SILICA-IMMOBILISED SALOPHENS FOR THE SYNTHESIS OF CYCLIC CARBONATES

William Pointer

Thesis for the degree of Masters (by Research)

Under the supervision of

Professor Michael North

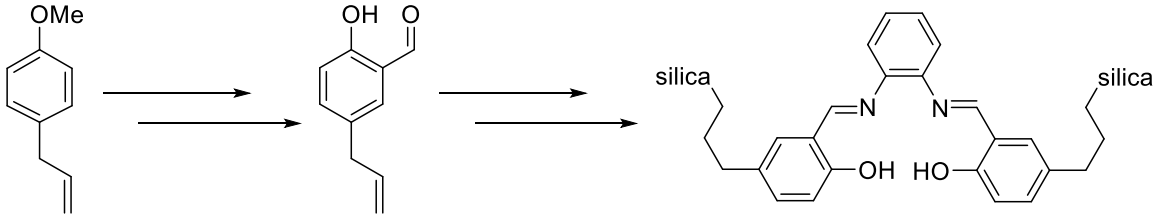

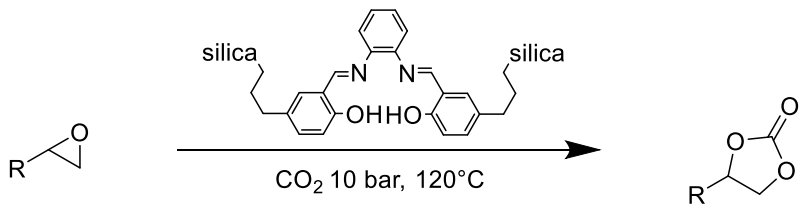

December 24, 2021

Department of Chemistry
University of York

Abstract

Cyclic carbonates are an important class of organic molecules with both interest from both the commercial and academic world. These valuable chemicals can be produced from corresponding epoxides and CO_2, catalysed by salen or salophen complexes and ligands. One drawback of this method of production is the high cost of the catalyst and purifying the product.

A green synthetic route to produce symmetrical salophens immobilised onto silica has been developed from 4-allylanisole, a cheap and naturally occurring compound. This process is split into three key phases, the preparation of a salicylaldehyde **3a**, the hydrosilylation for **4a**, and the salophen formation and immobilisation to produce immobilised salophen **6a**. Control over the immobilisation ratio of silica to salophen has been demonstrated by varying the stoichiometric ratio of **5a** to tetraethyl orthosilicate. This scheme has been developed with the 12 principles of green chemistry in mind and each step has been analysed for its environmental impact.

Once prepared these immobilised salophens have been shown to be active as catalysts for the formation of cyclic carbonates in the reaction between epoxides and gas phase CO_2. Seven cyclic carbonates have been produced utilising these immobilised salophens with activity matching that of the homogeneous equivalent.

List of Contents

List of Figures

List of Schemes

List of Tables

Acknowledgement

I would like to thank Professor Michael North for his guidance and patience, as well as him presenting me the opportunity to undertake this research. I would also like to thank the entire staff network within the Green Chemistry Centre of Excellence at the University of York. In particular, I would like to thank Dr Richard Gammons. Finally, I am immensely grateful for the members of the Mike North Research Group, with whom it was a privilege to work: Dr Xiao Wu, Ryan E. Barker and Marcell Haselwood.

Declaration

The work described herein has been undertaken solely by the author within the Green Centre of Chemical Excellence within the Department of Chemistry at the University of York between the dates of October 2020 and September 2021. This thesis contains no material that has been accepted for the award of any other degree in any other institutions. This thesis contains no material previously written by any other person, except where reference has been made within the text.

Chapter 1 Introduction

1.1- The Growing Climate Crisis

2020 Marked the end of the warmest decade since reliable records began (Figure 1).[1,2] Since the start of the 1920s the average global surface temperature and global oceanic anomaly temperature have risen by an average of 0.11°C and 0.14°C per decade respectively, with the average surface temperature of the Earth now being more than 1°C warmer than the same point of the last century.[3,4] Not only is the current global temperature the highest on record and consistently rising, the rate of warming is also increasing, with the decadal increase of the last twenty years being more than double that of the average of the previous one hundred (Figure 1).

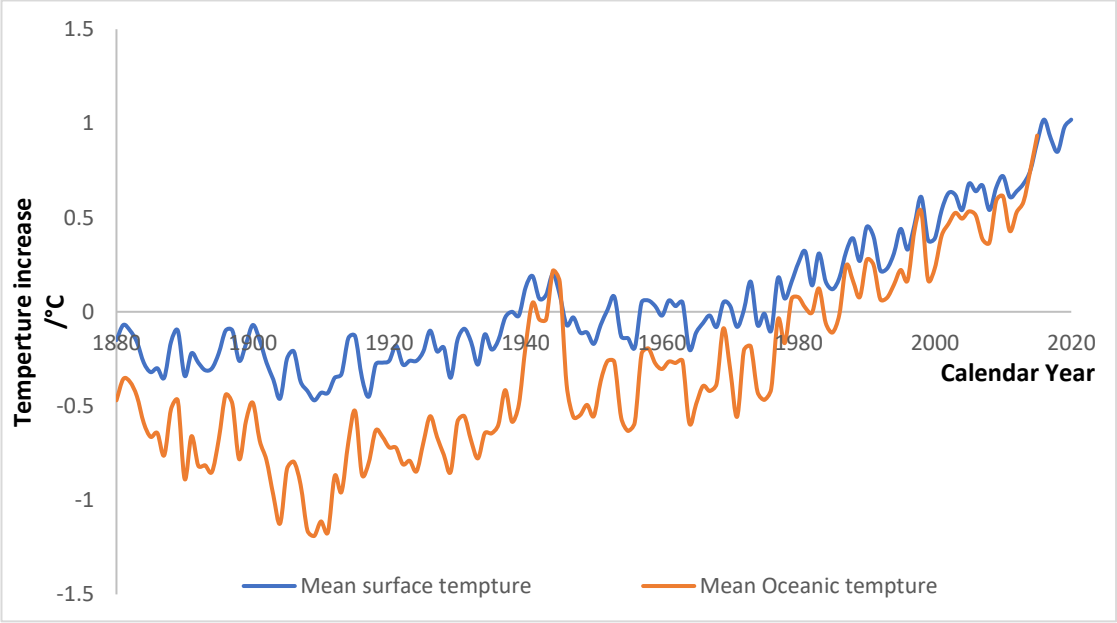

Figure 1:Graph showing the average surface temperature between 1880 and 2022 and the mean oceanic temperature anomaly between 1880 and 2015.[3]

This increase of the Earth's temperature is showing no signs of slowing, estimates predict that mean surface temperatures are likely to exceed 2.2 °C higher than the 1951-1980 baseline by the end of this century, with some, more extreme, predictions forecasting a

rise as high as 5 °C above the baseline.[1,3] The International panel for climate change (IPCC) predicts that the increase in land temperature will exceed that of the oceanic temperature and increases in the Arctic will be the most pronounced.[5] The highest levels of oceanic warming will occur in surface waters in the tropical and subtropical regions. Estimates place average oceanic warming between 0.6-2 °C for the top 100m and between 0.3-0.6 °C for the top 1 km of the ocean by the end of this century.[1,5]

It is crucial to note however, that temperatures have not risen uniformly across the globe and that these forecasts represent the predicted average global temperatures. As seen in Figure 2, there is likely to be wide variation in temperature increase by geographical region, with high latitudes and inner continental areas experiencing the most severe rises.[2]

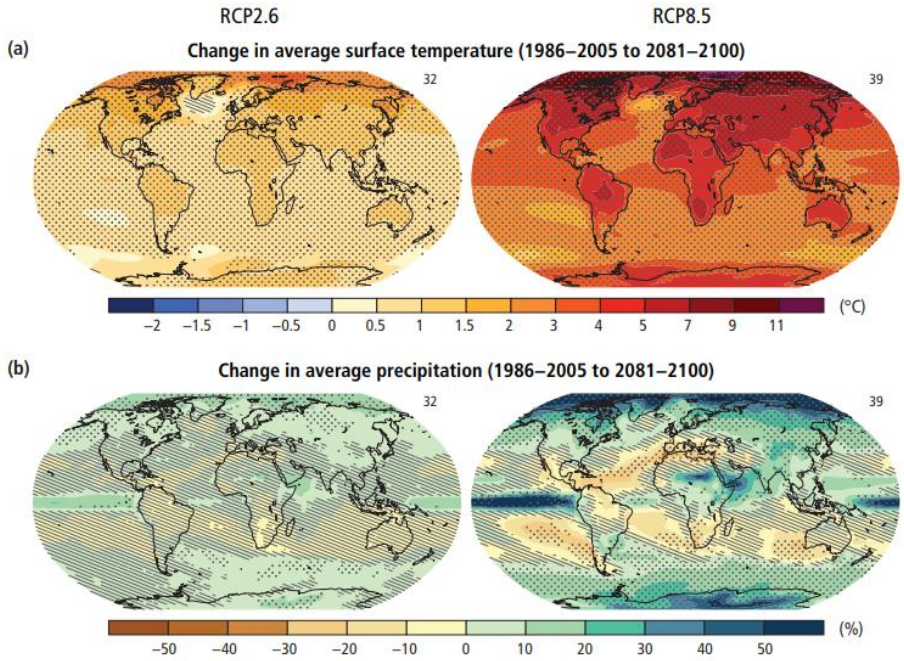

Figure 2: a)- Geographical variation of temperature change forecast by the IPCC. b) Geographical variation of precipitation change forecast by the IPCC. RCP2.6 represents a "best case scenario" with RCP-8.5 representing the most extreme prediction.[1]

1.1.1- Results of Temperature Increase

The effects of the 1-2 °C temperature increase will vary by region, however there is no doubt that it will be devastating to Earth's ecosystems. Much of the effect will be observed through changes to the global and local water cycles, mainly through changes to rates of evaporation and precipitation.

Global average rates of evaporation are predicted to rise with higher average temperatures. This will be more pronounced in regions that are currently dryer; southern and north-western Africa, the southwestern United States and the Mediterranean are likely to be affected and have already started displaying this trend.[5–7] Following on from increased rates of evaporation, these areas are likely to experience drops in soil-moisture content, possibly rendering vast swathes of land useless as arable land.[5]

Increasing rates of evaporation invariably lead to higher atmospheric humidity levels, which, in turn, lead to higher global precipitation levels. Different models predict an average increase between 0.5% $°C^{-1}$ and 4% $°C^{-1}$. High latitude areas will experience significantly increased precipitation while there is likely to be a decrease in the drier regions described previously.[5]

1.1.2- Effects on society

In wetter regions, increasing precipitation will result in shorter growing seasons, higher cloud coverage, an increase in the demand for fertilisers and a reduction in arable land area. Again, this will result in a drastic drop in agricultural product. In depth socio-political and economic analysis of the effects of climate change are well beyond the scope of this thesis, suffice it to say that the scale of the existential threat posed to the natural world has not been seen since the advent of human civilisation.

1.2- The Greenhouse Effect

The "greenhouse gas" effect is a well understood concept that has its origins in fundamental chemistry; the ability of chemical bonds to absorb and re-emit infrared (IR) radiation. Any gas present in the Earth's atmosphere that absorbs IR radiation is given the name a greenhouse gas (GHG). Notably oxygen and nitrogen, which collective comprise over 98% of the Earth's atmosphere are not able to absorb IR radiation, however they can gain energy from colliding with an excited GHG.

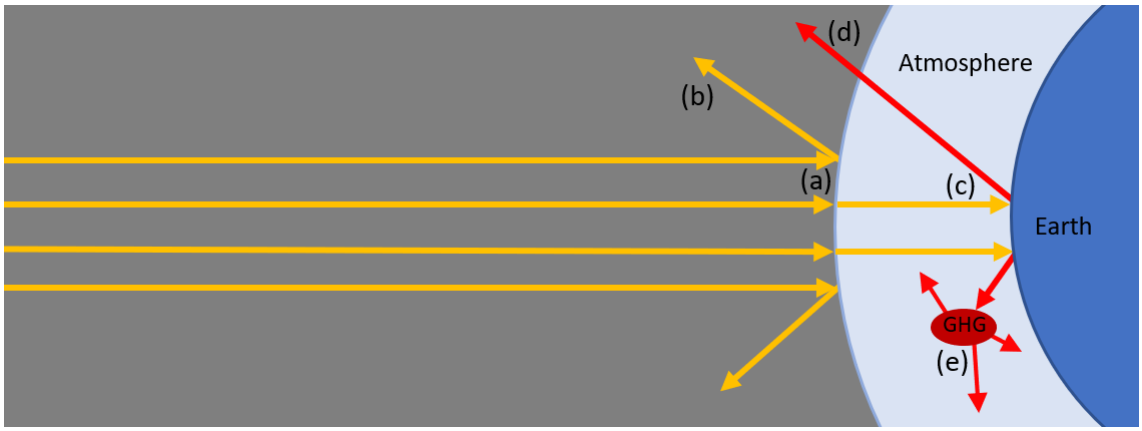

Figure 3: Schematic diagram of solar radiation reaching the Earth's atmosphere (a), radiation reflected back into space; (b), absorption of the radiation by the Earth and re-emitting as IR radiation; (c), IR radiation escaping the atmosphere and; (d), absorption of IR radiation by GHGs.

The fundamental cause of the increasing temperature of the Earth's atmospheric system is that more energy is being absorbed by GHGs and transferred to the atmosphere than previously.

1.2.1- Greenhouse Gases and Global warming Potential

Annex A of the 1997 Kyoto protocol identifies four specific gases and two groups of chemicals as being the major contributors to the global greenhouse effect.[8] These are: carbon dioxide (CO_2), methane (CH_4), nitrous oxide (N_2O), sulphur hexafluoride (SF_6), hydrofluorocarbons (HFCs) and perfluorocarbons (PFCs). Water vapour (H_2O) and ozone

(O_3) are both also strong IR absorbers and it is likely that water vapour is responsible for around 75% of the total greenhouse effect in the atmosphere.[9]

Water vapour has a short lifetime within the atmosphere and the vapour distribution is determined by complex series of condensation, evaporation and vertical and horizontal movements but is determined largely by temperature. To a large degree, water vapour distributions are part of a natural response to external temperature changes; be this from the presence of long-lived GHGs or heightened solar activity. It is therefore ignored by international policy makers as a cause of global warming.[9]

The individual contributions of these species to the global greenhouse effect are determined by their global warming potential (GWP) and atmospheric concentrations. The GWP of a gas is a function of the lifespan of the species in the atmosphere, and its efficiency to absorb IR radiation, compared to the properties of the same mass of CO_2.[10]

Table 1- Global Warming Potentials for the species identified by the 1997 Kyoto protocol.[11]

Gas	*Lifespan (Years)*	*20 Year GWP*	*100 Year GWP*	*500 Year GWP*
CO_2		1	1	1
CH_4	12	56	21	6.5
NO_2	120	280	310	170
SF_6	3200	16,300	23,900	34,900
CCl_2F_2	100	11,000	10,900	5,200
CF_4	50,000	5,210	7,390	11,200

As can be seen in Table 1, CO_2 has the lowest GWP of the species identified by the 1997 Kyoto protocol. However, atmospheric CO_2 levels are currently at 416ppm, more than a thousand times that of the next most abundant GHG. It is clear to see in Table 2 how the concentrations of the gases determine their individual contributions to the greenhouse effect, and that the high atmospheric concentration of CO_2 is the dominant factor in the total greenhouse effect.

Table 2:GWPs and the effect of atmospheric concentration.[11]

Gas	*100 Year GWP*	*Atmospheric Concentration (ppm)*	*GWP x Concentration*	*Relative to CO_2*
CO_2	1	416	416	1
CH_4	21	1.73[12]	36.3	0.087
NO_2	310	0.319[12]	98.9	0.24
SF_6	23,900	0.000004[13]	0.0956	0.00023
CCl_2F_2	10,900	0.00053	5.78	0.0139
CF_4	7,390	0.000085-	0.628	0.00151

1.2.2- Historical CO_2 Levels

Atmospheric CO_2 levels have varied greatly during the Earth's history. Over the last 800,000 years, CO_2 levels have risen and fallen, see Figure 4, but have consistently stayed between 170 ppm and 300 ppm. On a more human timescale, between the start of the Iron age (~1200 BCE) and the dawn of the industrial revolution in the 1800s, CO_2 levels have remained stable at around ~280ppm, as shown in Figure 5. The question of the source of the increased CO_2 levels is answered by the relation to the growth of human industry, specifically our increasing use of petrochemicals derived from fossil fuels. As seen in Figure 5, the onset of the industrial revolution and the largescale exploitation of petrochemicals heralded an explosive rise in CO_2 levels, there is no basis to assume that the rise in CO_2 level would have occurred without human intervention.[14] As stated in section 1.2.1- higher CO_2 levels ultimately result in a larger greenhouse effect, and the increase in global temperatures seen in Figure 1.

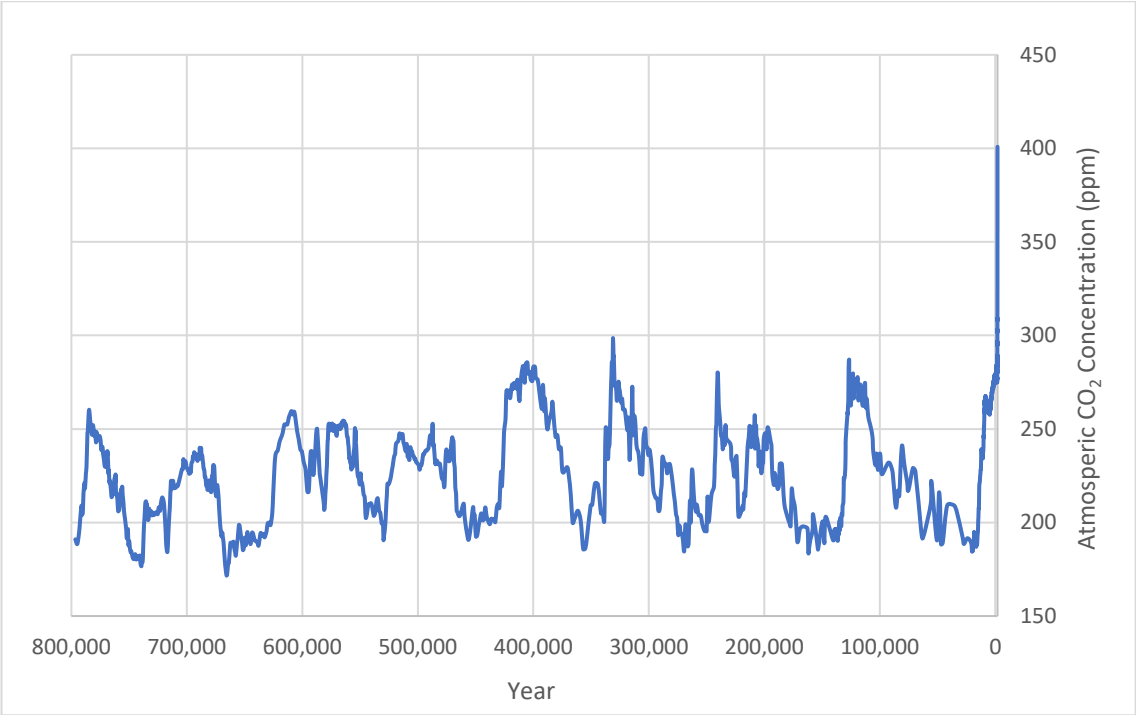

Figure 4: Graph showing Atmospheric CO_2 levels over the last 800,000 Years.[3]

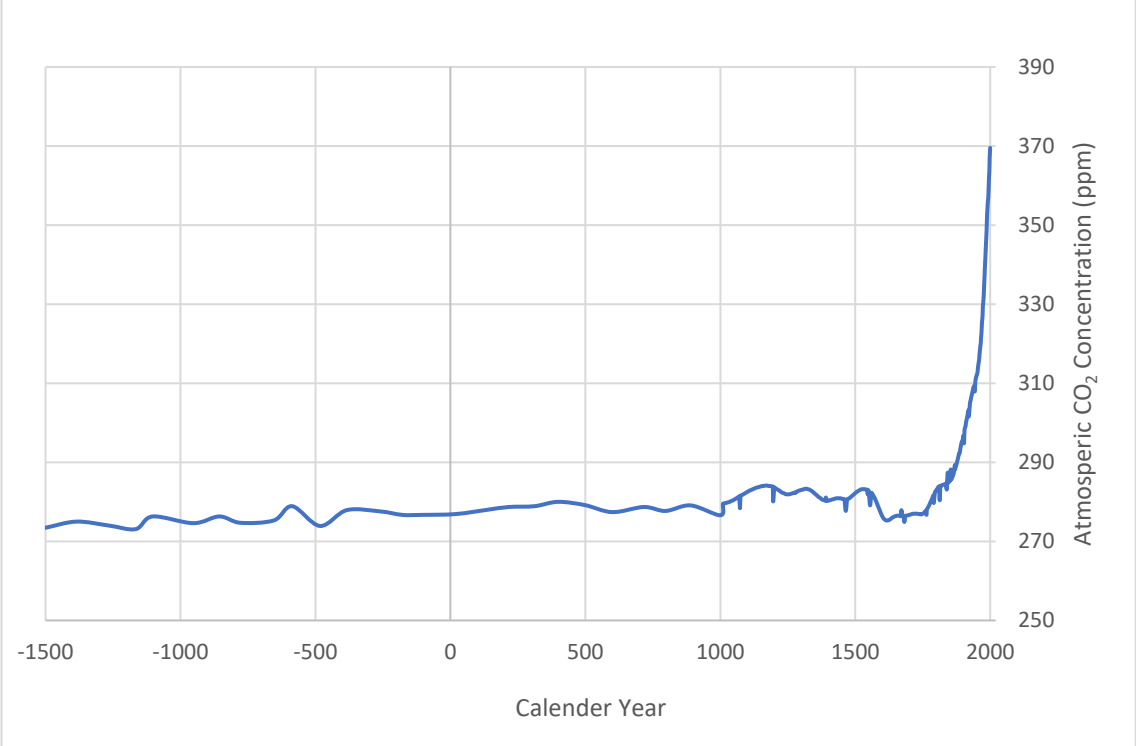

Figure 5: Atmospheric CO_2 concentrations over the timeframe of western civilisation.[3]

1.2.3- CO_2 Capture, Storage and Utilization

Reducing the CO_2 content of the atmosphere is essential for the preservation of the Earth's current environmental state. For this to be accomplished two criteria must be met; A reduction in CO_2 emissions, and an increase in the rate at which CO_2 is removed from the atmosphere.

Both methods require the development and implementation of carbon capture (CC) technologies, either in the form of Ultralow CC (such as from atmospheric levels ~0.04% CO_2) or from high-concentration gas samples (such as flue gas lines or from urea production 5-100% CO_2). Ultralow CC has the advantages of being a universal source, placing no demands on the location of CC facilities, though low CO_2 concentrations would require thousands of facilities with exceedingly high-volume throughput to have any noticeable effect on the global scale. High-concentration CC has almost the opposite qualities, the potential for high masses of CO_2 capture from large stationary producers.[15–18] Ultimately, optimisation of both is required.

Multiple technologies exist for CC; liquid absorption, solid adsorption and membrane separation.[19] Liquid absorption such as amine absorbent technologies are well established, finding use in small/medium scale facilities, though high costs of solvents, reliance on temperature swings and the production of hazardous by-products are less than satisfactory for widescale use.[18] Solid state sorbents function by selectively adsorbing CO_2 onto solid surfaces; zeolites, metal-organic frameworks[20] (MOFs) and carbonaceous materials are three major players.[15] None of these however have ideal properties. Zeolites have poor loading capacities and stability in the presence of impurities, MOFs are difficult to produce in the bulk required in an environmentally friendly way and carbonaceous material have poor adsorption properties at mild temperatures.[19] Once captured, the CO_2

can either be treated as a waste product, fated for processing and long-term disposal, or as valuable resource. Either option must result in the prevention of it from re-entering the atmosphere.

The utilisation of CO_2 as a reagent in the production of pharmaceuticals as well as fine and bulk chemical is a very attractive and potentially very lucrative opportunity. Synthesis of cyclic carbonates via catalytic processes;[21–24] complex hydrocarbons via Fischer-Tropsch chemistry[25–27] or even the production of methane using the Sabatier reaction[28,29] may well be sufficient to financially justify the capital cost of capturing CO_2. This is likely to become even more lucrative as dwindling fossil fuel reserves may drive up the cost of traditional chemical feedstocks.

Due to the scale of the issue, long term storage of CO_2 will have to be employed to deal with the bulk of the CO_2 recovered from the atmosphere. Dissolution of CO_2 in oceanic deepwater[30] or ocean sediment[31] has largely been dismissed as a potential route, as it is likely to solve one environmental crisis by creating another.[11] Mineralization of CO_2 is a highly interesting option[32,33] and would produce a potentially useful material for the construction industry.

1.3- Cyclic carbonates and their applications

Cyclic carbonates[21,34] are a subgroup of organic carbonates, esterified forms of carbonic acid. This group of chemicals possess a carbonyl oxygen and two alkoxy groups attached to a central carbon. In the case of cyclic carbonates, the two alkoxy groups are joined either 1,2- or 1,3- to each other, forming a five or six membered ring (Figure 6).

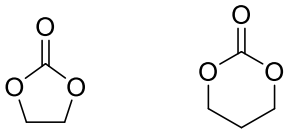

Figure 6:examples of cyclic carbonates

Other forms of organic carbonates exist: polycarbonates[21,35] and acyclic carbonates.[21] All three forms are industrially relevant for a multitude of purposes, and all are produced in multi-tone scales and employed commercially. [36]

1.3.1- Current methods of cyclic carbonate production

Two routes exist for cyclic carbonate formation: transesterification of 1,2 and 1,3 diols with phosgene (Figure 7a) [36] and the coupling of CO_2 with heterocycles[36,37] (Figure 7b). High atom economy and the lack of highly toxic reagents make the latter option highly appealing. Additionally, the CO_2 required for the synthesis could be obtained directly from the air, thus lowering material costs, and addressing the problems raised in section 1.1-.

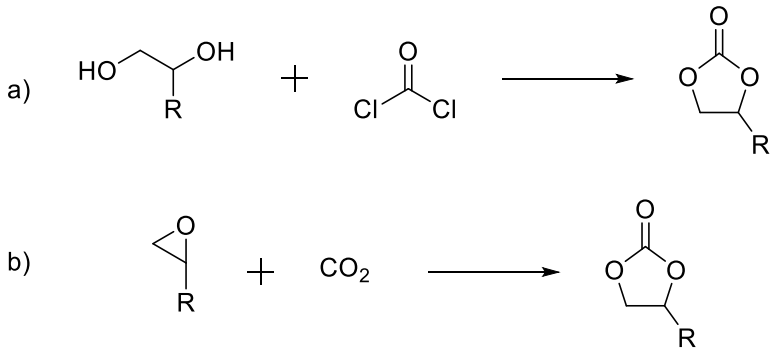

Figure 7: a) Cyclic carbonate synthesis from 1,2-diol and phosgene gas. b) Reaction of epoxides and CO_2 producing a cyclic carbonate.

Cyclic carbonates have also been formed via reaction of alkali metal carbonates with epoxides, and through transesterification, however these reactions are more complex and less reliable than direct synthesis from epoxides and CO2.[38–40]

Direct synthesis from CO_2 can be accomplished in some cases (such as with propylene oxide) without the use of a catalyst, and proceeds via a nucleophilic attack of a CO_2 oxygen to one of the carbons within the epoxide ring.[41] Typically this reaction does not proceed in high yields under mild conditions, therefore it is necessary to employ a catalyst. Several catalytic systems have been developed, both homogeneous and heterogeneous, which operate under milder conditions with high yields.[23,41–44]

1.3.2- Applications of Cyclic Carbonates

Cyclic carbonates are versatile chemical building blocks for both the production of fine chemicals and pharmaceuticals and find uses in the bulk chemical industry. They are commonly produced as precursors to both polycarbonates and acyclic carbonates.

1.3.2.1- Applications in Polymer Technology

The interest in cyclic carbonates for use in polymer chemistry has grown significantly over the past few years, specifically the incorporation of five membered carbonate rings

both within the backbone of polymers and as pendants attached to them. One application of particular interest is developing cyclic carbonates for the production of polyhydroxyurethanes without the need for hazardous isocyanates.[40,45,46] Polyurethanes are one of the largest polymer types currently produced with an estimated 21 million tonnes produced each year, finding applications in several materials such as clothes, foams, adhesives, sealants and elastomers, further development of cyclic carbonates could allow this entire sector of the polymer industry to be actively utilising CO_2.[46]

Cyclic carbonates have also been used to alter the physical and mechanical properties of epoxy resin systems.[47,48] Properties such as mixture viscosity, gelling time and peak exotherm were reduced in epoxy resin systems that had been mixed with cyclic carbonates, these systems also showed improved mechanical properties of the resulting resin, such as higher impact resistance, flexibility, and adhesion.

Another, crucial application of cyclic carbonates within polymer chemistry is the development of polycarbonate plastics. Cyclic carbonates are often produced as a pseudo-intermediate of polycarbonate species, the formation of which utilises the incorporation of CO_2 into heterocyclic monomers. These polycarbonates are distinguished by their high strength, durability, heat resistance, low weight, and optical transparency.[49]

1.3.2.2- Applications as Solvents

There has been tremendous levels of research into the use of cyclic carbonates as green solvents for chemical reactions and industrial processes.[36] Cyclic (and linear) carbonates have several advantages as solvents and have been suggested as replacements for the commonly used volatile organic compounds (VOC). The liquid-phase temperature range of most cyclic carbonates is suitable for their use as polar solvents, and their readily availability from renewable resources makes them attractive from both a financial and

environmental standpoint. Coupled to this is their relatively low toxicity, complete biodegradability, and their potential to be produced in a way that utilises atmospheric CO_2.[36]

1.3.2.3- Use as Electrolytes and Battery Additives

One of the most valuable functions of cyclic carbonates, is their application in high efficiency Li-ion batteries.[50,51] Lithium ion battery technology has exploded over the last two decades as demands for their incredibly high energy density and stable cyclability for use in portable electronics and electric vehicles has increased. Whist linear carbonates have often made up the bulk of the electrolyte systems, cyclic carbonates have played a crucial role in the development of battery technology, acting both as the sole electrolyte and as additives for electrolyte mixtures. Due to extensive and ongoing safety concerns of traditional Li-batteries, caused in no small part by the high flammability of linear carbonates, liquid electrolyte systems have been pushed to the backseat as solid-phase[52,53] and gel-polymer[54] electrolyte systems have been investigated. Cyclic carbonates are key to both new electrolyte systems and are equally key to the development of novel lithium metal batteries, where they have been shown to profoundly enhance the stability of the lithium metal anode.[55]

1.4- Catalysis

The field of catalysis is one of the key foundations in the development of green chemistry and has fundamentally facilitated the explosion of technological growth seen over the last 100 years.[56] Beginning in the early 1900s with the Haber-Bosch process, catalytic chemistry has changed the way in which chemical research and production has been carried out; currently more than 80% of all chemical manufacturing processes worldwide employ catalysts.[56,57] The contributions of catalytic processes to society is incredibly large, contributing towards almost every basic need of mankind.[56] Over 90% of the worldwide production of fertilizers utilises ammonia produced from the Haber process, one of the earliest examples of an industrial catalytic process.[58,59] Catalysts are also used extensively in non-industrial contexts, such as their employment for reducing toxic gas emissions from motor vehicles.[60] As of July 2021 the estimated value of the catalyst industry passed 20 billion dollars.[61]

The general description of a catalyst is: a material used in a reaction that lowers the activation energy without the consumption of the catalyst.[62–65] While this description lacks nuance, it is adequate to describe the role of a useful catalyst.[63] The effect of including a species in the role of a catalyst usually comes in the form of: enabling reactions under less extreme conditions, lowering temperatures, times required or pressures, forcing equilibria, or increasing selectivity for a desired product.[62,63]

Catalytic systems can be as simple as acid or base catalysed reactions but increase in complexity all way up to vast organic ligands hosting metal ions, such as platinum, rhodium, and copper.[60] Broadly speaking, catalysts fall into one of three groups, homogeneous, heterogeneous, and biological or enzymatic catalysis.[57,62]

Enzymatic or biological catalysis is possibly the oldest catalyst used by human beings, fermentation of sugars to ethanol has been employed by almost every culture of mankind on the planet, and is employed commercially to this day.[66–68] Whilst ancient humans had no understanding of fermentation, we now know the process is catalysed by the zymase enzyme found within yeast.[67] In more modern times our understanding of enzyme chemistry has improved, enzymatic catalysis has undergone a dramatic boom in interest as demand for complex, and enantiomerically pure organic molecules continues to rise.[69] This is driven in large parts by the pharmaceutical and food industries requirements for high purity chiral building blocks, the regioselectivity, chemoselectivity, and enantioselectivity offered by enzymatic transformations and the mild conditions under which they operate.[70] Enzymatic catalysis is a school unto itself and will not be discussed further in this thesis.

More ‘traditional’ methods of catalysis are split between homo- and heterogenous catalysis. Homogeneous catalytic systems operate with the catalyst and reagents being mixed in the same phase, normally in solution phase.[64] This comes with several distinct advantages, high rates of reaction, high selectivity, mild conditions, and easily tailorable chemistry.[57,71] However, when scaling up to industrial processes, difficulties in recovering and reusing catalysts severely limit their attractiveness to both industry and research.

Heterogeneous systems involve a bi-phasic or tri-phasic system whereby the catalyst and reagents are not within the same phase.[65] Most commonly these tend to be solid catalysts with solution or gas phase reagents passing over them. In contrast to homogeneous catalysis the advantage of heterogeneous systems is that being in separate phases, the reagents and products are easily separated from the catalysts, dramatically improving the recovery and reuse of the catalyst, and enabling continuous use in flow systems.[72] This is

highly appealing from a commercial view, as this reduces the cost per reaction of using a catalyst and can commercially justify the high cost of elements such as platinum.

1.4.1- Hetrogenising catalysts

Some catalytic species, such as macromolecules, nanoparticles, and Pt group metals, are effectively insoluble in most solvents, however transition metal complexes, salts, and organo- catalysts are largely soluble in common organic solvents or water. The selection of the solid material is not trivial, it must be insoluble for the given solvent system and stable within the solution. It also must not interfere with the chemistry of the reaction. Most crucially it must be able to host the catalyst in such a way that does not affect the catalytic activity.

Rendering homogeneous catalysts insoluble is possible by ‘immobilising’ the catalyst onto a solid support such as silica or zeolites, though the use of an organic bridge. This produces a material which is mechanically heterogeneous but catalytically homogeneous. [71]

Catalysts produced through these methods are not true heterogeneous catalysts, and have several drawbacks, the most obvious of which is leaching. Leaching occurs as metal ions are removed from the solid anchor and dissolved into the solvent. This is highly problematic for several reasons, chief amongst them being the decline in catalytic activity with the loss of the active sites. This presents a significant cost when using precious elements, in terms of decreasing yields or adding more catalyst. More alarmingly, this also presents a huge danger both toxicologically and environmentally.

1.5- Salens and Salophens

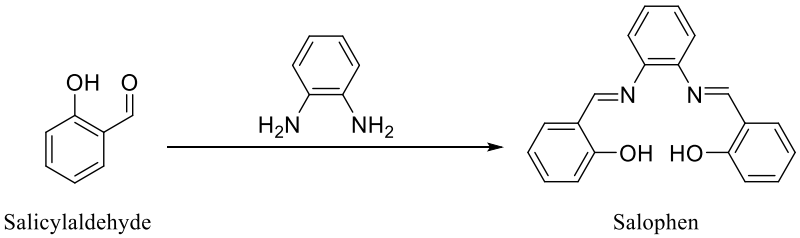

Figure 8: Salophen formation from a salicylaldehyde with phenylene-1,2-dimine.

Salens and salophens are two classes of Schiff base, tetradentate ligands formed by the coupling of two salicylaldehyde molecules with a 1,2-dimine, as seen in Figure 8.[73] They were first developed for use as catalysts by Jacobsen in 1991 in the, now famous, enantioselective epoxidation of alkenes.[74] Sometimes referred to as "Privileged ligands", salens and salophens are able to catalyse a vast number of transformations with high yield.[75,76] These include the hydroxylation and epoxidation of alkenes[77], The aziridination of alkenes[78], Diels Alder reactions[79,80], and the oxidation of sulfides to sulfoxides[81]. Their wide applications as catalysts stems partially from their capability to complex to a large variety of metal ions in multiple oxidation states, such as zinc, manganese, copper and even uranium.[75,76,82] Salens and salophens can act as catalysts independently or via bimetallic pathways, this is advantageous as bimetallic catalysts are able to active both nucleophilic and electrophilic reactants simultaneously, this can drastically improve selectivity and the kinetics of a reaction.[82–84] Salens have a highly contorted geometry which enables their complexes to display high levels of catalytic enantioselectivity [80,85]

1.5.1- Current methods of production

The key bond in the formation of both salens and salophens is the secondary aldimine formed during a condensation reaction between the aldehyde group of the salicylaldehyde and the amine from the 1,2 diamine.[74,86] In the production of salophens the 1,2-diamine

must be phenylene-1,2-diamine, for salens ethylene-1,2-diamine, and 1,2-diaminocyclohexane are typical.[87] The identity of the diamine bridge pays a large role in the catalytic properties of the ligand.

1.5.2- Applications in catalysis

Salens and salophens are known primarily for their catalytic activity. Epoxidation of alkenes using a manganese salen complex is one of the most well-known examples[74,77]; there are countless more reactions catalysed by salens or salophens including; The aziridination of alkenes using a copper salophen complex[78], Diels Alder reactions using uranyl or cobalt salens complexes[79,80], and the oxidation of sulfides to sulfoxides with salen oxo vanadium complexes[81]. Salen complexes also form multi-metalic species which can behave as multicatalysis in cooperative catalysis.[88] Salens, due to their contorted nature, are highly efficient asymmetric catalysts, giving products with high enantioselectivity.[88]

The broad range of transformations possible with salens and salophens make them attractive for study as potential targets for heterogenization. [88] Anchoring of salens and salophens has been investigated previously, in order to improve their recoverability and potential to be reused. Methods of immobilisation have been split between organic and inorganic, mainly silica, supports.

So called “grafting” of salen complex onto polymeric materials has been documented extensively with some success.[88–90] Immobilisation using covalent hetero-atom chemistry and via coordination of the support to the metal centre have been achieved. However a noticeable drop in selectivity and activity of the catalysts were observed, when compared to homogeneous equivalents, but they did display good recoverability and maintained their activity.

Additionally, to be immobilised onto polymers, salen derivatives have been designed to be included within the polymerisation process. The work done on this ideal is expansive and is shown to be effective utilising copolymerisation, anionic polymerisation, atom transfer radical polymerisation and many more methods. Immobilised salens produced under these methods have their own strengths and drawbacks and cannot be easily summarised. Given the wide application of salens and the even wider variety of polymers, monomers and polymerisation techniques, it is possible to tailor specific polymer-immobilised salophens for each specific purpose.[88]

Metal organic frameworks have also been investigated as a method of heterogenising salens and have been shown to be highly effective for a number of asymmetric transformations.[91–93] The topic of MOF-immobilized salens is as large as polymer immobilised salens. High catalytic activity and selectivity, surpassing that of the homogeneous equivalent, has been achieved. [91–93]

Salen immobilisation onto silica has also been accomplished previously with varying results.[87] Typically these methods are accomplished via either immobilisation using an organic tether apical coordinatively bonded to the metal centre or through linkers covalently bonded to either the amine bride or via substituents on the aromatic rings. These linkers universally require carbon-heteroatom bonds to bridge between the silica and the salen.[87] These covalently bound salens typically have very high activity, though can suffer from decreased enantioselectivity, and difficulties in characterising the catalyst loading and purity.[87]

Chapter 2 Project Aims

The goal of this project was to develop a sustainable synthesis route for silica immobilised salophens for the use in heterogeneous catalysis of cyclic carbonates, from epoxides and CO_2. Secondary goals were demonstrating control over the ratio of the salophen ligand to the silica matrix and conducting the research in a manner that limited its environmental impact, as defined by the principles of green chemistry. The commercial importance of cyclic carbonates has been discussed in section 1.3-, the commercial and chemical importance of salophens in section 1.5.1- and the advantages of hetrogenizing catalysts in section 1.4-. An additional goal of this project was to develop a flexible and versatile synthesis route that would allow for further modification of the immobilised salophens.

2.1.1- Green Technology and Green Business

The issues of climate change, global warming and environmental degradation are not problems for the chemist alone; these issues are entrenched in political, societal, and economic considerations. Whilst these problems are beyond the scope of this thesis, it does not demean the necessity of conducting novel research in a manner so as to limit the environmental impact of that research.

The principles of green chemistry (PoGCs, Figure 9) were laid out in 1990 by Paul Anastas and Nicolas Eghbali, intended as a guide for chemical and engineering industries and research.[94] These principles are straight forward, each being chosen to lower the environmental impact of a procedure. This research project has held fast to several of these principles, specifically, principles 1, 2, 7, and 9 which were focused on when planning the work.

1. Prevention of waste
2. Atom economy
3. Less hazardous synthesis
4. Designing safer chemicals
5. Safer solvents
6. Designed for energy efficiency
7. Use of renewable feedstock
8. Reduce derivatives
9. Catalysis
10. Design for degradation
11. Real-time analysis of pollution prevention
12. Inherently safer chemistry for accident prevention.

Figure 9: The principles of green chemistry as laid out by Paul Anastas and Nicolas Eghbali

Within chemical synthesis, prevention of waste is an area with large scope for improvement. Large volumes of plastic and glass consumables, hazardous chemical waste and solvents are produced, even when doing the most basic of procedures. Efforts were made to eliminate large volumes of solvents and to actively seek ways of reducing the amount of extraction and purification steps involved with the synthesis.

Atom economy is a straightforward concept that is often forgotten. It is the number of atoms that are present in the reagents that are present in the final product, including atoms present in solvents and catalysts. This is a powerful way of measuring the waste produced in a reaction, conceptually focusing down on the product. The concept of atom economy disincentivises wasteful procedures such as the incorporation of protecting groups.

The use of renewable feedstocks is highly important in the current day and age, as discussed in section 1.1-, the exploitation of fossil fuels is one of the largest driving forces behind climate change and global warming. Fossil fuels are known to be a finite resource, thus developing synthesis schemes entirely dependent on them is short-sighted, this

project has made efforts to use alternative feedstocks where possible, specifically in the use of 4-allylanisole as a starting point.

As discussed in section 1.4-, catalysing reactions, either heterogeneously, or homogeneously presents benefits environmentally including reducing the production of unwanted regio-, or stereoisomers, lowering the pressure and temperature reactions can proceed at and reducing the duration of a reaction. Specific efforts were made to utilise catalysts when appropriate. Additionally, the use of heterogeneous catalysts was preferred.

Chapter 3 Synthesis of Silica Immobilized Salophens

3.1- Silica Supported Salophens from 4-Allylanisole

Also known as methyl-chavicol and estragole, 4-allylanisole **1** is a phenylpropenoid obtained from plant sources and has a wide variety of uses in consumer industries.[95,96] 4-Allylanisole is produced naturally by common aromatic plants and herbs, including tarragon, sweet basil, sweet fennel, star anise and anise vert. As one might expect, it is commonly used as a food and drinks additive and finds applications in the fragrance industry,[97] but it also shows potential as a repellent to certain insectoid pests.[98] While generally recognised as safe, there is evidence that it displays some carcinogenic effects.[99] As 4-allylanisole is a naturally produced material with a pre-existing commercial interest, it is the ideal starting material for this synthesis as both the environmental and financial costs are low. It is highly advantageous, from a green chemistry perspective, that 4-allylanisole is not derived from fossil fuel reserves.[100] The 4-allylanisole used in this work was characterised by a combination of ^{1}H-NMR, ^{13}C-NMR, ESI-MS and IR spectroscopy (see appendix).

The proposed synthesis scheme utilises well-understood reactions that are reported to proceed with high conversions and yield. It comprised of five synthetic steps and is broadly divided into two major segments, as shown in Scheme 1: synthesis of the key intermediate 2-hydroxy-5-(3-triethoxysilylpropyl)benzaldehyde **4a**; and salophen formation and immobilisation onto silica

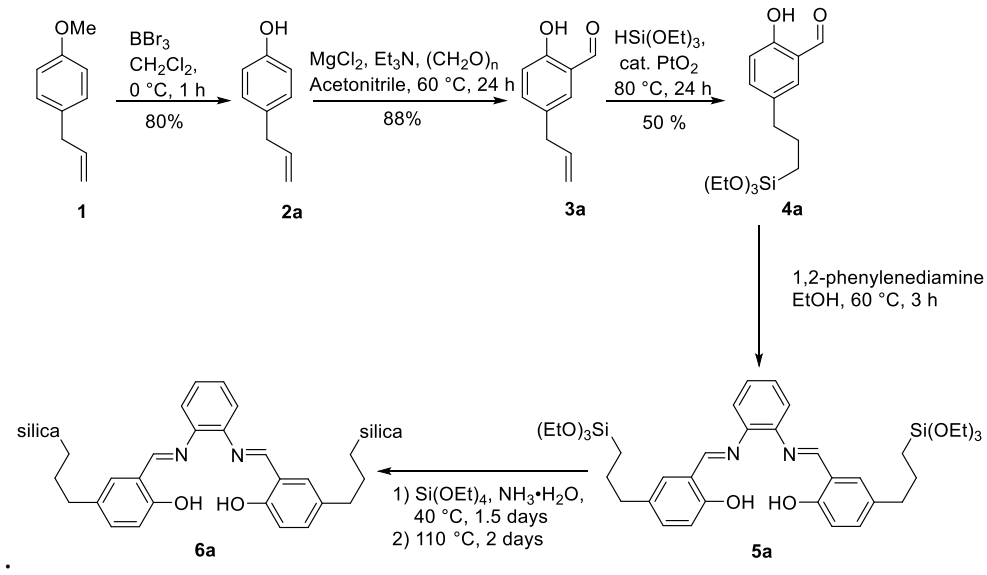

Scheme 1: Proposed synthetic scheme for silica immobilised salophens

The first stage of this synthetic route is designed to form the salicylaldehyde (half salophen) with the added functionality of a triethoxysilyl group attached via a propyl chain. The two areas of functionality, the salicylaldehyde and the triethoxysilyl group facilitate the second stage of the synthesis; imine formation with a 1,2-diamine to form the salophen and the immobilisation of the salophen using the sol-gel procedure. The sol-gel procedure is where the control over the silica: salophen incorporation ratio will be achieved. This scheme is designed to produce a doubly immobilised symmetrical salophen, with both sides of the ligand bearing a propyl-chain and the silica anchor. Modification of this procedure to allow the synthesis of unsymmetrical salophens, or the introduction of additional functionality should be feasible. Additionally, this procedure has only been completed using 1,2-phenylenediamine as the central bridge; 1,2-diamoinoethane and 1,2-diaminocyclohexane are also potential bridges, forming the equivalent salens.

3.2- Demethylation

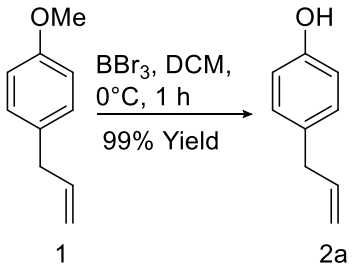

Scheme 2: Demethylation of 4-Allylanisole

Synthesis of 4-allylphenol, **2a,** is achieved by demethylation of 4-allylanisiole, **1**, following an established procedure (Scheme 2).[101] Demethylation using BBr_3 is well understood and the mechanism is displayed in Scheme 3. The product, 4-allylphenol, is commercially available, all be it at £830 per gram. At this price it is significantly more economical to produce it in-house from 4-allylanisole (£0.68 per gram) and BBr_3 (£1.64 per gram) using the method described herein.[95]

Demethylation was initially accomplished using 1.5 equivalents of BBr_3 in dichloromethane under dry conditions and an atmosphere of nitrogen. Using BBr_3 proved method of demethylation with consistent conversion of >99% to products, as seen in the crude ^{1}H-NMR (Figure 14) spectrum the characteristic methyl signal of compound **1** (3H, Singlet, 3.8 ppm) is entirely absent. Purification of this reaction was accomplished using column chromatography with silica gel (50g) eluting with EtOAc/Hexane (1/9) to give 4-allylphenol **2a** in 51% yield.

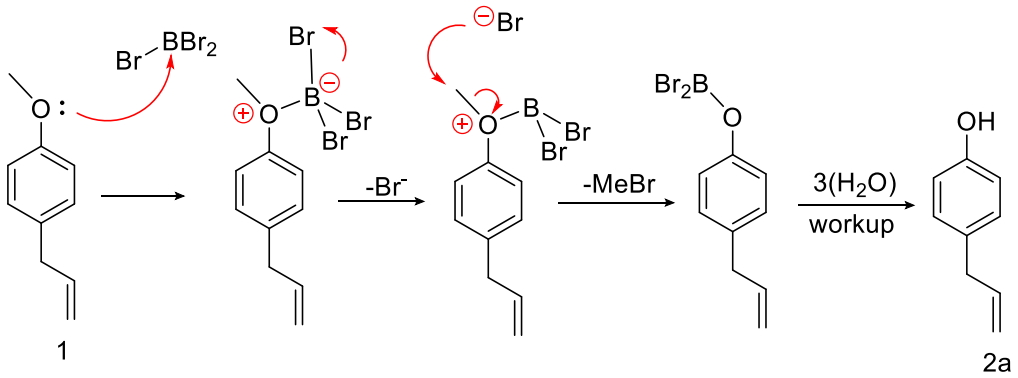

Scheme 3: Mechanism of demethylation.

Characterisation of **2a** was achieved using ^{1}H-NMR (Figure 10) and ^{13}C NMR spectroscopy. Within the ^{1}H-NMR spectrum, the four aromatic hydrogens are visible as two doublets at 7.08 ppm (*J = 8.3 Hz*) and 6.80 ppm (*J = 8.3, 2.1 Hz*), the hydrogen on carbon two of the propyl chain appears as a doublet of doublet of triplets at 5.98 ppm (*J = 16.0, 10.7, 6.7 Hz*), the terminal hydrogens appear as two doublets of triplets at 5.09 ppm (*J* = 16.0, 1.6 Hz) and 5.08 ppm (*J = 10.7, 1.6 Hz*), with the two hydrogens on carbon 1 appearing as a well resolved doublet at 3.33 ppm (*J= 6.7 Hz*).

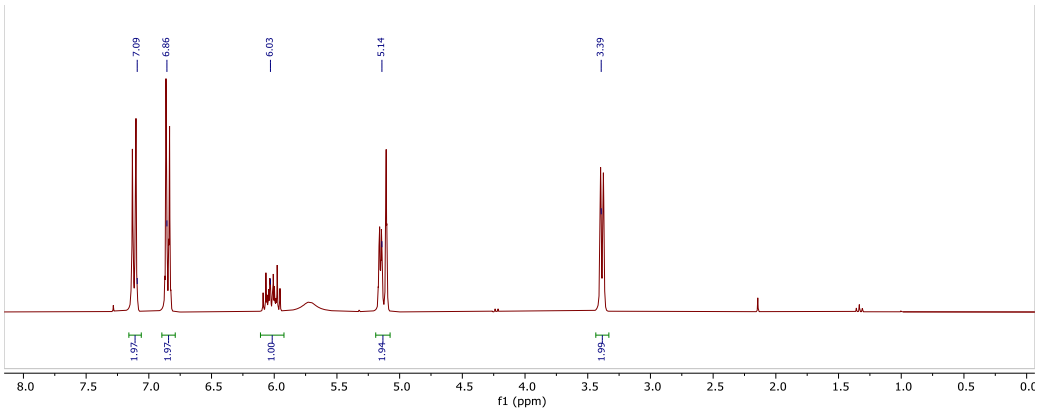

*Figure 10: The ^{1}H-NMR spectrum of purified 4-allylphenol, **2b**.*

A broad peak corresponding to the phenolic hydrogen can be seen at 5.75 ppm, though the exact location of this peak varied. The ^{13}C-NMR spectrum of **2a** can be seen in Figure 11. The peak due to the phenolic carbon can be seen at 153.8 ppm and three other aromatic carbons can be seen at 137.8 ppm, 132.3 ppm and 129.7 ppm. Two peaks at 115.2 ppm

are caused by the two alkene carbons, and a peak at 39.2 ppm is due to the alkyl carbon in the propylene chain.

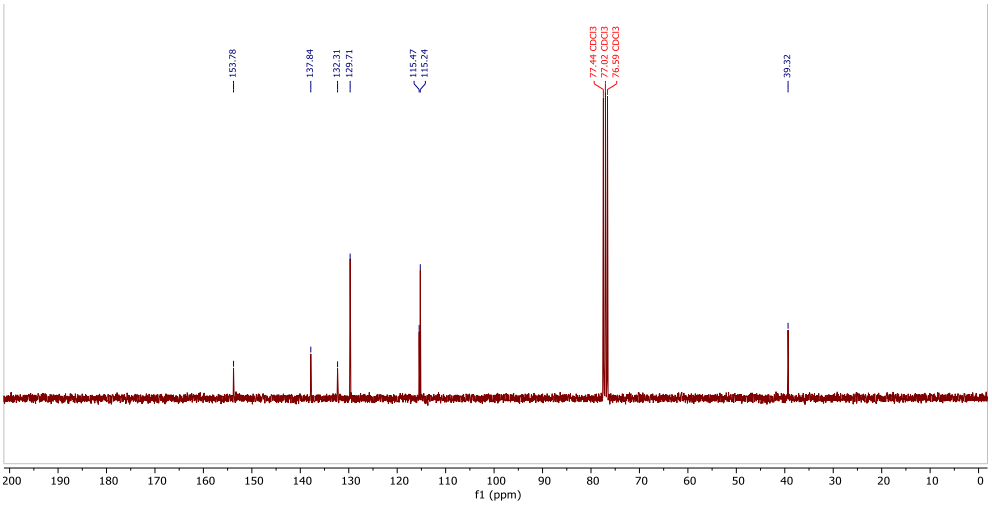

*Figure 11: ^{13}C-NMR spectrum of purified 4-allylphenol, **2a**.*

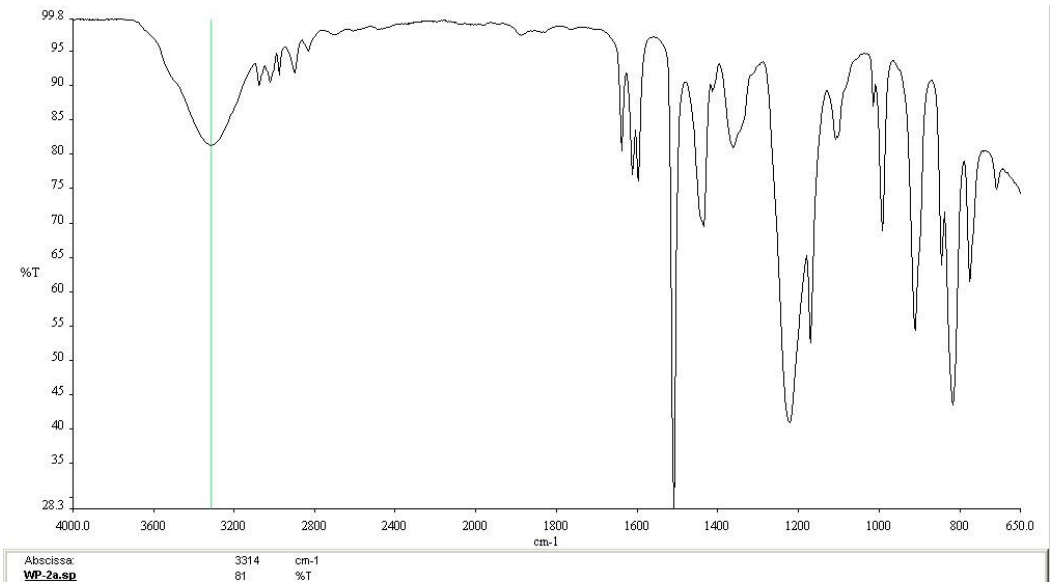

*Figure 12: IR Spectrum of 4-allylphenol, **2a***

The IR spectrum shown in Figure 12 shows a broad O-H peak at 3314 cm^{-1} and C-O stretches at 1220 cm^{-1} and 1180 cm^{-1}. Additionally, there are weak alkane and aromatic C-H stretching peaks between 2800 cm^{-1} and 3150 cm^{-1} and C=C alkene and aromatic peaks at 1600 cm^{-1} and 1650 cm^{-1}.

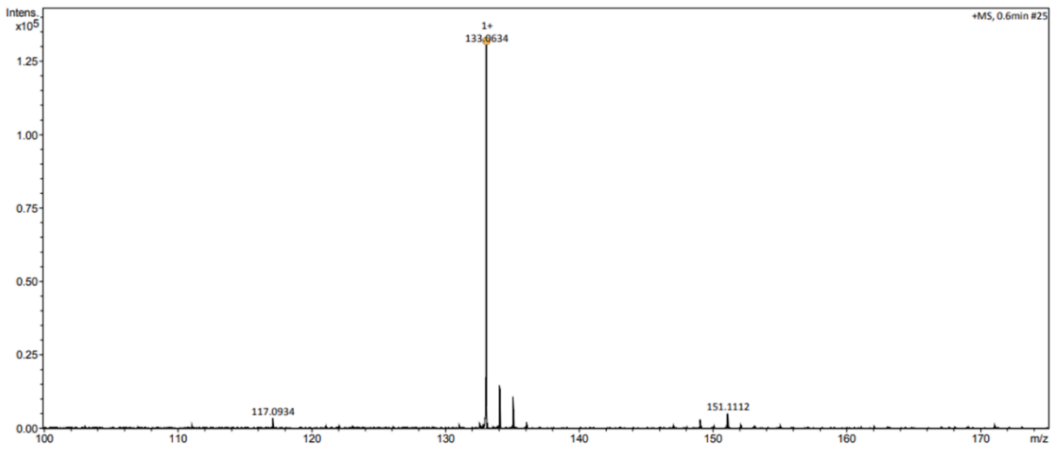

Figure 13: ESI- Mass Spectrum of of 4-allylphenol, ***2a***

It was determined by ESI-mass spectrometry (Figure 13) that the molecular ion peak at m/z 133 matches the predicted mass of **2a**, minus the phenolic hydrogen.

3.2.1- Bromination Side Reaction

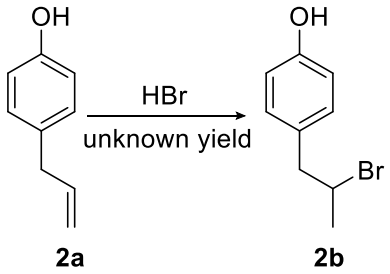

Scheme 4: Proposed scheme for the bromination of 4-allylphenol.

During the demethylation a significant proportion (up to 50%) of the material underwent a further reaction, yielding 4-(2-bromopropyl)phenol, **2b** (Scheme 4). Evidence of this is seen in the ^{1}H-NMR spectrum shown in Figure 14. The cause of this is the use of excess BBr_3 (1.1 equivalents), resulting in 0.1 equivalents of BBr_3 remaining in the reaction mixture after the reaction has run to completion. When the reaction mixture is quenched with water, the remaining BBr_3 reacts with the water to form H_3BO_3 and 3HBr; the HBr then proceeding to brominate the allylic bond to produce **2b** (*Scheme 5*).

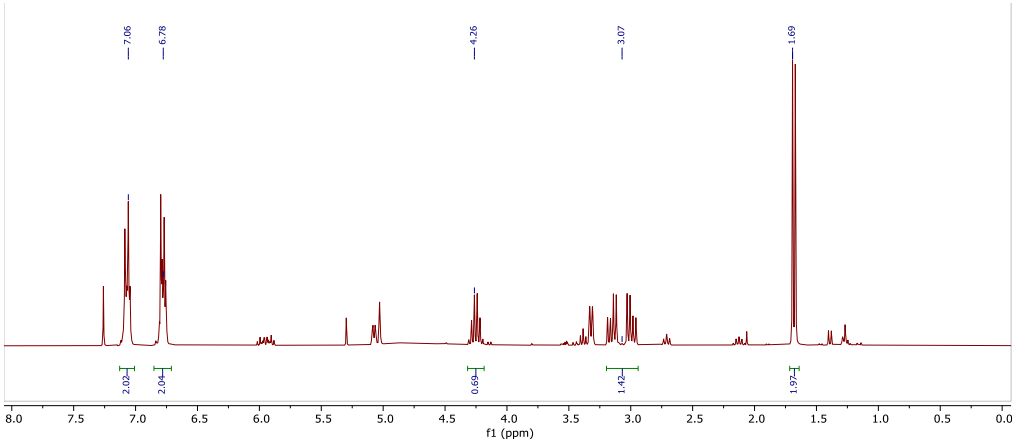

*Figure 14:[1]H-NMR spectrum showing product **2b** produced as a side product during the synthesis of 4-allylphenol, **2a**.*

The identity of compound **2b** was determined by use of ^{1}H-NMR and IR spectroscopy and mass spectrometry. The ^{1}H-NMR spectrum does not contain a peak caused by the phenolic hydrogen; however, the aromatic hydrogens can be seen as two doublets of doublets of doublets at 7.06 ppm and 6.78ppm respectively. The peaks caused by the hydrogens in the propyl chain have been altered by the addition of H-Br across the alkene bond. The terminal CH_3 appears as a doublet at 1.69 ppm, the Br-C-H hydrogen is present as a well resolved sextet at 4.26 ppm and a pair of doublets of doublets at 3 ppm are formed by the CH_2 group.

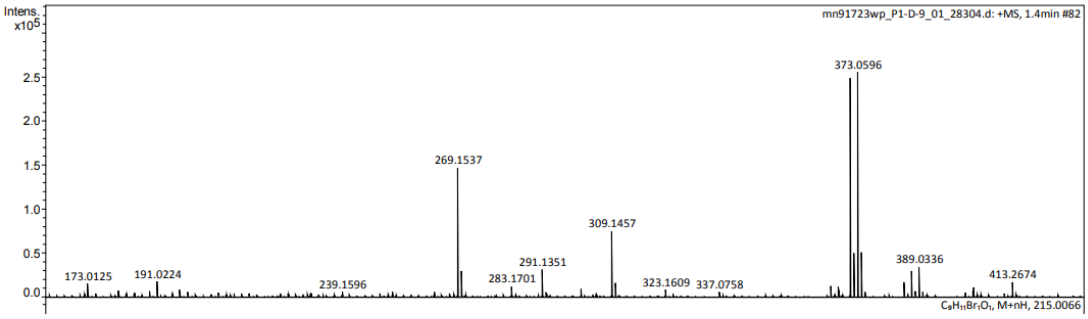

*Figure 15: ESI-Mass Spectrum of **2b***

A peak at the calculated m/z of **2b** (215 au for MH^+) is not seen in the mass spectrum shown in Figure 15. However, the twin peaks at 371 and 373 are characteristic of the

presence of the two isotopes of bromine. These peaks at 371 and 373 correspond to two molecules of **2b**, after the loss of HBr and gaining of one sodium ion.

Figure 16 shows the IR spectrum of **2b** which is similar to that of **2a**. Noticeably, the C=C stretch region at ~1600 peaks cm^{-1} only contains 1 peak, likely an aromatic C=C stretch, with the C=C alkene peak no longer present.

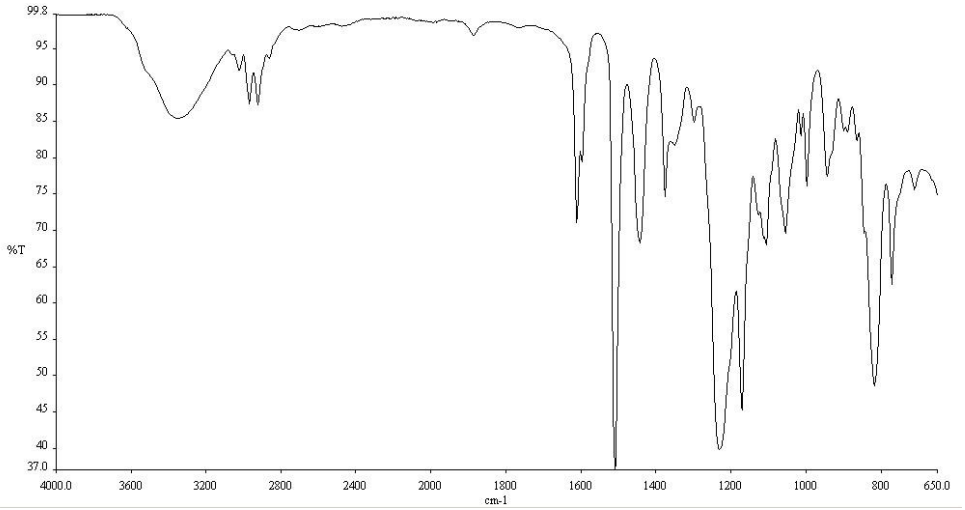

*Figure 16: IR Spectrum of **2b.***

As shown in Scheme 4, the bromination is dependent on the presence of HBr and therefore H_2O. It was assumed that **2a** is brominated to **2b** as the reaction mixture is quenched, rather than the bromination of **1** then demethylation to form **2b**, due to the necessity of the presence of H_2O. Two methods of avoiding the formation of this side product were investigated: precise stoichiometric control over the ratio of **1** to BBr_3 and elimination of the production of HBr during the quench.

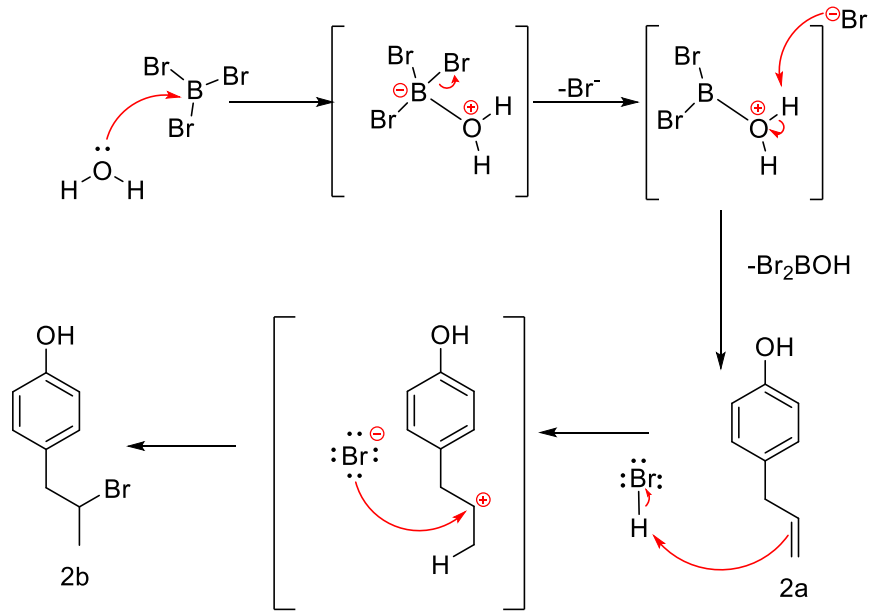

Scheme 5: Proposed mechanism of the bromination of 4-allylphenol

As seen in Scheme 3 the demethylation of 4-allylanisole **1** requires fission of the B-Br bond in BBr_3. As there are three B-Br bonds present in each equivalent of BBr_3, theoretically each of these could be used for demethylation. Therefore, a theoretical minimum stoichiometric ratio of 1:0.33 would be sufficient for this reaction to run to completion and should eliminate the production of any HBr. Hence, reactions were conducted using 5 mmol of **1** and 0.4 equivalents of BBr_3, a theoretical excess. The other reaction parameters were unchanged. Crude conversions are given in Table 3.

Table 3: Crude conversion of demethylations using 0.3 Equivalents of BBr_3

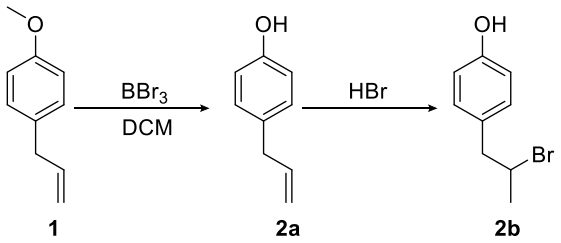

Duration Hours	***1 (%)***	***2a (%)***	***2b (%)***
1	81	10	8.8
3	50	33	17
3 (Hexane)	53	35	10
24 (Hexane)	50	30	20

After reacting for 1 hour (standard conditions), approximately 20% of the starting material had reacted, with 8% then being brominated, indicating that there was remaining BBr_3 in the reaction mixture and therefore that the reaction had not gone to completion. Increasing the duration of the reaction to 3 hours improved the conversion to 50% with 17% becoming brominated. That 50% of **1** had reacted proves that each molecule of BBr_3 can demethylate more than once. However, the presence of **2b** also indicates that there is still active BBr_3 in the reaction mixture. These results were repeated using hexane as the solvent. Hexane was chosen primarily because of the ready availability of BBr_3 in hexane solution but will be discussed further in section 3.2.3-.

It is likely that the first instance of nucleophilic attack of the oxygen to the BBr_3 boron centre occurs much more rapidly than the interaction between a phenolic oxygen and BBr_2OH, which in turn is much more rapid than with $BBr(OH)_2$. When the reaction was conducted for 24 the conversions were almost identical to the 3 hour reaction, suggesting

that this quantity of BBr_3 was unlikely to proceed to any higher conversion in a reasonable timeframe. The presence of **2b** in the reaction mixture and the poor conversion suggests that it is not feasible to prevent the formation of **2b** via stoichiometric control.

The alternative method of eliminating the production of **2b** was quenching with a basic aqueous solution. Initially, an experiment starting with 5 mmol of **1a** and quenching with 20 mL of 1M NaOH, neutralising with 1M HCl then extracting with dichloromethane was carried out. However, **2b** was still present in the crude mixture. This was repeated using 20 mL of 2M NaOH solution with more success, as can be seen in Figure 17, the characteristic peaks of **2b** are entirely absent.

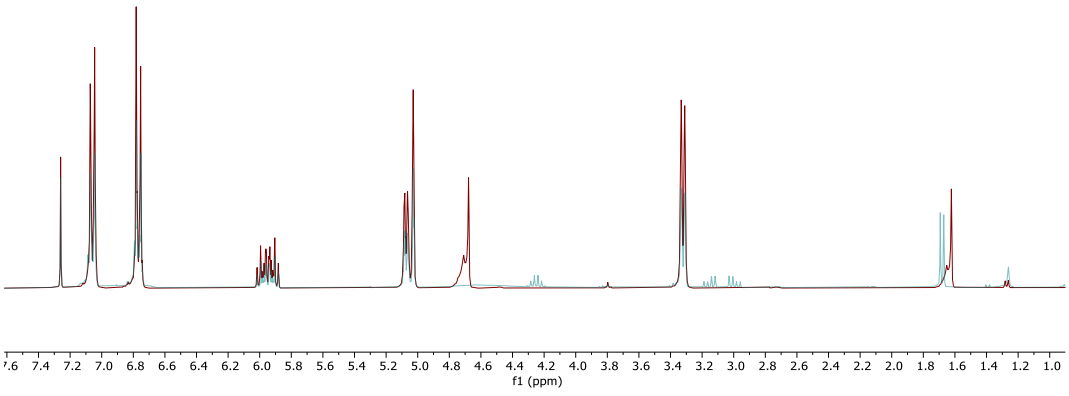

*Figure 17: Crude NMR spectra of a demethylation reaction using a 2M NaOH quench (red) and a standard demethylation (blue). Peaks at 4.25, 3.1 and 1.6 ppm, caused by the presence of **2b** are entirely absent from the red trace.*

This result was verified by repeat testing using the same conditions, but on a larger scale, with identical results. Interestingly, the peaks at 4.69 ppm and 1.63 ppm were present in both runs of this experiment and were not removed during purification. However, the peaks relating to product, as described previously, are unchanged. The isolated yield of this modification was 88%, slightly higher than that obtained via the water quench, but short of the >99% conversion indicated by the crude NMR spectrum.

3.2.2- Purification and Telescoping

For the initial attempts of this reaction, purification of the product was achieved by column chromatography using ~50g of silica, eluting with 1:9 EtOAc: hexane. This column was efficient for separating the products **2a** and **2b** from **1**. However, the major by-product **2b** had a similar retention factor to **2a** under these conditions, causing the two products to co-elute. This raised the question of the necessity of purifying the reaction mixture at this stage, as any remaining **1** would not undergo the *ortho*-formylation, and while both **2a** and **2b** would react, they might be more easily separated later in the synthesis. Hence, optimisation at this stage was deemed unnecessary and the purification step was eliminated, allowing the reaction to be telescoped to the subsequent *ortho*-formylation. Eliminating this chromatographic purification is a major advantage, as it significantly reduced both the time and environmental cost of the synthesis.

3.2.3- Alternative Solvents

Experimentation was also conducted into carrying out this reaction with alternative solvents. Literature precedent had used dichloromethane with good results; however, this presents difficulties from a green chemistry perspective. Chlorinated solvents should be avoided wherever possible due to the potential health risk and the environmental and financial cost of processing the waste.

Investigations into alternative solvents were directed by which BBr_3-solvent systems were commercially available. At the time of investigation only a BBr_3 hexane solution was readily available but proved to be an effective solvent to use in this system. Used in equal volumes in place of dichloromethane, the crude conversion and isolated yield of the demethylation was not affected by the change. The reaction could also be conducted in a hexane, dichloromethane mixture with no adverse effects, however, in this case, it must

be noted that the aqueous work-up was made problematic as the density of the mixture was not different enough from water to separate effectively. Throughout this project, this reaction was performed either in dichloromethane, hexane, or a mixture thereof, depending on the availability of BBr_3.

3.2.4- Green Chemistry Analysis

Under the original conditions, this reaction had a 24.8% atom economy. This value has been calculated without considering the production of **2b**, if included the atom economy shrinks to 22.9%. This value also excludes the use of solvent, eluent and silica used in this reaction. This poor performance is mainly a result of the use of highly brominated species in the 1.5 equivalents of BBr_3 producing high amount of brominated wate in the form of MeBr and BBr_2OH.

$$\%\ Atom\ economy = \frac{Mass\ of\ atoms\ in\ desired\ product}{Mass\ of\ atoms\ in\ all\ products}\ x\ 100$$

$$\%\ Atom\ economy = \frac{134.28\ gmol^{-1}}{134.18\ gmol^{-1} + 94.94\ gmol^{-1} + 187.63\ gmol^{-1}}\ x\ 100 = 32.3\%$$

With the modifications developed for this reaction, the atom economy rises back to 32.2%. Given the nature of this reaction, being a demethylation, the atom economy is inevitably poor, however the elimination of the production of **2b**, the necessity of purification and the reduction of BBr_3 equivalents have all been beneficial for the environmental impact of this reaction.

The work conducted on this reaction fulfils several other of the PoGCs, namely the prevention of waste, investigation of safer solvents, the use of renewable feedstock and the reduction of derivatives. A key area that could be investigated further with this

reaction is reducing the energy cost of thermal control, an area which was not investigated in this project.

E-factor analysis can be applied to this reaction, though this analysis may be contentious depending on what is classified as a waste product during the reaction. Taking the "Worst-case-scenario" and classifying all material other than product **2a** as waste, including silica, solvents, and all by products a E-factor of 619.2 is obtained.

$$E\ Factor = \frac{Total\ Mass\ of\ Waste}{Total\ Mass\ of Product}$$

$$= \frac{99.09\ g\ (CH_2Cl_2) + 90\ g(H_2O) + 50g\ (silica) + 400g\ (eluent) + 3.64\ (chemical\ waste^*)}{1.038}$$

$$EFactor\ = 619.2\ (chemical\ waste = all\ by\ products\ and\ drying\ agents)$$

The relevance of this is highly dependent of the categorisation of waste; for example, if one assumes solvent and water used can be recovered then the E-Factor falls to 244.4, if one deems silica as a re-processable resource or, as in the case of this research eliminates the need for purification, then the E-factor rests at 3.51. This ambiguity in measuring E-factor limits its usefulness as a measurement and prevents it from painting a comprehensive picture of the environmental cost of a reaction. It also fails to account for the type of waste produced, in this case the halogenated MeBr and BBr_2OH side products pose a higher environmental cost to process than the solvent, waste water and silica, despite contributing less to the E-Factor value.

The key metric that could be employed in assessing the environmental impact of this reaction (and entire scheme) is life cycle analysis. This analysis is a comprehensive study into the environmental cost of producing a product, taking into account the cost of producing each element from the raw starting material and the cost of processing all of the waste produced. It also includes the environmental impact of using the product and

disposing of it at the end of its life cycle. LCA is not a trivial study, though further work on this project would benefit fit from it.

3.3- *ortho*-Formylation

The formation of 2-hydroxy-5-allylbenzaldehyde **3a** was achieved via the *ortho*-formylation of 4-allyphenol, **2a** (Scheme 6). This technique is well known in our research group and was easily applied to this substrate. To achieve suitable reaction times, a large excess (10 equivalents of paraformaldehyde, 2.5 equivalents of $MgCl_2$ and 4 equivalents of Et_3N) were used.[102]

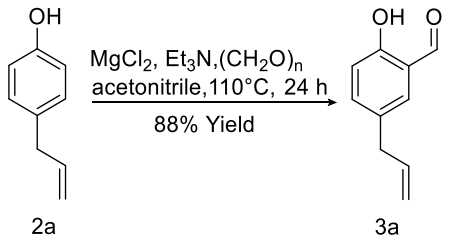

*Scheme 6: Synthesis of 2-hydroxy-5-(2-bromopropane) benzaldehyde **3b** is not produced in this reaction.*

The proposed mechanism is shown in Scheme 7, this demonstrates why it is not necessary to purify after the demethylation of 4-allylanisole, as the *ortho*-formylation mechanistically requires the phenolic OH to proceed, therefore any remaining 4-allylanisole will not react.

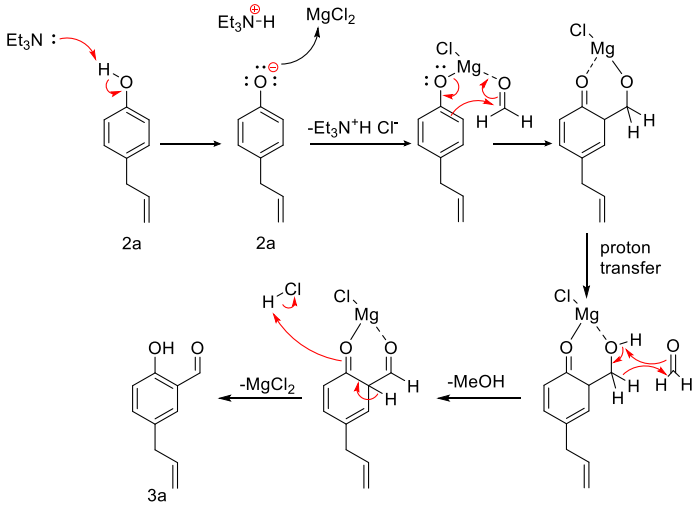

Scheme 7: Mechanism of orthoformylation of 4-allylphenol.

This reaction proceeds without producing any additional products. That is to say that it does not produce the double formylated product at all, as the aldehyde group strongly deactivates the phenol ring. Additionally, when the crude product of the demethylation was used, the theoretical ortho-formylated product of **2b**, 2-hydroxy-5-(2-bromopropane) benzaldehyde **3b** was not observed in any of the experiments undertaken (Scheme 8). Mechanistically it is not clear why **3b** is not formed, it is possible that the presence of the bromine deactivates the species, reducing the rate of reaction further. This could be investigated by direct inspection using **2b** and larger equivalents of $MgCl_2$, Et_3N and paraformaldehyde, or increased temperature or reaction durations.

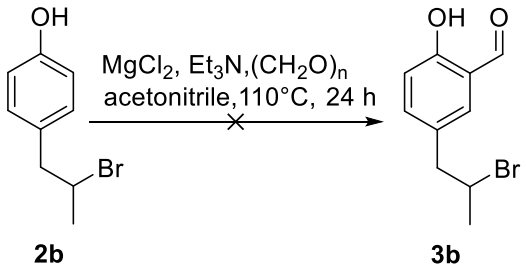

*Scheme 8: 2-hydroxy-5-(2-bromopropane) benzaldehyde **3b** is not produced in this reaction.*

Characterisation of **3a** was accomplished through a combination of ^{1}H-NMR, ^{13}C-NMR, IR spectroscopy and ESI mass spectrometry. The ^{1}H-NMR spectrum can be seen in Figure 18. The phenolic hydrogen resolves as a sharp peak at 10.9ppm, this is characteristic of phenolic hydrogens ortho to aldehyde groups, as there is an intramolecular hydrogen bond between the phenolic hydrogen and the carbonyl oxygen, forming a pseudo-6-membered ring, and limiting the rotational freedom of the hydrogen. At 9.98ppm, a peak corresponding to the aldehyde hydrogen can been seen as a sharp singlet. Within the aromatic region, two multiple peaks appear, at 7.38 and at 6.95ppm. The peaks corresponding to the hydrogens on the propenyl chain remain unchanged from **2a**.

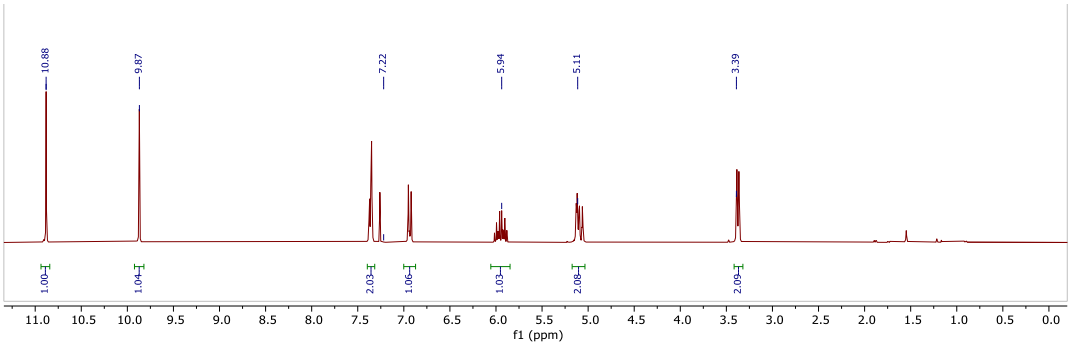

*Figure 18: [1]H-NMR spectrum of 2-hydroxy-5-allylbenzaldehyde **3a***

The [13]C-NMR spectrum (Figure 19) contains further proof of the successful *ortho*-formylation with the addition of a singlet at 196.5 ppm, which is typical for aldehyde carbons. The additional substituent on the aromatic ring has removed the symmetry of the ring, and therefore the individual carbons can be differentiated. The aromatic aldehyde peak appears at 196.5 ppm. The phenolic carbon can be seen at 160.1 ppm. Five aromatic peaks can be seen, alongside two alkene peaks between 137.6 ppm and 116.4 ppm. The alkane carbon can be seen at 38.8 ppm

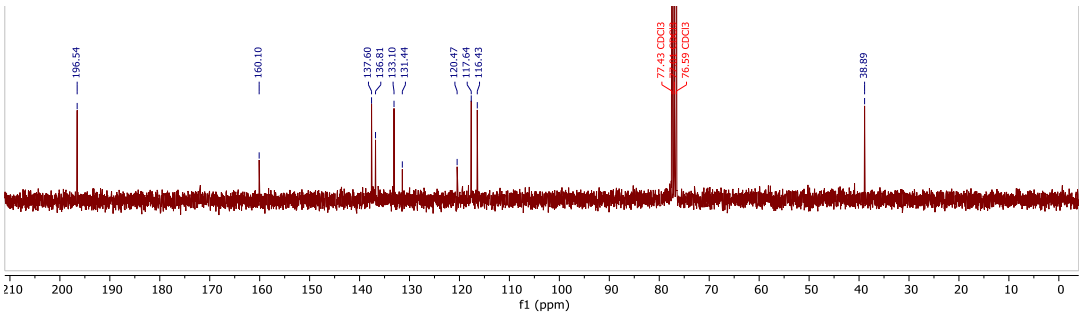

*Figure 19: [13]C-NMR spectrum of 2-hydroxy-5-allylbenzaldehyde **3a***

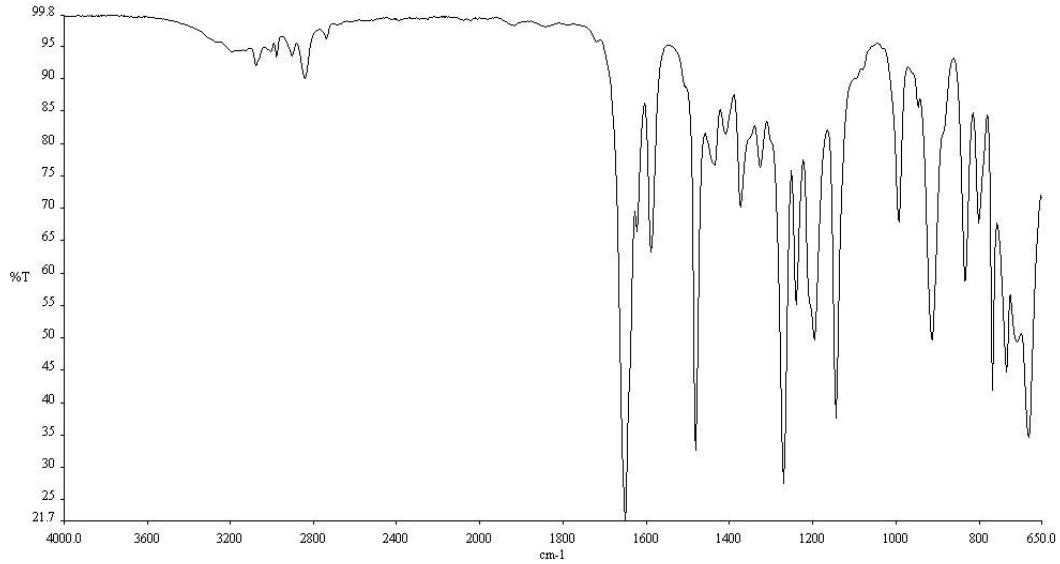

*Figure 20: IR Spectrum of 2-hydroxy-5-allylbenzaldehyde **3a***

The spectrum shown in Figure 20, contains a strong C=O stretching peak at 1650 cm^{-1}, overlapping with a C=C stretch at 1590 cm^{-1}. The broad O-H peak seen in Figure 12 has been greatly supressed, this is likely due to the pseudo- 6-membered ring formed by the hydrogen bonding interaction between the phenolic hydrogen and the oxygen on the aldehyde. The negative ion mode ESI Mass Spectrum of **3a (** Figure 21), contains further proof of the identity of this species. The large signal at 161 m/z arises from the ionised form of **3a** (lacking a hydrogen).

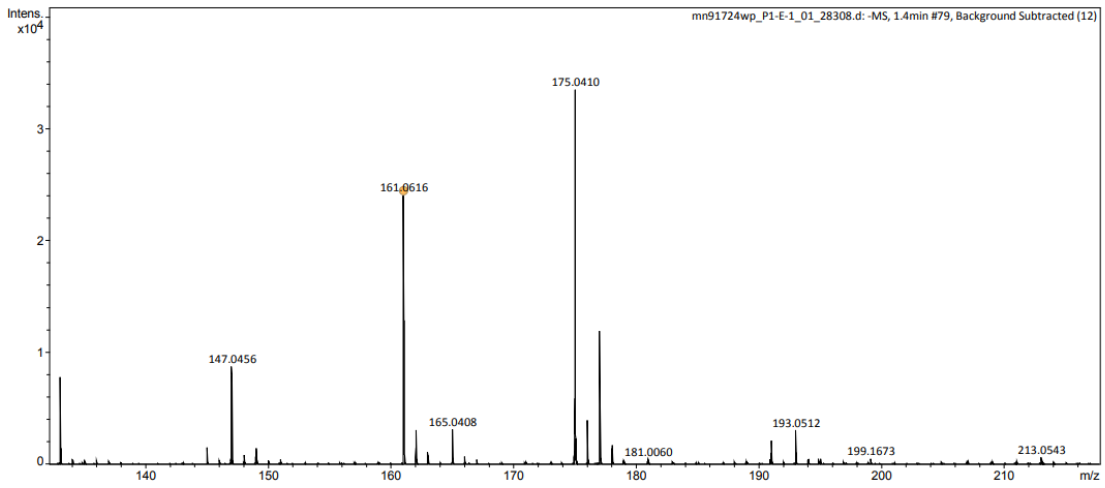

*Figure 21: ESI Mass spectrum of 2-hydroxy-5-allylbenzaldehyde **3a***

The purification of this product was achieved via column chromatography using 50g of silica, eluting with Pet-Ether-(40/60) 15:1 EtOAc. It was necessary to purify at this stage, as it was unknown what effect **2b** would have on the hydrosilylation. Additionally, any unreacted **1** would undergo hydrosilylation, then become more problematic to separate. This purification method proved to be effective for the separation of **3a** from both **1** and **2b**, with little overlap of the fractions. The necessity of this purification step is frustrating, as it reduces the overall yield of the scheme, and adds a time and environmental cost that could be avoided.

Another drawback of this reaction is the poor rate of reaction, large excesses of Et_3N, paraformaldehyde and MgI_2 are required to reduce the time required for this reaction to under 24 hours. The reaction must also be heated to reflux at 110 °C for the full duration. These factors result in high material and energy cost, increasing the environmental impact of this synthesis.

3.3.1- Green Chemistry Analysis

The atom economy of this reaction is surprisingly high at 83.5%. This is a result of there only being one by-product of this reaction- MeOH, the large excess of reagents used do not formally contribute to the Atom economy.

$$\%\ Atom\ economy = \frac{Mass\ of\ atoms\ in\ desired\ product}{Mass\ of\ atoms\ in\ all\ products}\ x\ 100$$

$$\%\ Atom\ economy = \frac{162.19\ gmol^{-1}}{162.19\ gmol^{-1} + 32.04\ gmol^{-1}}\ x\ 100 = 83.5\%$$

As atom economy is unable to take full account of the waste produced E-Factor analysis can be used, though it must be sated that the aforementioned criticism of E-fact analysis still stands. A value of 1053.1 is obtained when taking eluent, solvents, silica and all waste into account.

$$E\ Factor = \frac{Total\ Mass\ of\ Waste}{Total\ Mass\ of Product}$$

$$= \frac{117.3\ g\ (solvent) + 130.4\ g(H_2O) + 35\ (silica) + 400g\ (eluent) + 10.42\ (chemical\ waste^*)}{1.102}$$

$$E\ Factor\ = 1053.1\ (chemical\ waste = all\ by\ products, excess\ SM\ and\ drying\ agents)$$

It is necessary to purify the product due to the large excess of reagents is causes a large mass of waste silica, solvent, and eluent therefore a 'best case scenario' is hard to determine. It may be feasible to reduce or recycle the solvent, however this was not accomplished through the duration of this research. Taken together the atom economy and E-factor provide some indication of the environmental impact of this reaction, the poor E-factor analysis would appear to be quite damming, however this is a result of poor reaction kinetics rather than an inherently wasteful reaction, as demonstrated by the atom economy. Both methods of evaluating this procedure also fail to take into account the energy cost of producing the high temperatures for extended duration required by this procedure, additionally neither account for the wastewater used in condensers and rotary evaporators which is not insignificant.

3.4- Synthesis of 2-hydroxy-5-(3-triethoxysilylpropyl) benzaldehyde

Production of 2-hydroxy-5-(3-triethoxysilylpropyl)benzaldehyde **4a,** is a key step in this reaction scheme, as it is the incorporation of the silyl-group that facilitates the immobilisation of the ligand onto silica. The method chosen to produce **4a** was the hydrosilylation of 2-hydroxy-5-prop-2-enylbenzaldehyde **3a**, following a method reported by Amarasekara *et al*. using a similar substrate,[103] (Scheme 9). This method utilised a heterogeneous PtO_2 catalyst (1 mol%) and equimolar amounts of **3a** and triethoxysilane. The reaction mixture was heated to 80°C in a sealed glass vial and stirred for 24 hours. This method did produce **4a**, with an isolated yield of 35% with the structure confirmed by ^{1}H-NMR (Figure 22).

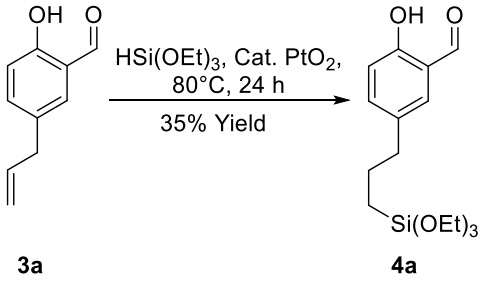

Scheme 9: Reaction scheme of the Hydrosilylation of 2-Hydroxy-5-prop-2-enylbenzaldehyde

The ^{1}H-NMR spectrum of **4a** is shown in Figure 22 This material is easily differentiated from **3a**, by the loss of the alkene hydrogen peaks, replacing them are a triplet at 0.57 ppm (*J=8.1 Hz*) corresponding to the terminal CH_2 of the propyl chain, and a triplet of triplets at 1.72 ppm (*J= 8.1, 7.6 Hz*) forms corresponding to the hydrogen on carbon 2 of the propyl chain. These assignments, as well as the triplet at 2.56 ppm (*J= 7.6 Hz)* assigned to carbon 1 were confirmed by the ^{1}H-COSY NMR, shown in Figure 25. The ethoxy groups attached to the silicon can also be observed with the CH_2 appearing as a

well resolved quartet at 3.80 ppm (*J= 6.9 Hz*) and the terminal CH_3 as a triplet at 1.1ppm (*J= 6.9Hz*). The aldehyde, and phenolic hydrogens peaks remain unchanged, as do the peaks caused by the aromatic hydrogens.

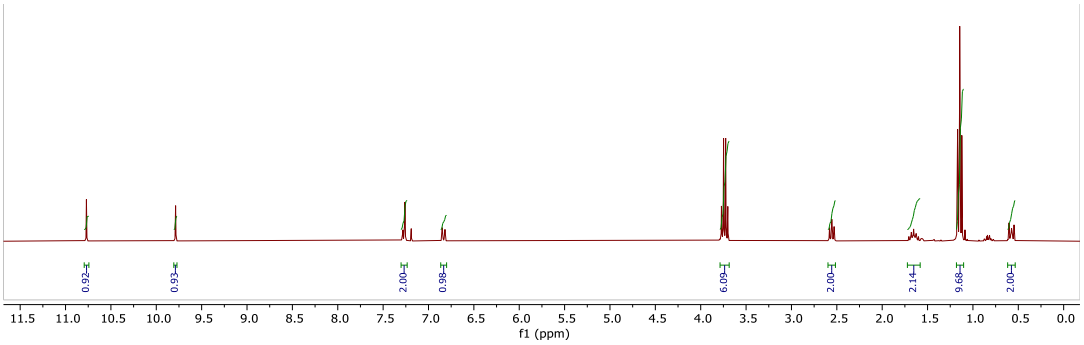

Figure 22 [1]H-NMR of 2-hydroxy-5-(3-triethoxysilylpropyl) benzaldehyde

Initial attempts at this procedure using **3a** were conducted thermally, using 200 mg of sample. It was found that **3a** is a substantially less active substrate for this reaction than the related material used in the literature, with the reaction only producing an isolated yield of 35%, far short of the 100% yield reported by Amarasekara *et al*.[103]

The crude 1H-NMR spectrum of this reaction shown in Figure 23, indicated that **4a** was the major product, certainly higher that 35% of the product, but showed signs of multiple other materials being present. The low isolated yield also indicated that there was a significant amounts of product **4a** being lost during the purification process.

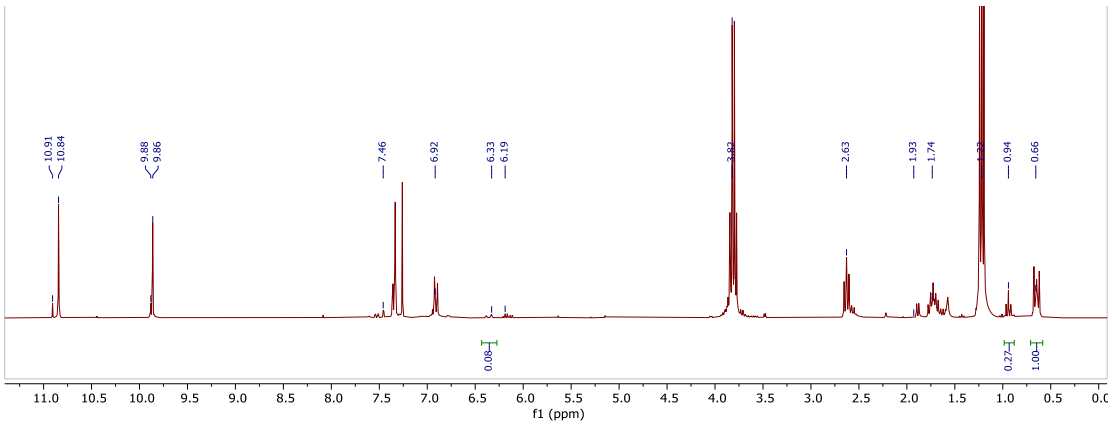

Figure 23: Crude [1]H-NMR of hydrosilylation reaction of 3a, conducted thermally.

3.4.1- Purification.

Initially, purification of **4a** was achieved by flash chromatography using a 12g silica column, eluting with petroleum ether 40-60/ EtOAc (15:1). This method was quickly abandoned as less than half of the crude mass of product was recovered. The fate of the lost material is unknown, it is likely that it is binding to the silica, either precipitating out of solution or otherwise being rendered immobile. Flushing the columns with pure EtOAc did not yield any more material. Following this discovery, it was decided to proceed without purification at this stage, and effort was instead placed on finding the optimal conditions for the primary pathway, eliminating, as much as possible, the formation of by-products and reducing the need for purification.

3.4.2- Isomerisation

Evidence of an internal isomerisation of the allylic bond from position 2 to position 1 of the propyl group to form 2-hydroxy-5-prop-1-enylbenzaldehyde, **3c** (Scheme 10), was observed in the ^{1}H-NMR of the crude product (Figure 23 and Figure 24). The characteristic multiplet of the alkene hydrogen on position 2 of the propyl chain of **3a** at 5.94 ppm is entirely absent, indicating full conversion to products has occurred. However, multiplets at 6.35ppm and 6.15ppm respectively are strong evidence for the existence of

two alkene hydrogens attached to carbons 1 and 2 in the propyl chain. This indicates that, whilst no **3a** remains, the hydrosilylation had not gone to completion and an internal alkene isomerisation had occurred. The terminal CH_3 of **3c** can also be seen as a doublet at 1.8ppm . Due to the difficulty in purifying these materials this species was not isolated from the reaction mixture.

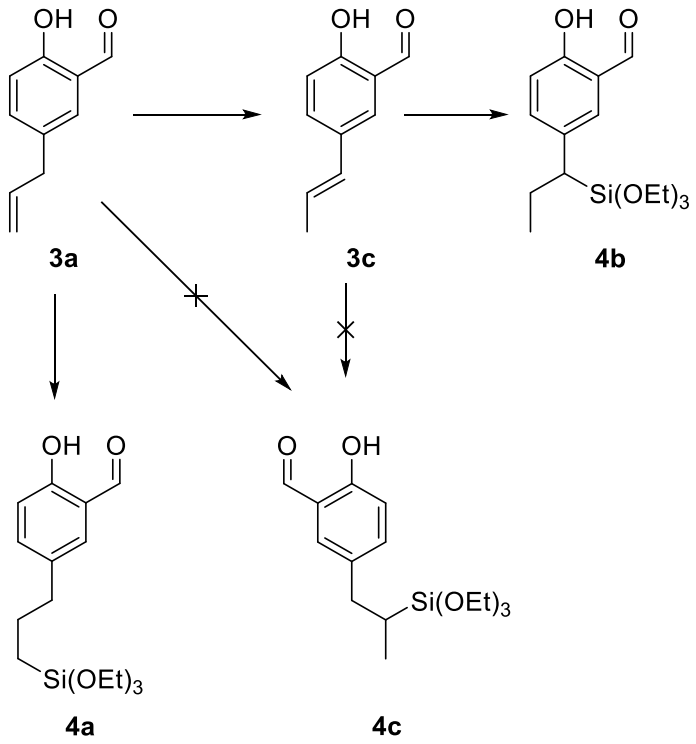

Scheme 10: Modified hydrosilylation reaction scheme

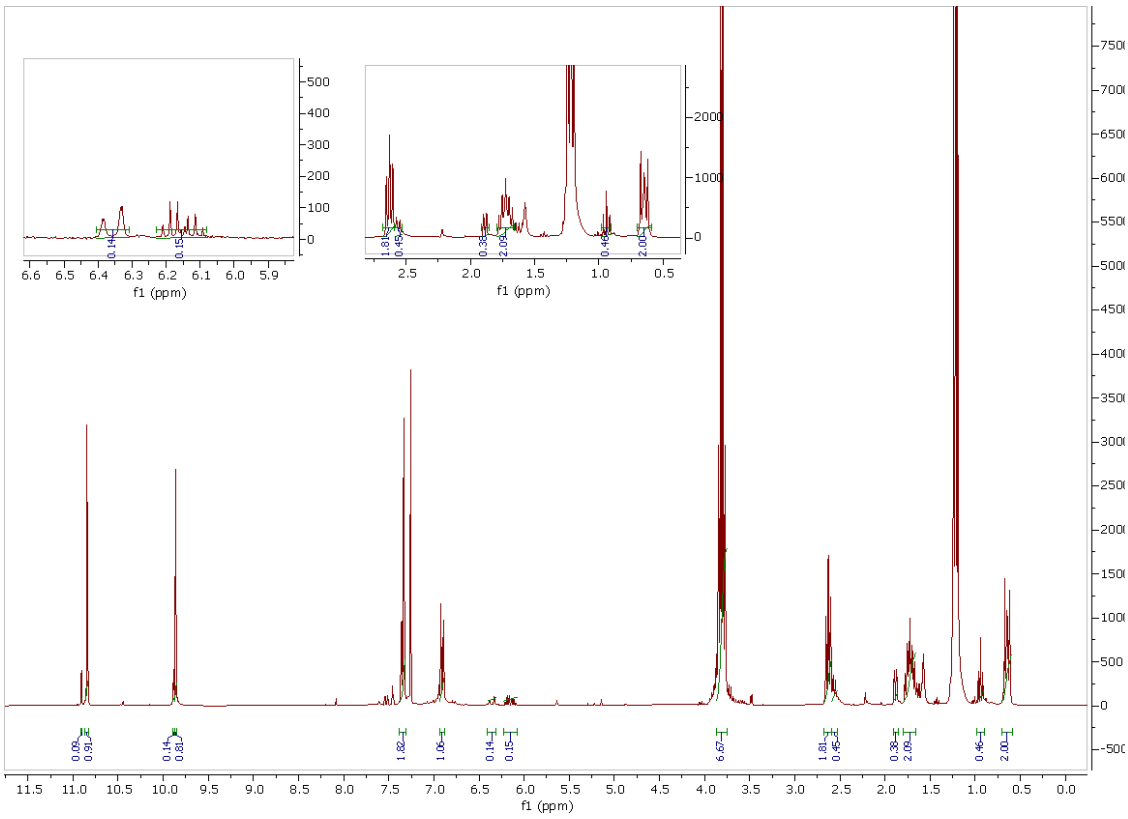

Figure 24: ^{1}H-NMR spectra of 2-Hydroxy-4(3-silyl-propyl)-Benzaldehyde

Within the spectra in Figure 24 a triplet at 0.9 ppm can be seen. The origin of this peak was initially unclear. However, a ^{1}H-COSY-NMR spectrum, Figure 25 showed coupling between this peak and a quartet, which is almost completely hidden underneath the CH_2 peak from carbon 2 in the propyl chain of product **4a**. The COSY analysis also showed the existence of another quartet, almost hidden under the CH_2 of carbon 1. The coupling patterns and chemical shifts of these three peaks match those expected from 2-hydroxy-5-(3-triethoxysilylpropyl)benzaldehyde, **4b,** a hydrosilylation product of **3c**.

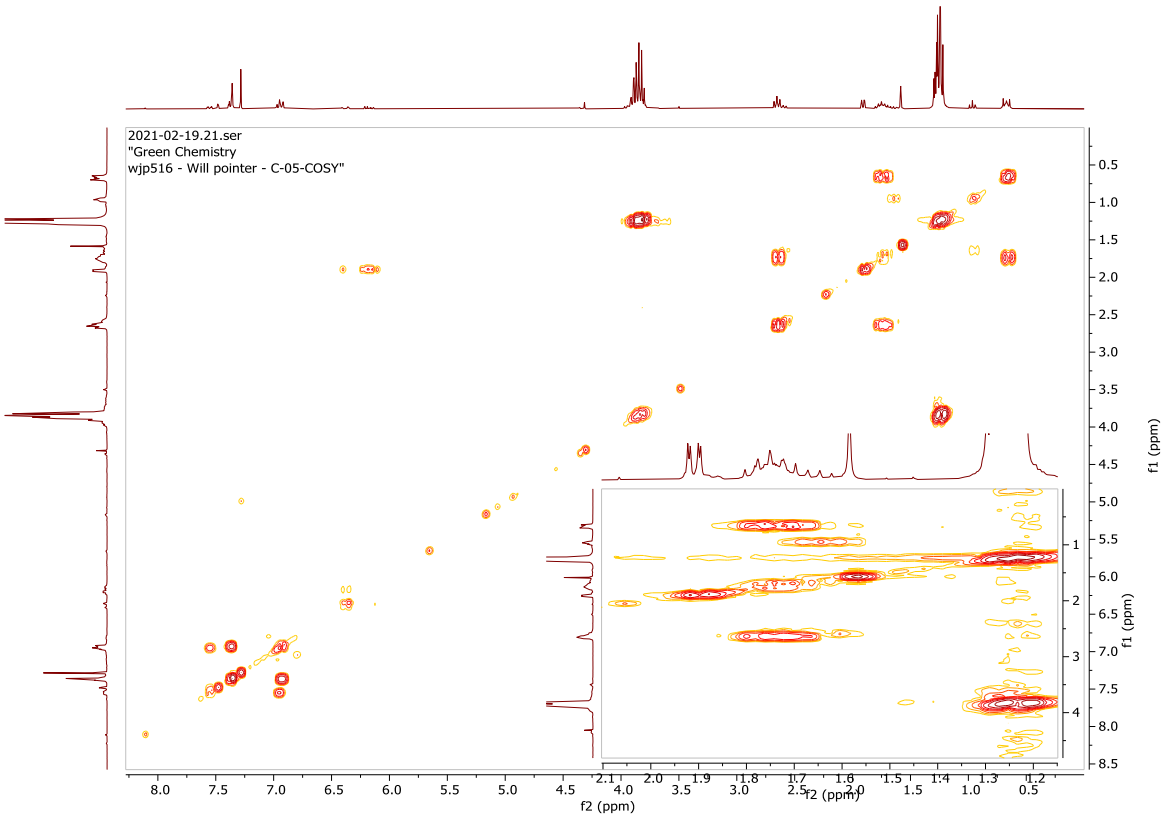

Figure 25: 1H COSY -NMR of the crude hydrosilylation reaction

These results were reproducible, giving a reasonable level of confidence in a modification to the reaction scheme, see Scheme 10. This model shows the isomerisation of **3a** to **3c,** and the hydrosilylations to form **4a** and **4b**.

Whilst this proposed model is theoretically sound there are a number of issues; firstly **3c** was never observed in large enough quantities to isolate, and therefore characterise, and attempts at forcing the isomerisation were unsuccessful. Therefore, its existence is not above question. Secondly, there is no evidence of the presence of 2-hydroxy-5-(2-triethoxysilylpropyl)benzaldehyde **4c,** which should be a possible product of the hydrosilylation of both **3a** and **3c**. This could suggest >99% anti-Markovnikov selectivity of the PtO_2 catalyst for **3a** and >99% Markovnikov selectivity for **3b**, which seems dubious. However, no other model produced explained the observe results of forming both **4a** and **4b** under the conditions used. Characterisation of both **4a** and **4b** was

achieved using a combination of ^{1}H-NMR (Figure 22), ^{13}C-NMR (Figure 26) and ESI Mass Spectrometry (Figure 27).

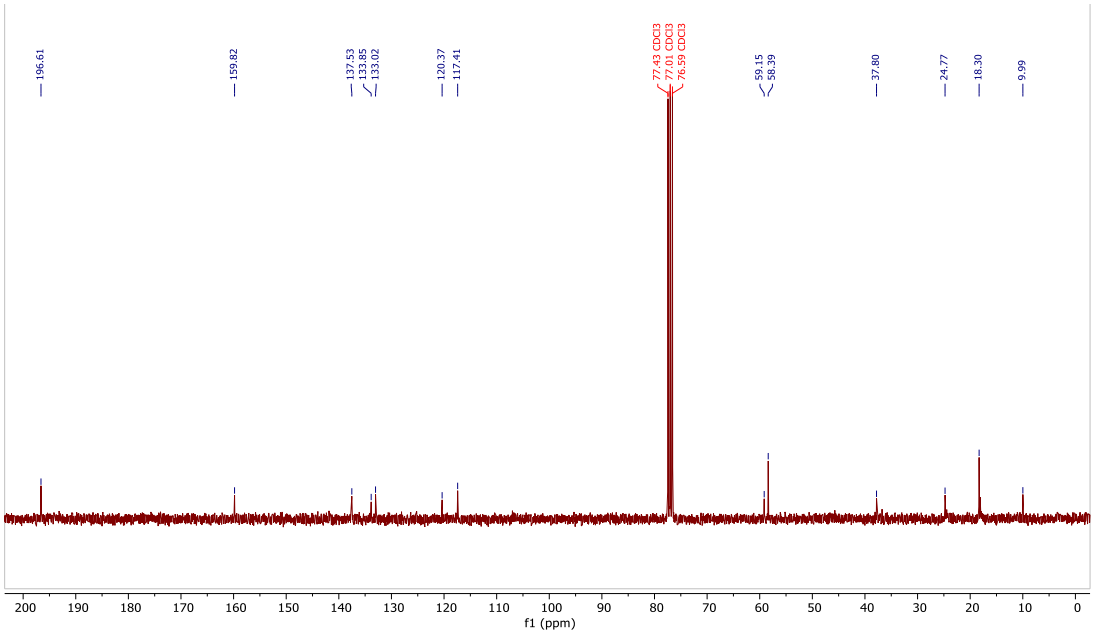

*Figure 26: 13C-NMR spectra of a mixed sample of **4a** and **4b.***

The ^{13}C-NMR of the **4a**/**4b** mixture (Figure 26), contains the aldehyde carbon peak at 196 ppm, seen in the ^{13}C-NMR of **3a**, the phenolic carbon, seen at 159 ppm, and 5 aromatic carbons between 117 ppm and 137 ppm. The alkene carbons peaks seen in Figure 19, are no longer present, instead there are an increase in the number of alkane carbon peaks between 9 and 60 ppm, as there are two structural isomers present each isomer has a unique return for each carbon position.

Figure 27 add further characterisation for **4a** and **4b**, the molecular ion peak is present at 349.1448 m/z correlating to the formular $C_{16}H_{26}O_5SiNa$ or the $[M+H+Na]^+$ ion.

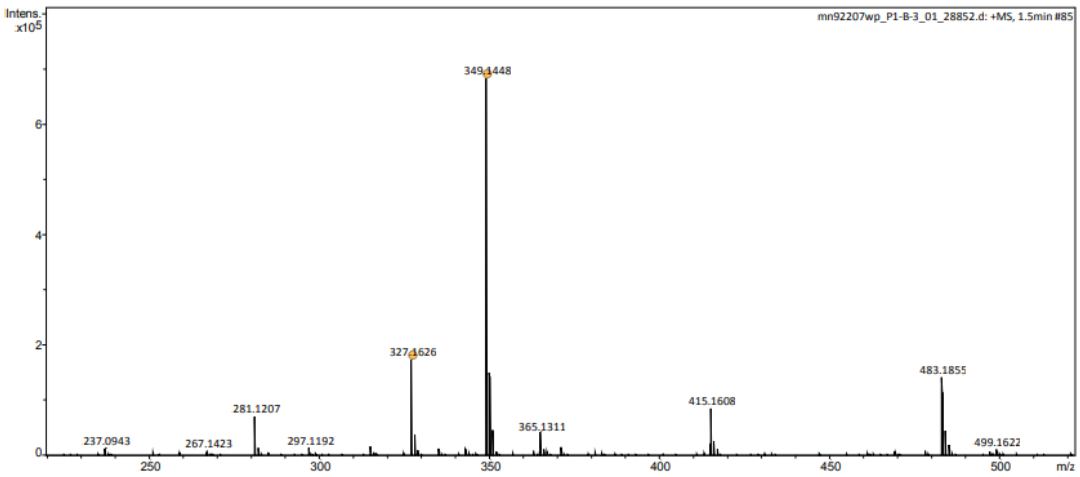

*Figure 27: ESI Mass Spectrum of of a mixed sample of **4a** and **4b.***

3.4.3- Microwave Study

Investigations were conducted into carrying out this reaction under microwave irradiation rather than thermally. An initial experiment was conducted using a CEM-Discover microwave with conditions as close to those used in the thermal reaction as was reasonably practicable. The initial test was set to 80°C for 10 minutes with the microwave power set to 100W. The results of this reaction were highly promising, the crude ^{1}H-NMR spectrum showed 66% conversion to **4a,** 22% to **3b** and 11% to **4b** with no **3a** remaining. These results are very similar to the result obtained under the conditions previously used, however the time reduction and lower energy usage are highly advantageous.

However, these results are not to be entirely relied upon. The method used on the microwave allowed full power to be used while ramping to temperature with the result that the sample tended to overshoot the maximum temperature by 10-25°C for anywhere up to 5 minutes.

A series of experiments were carried out using a blank. Power setting were reduced until an acceptable trade-off between ramp-rate and maximum overshoot temperature was reached. Detailed results can be found in appendix T1. A power setting of 80W was found to produce a ramp time of less than 48 seconds and would not overshoot 80°C by more than 2°C. Herein, a power setting 80W will have been used unless otherwise stated. Results from the first round of microwave testing, along with the result from the initial test are shown in Table 4. Without the maximum temperature being overshot, there is a dramatic reduction of all rates of reaction.

Table 4: Product composition from the initial round of Microwave testing.

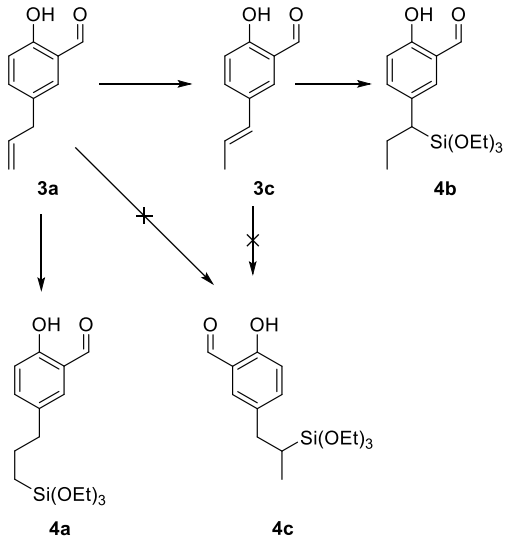

Exp Nu.	Temp /°C	Time (Min)	3a %*	3c%*	4a%*	4b%*
5B	80[a]	10	-	22	66	11
6E	80	10	72	6	19	3
7C	80	30	21.9	11.5	57	9
7D	80	60	-	19	65	15

*-Percentages calculated from ^{1}H-NMR integration ratios.

Investigations into the temperature dependency of the rate of reaction were undertaken with the results shown in Table 5. The rate of both routes of reaction drops significantly below 60 °C, however the presence of **4b** indicates that the hydrosilylation of **3c** has a lower activation energy than the isomerisation of **3a**. A temperature of 60 °C appears to be the lowest active temperature. There is no obvious difference in the distribution of the products when comparing the reactions at 60°C and 80°C, indicating that this difference is not large enough to affect the competing reaction rates.

As the minimum temperature for this system is 60 °C, this was selected for the lower energy costs. All **3a** is reacted between 45 and 60 minutes, with **4a** being the primary product, It can also be concluded that the hydrosilylation of **3b** occurs significantly slower than the hydrosilylation of **3a**, likely due to the steric hindrance from the proximity to the

aromatic ring. The isomerisation of **3a** to **3c** is seen to be temperature dependent regarding the forward direction,

The reaction was also conducted at 100°C, and 120°C. This was undertaken on the basis of the high conversion to **4a** seen in the experiments where the temperature was overshot. However, when carried out in a controlled manner, the levels of conversion seen previously were not replicated.

At 120 °C for 10 minutes, the isomerization pathway outcompeted the direct hydrosilylation route with the total percentage of isomerisation products surpassing 50%, however when the temperature was raised further to 140°C, the direct hydrosilylation to **4a** once again became the primary route, with the isomerisation products falling back below 40%.

Table 5: Results from microwave investigations of the hydrosilylation of 3a

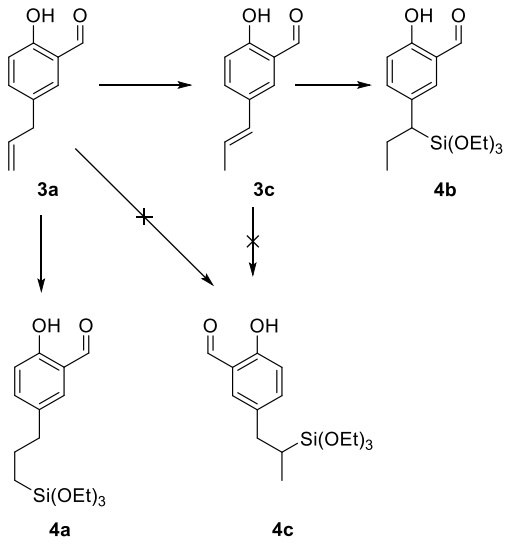

Exp Nu.	Temp °C	Time (mins)	3a % remaining	3b% conversion	4a % conversion	4b% conversion
6e	*80*	*10*	*72*	*6*	*19*	*3*
7c	*80*	*30*	*21.9*	*11.5*	*57*	*9*
7d	*80*	*60*	*-*	*19*	*65*	*15*
8a	*60*	*60*	*-*	*17*	*69*	*14*
9a	*50*	*60*	*87*	*0*	*9*	*3.15*
9b	*40*	*60*	*90*	*0*	*5.3*	*3.7*
8b	*100*	*3*	*58*	*10*	*27*	*3.7*
9c	*100*	*6*	*50*	*12*	*34*	*3.4*
9d	*100*	*12*	*22.2*	*19.3*	*55*	*4.8*
9e	*120*	*6*	*30.8*	*19.6*	*44*	*5.5*
10b	*120*	*10*	*-*	*15.2*	*49.3*	*35.5*
10c	*140*	*10*	*-*	*8.6*	*61.7*	*29.6*

3.4.4- Acid/ Base Selectivity.

Experimentation on the effect of conducting this reaction under acidic and basic conditions were attempted, with the results shown in Table 6:. Under basic conditions, after the addition of 0.1 ml of triethylamine (50 Mol %), the reaction went to completion and produced product **4b** with 100% selectivity. The ^{1}H-NMR and ^{1}H-COSY NMR are

shown in Figure 28 and Figure 29. Triethylamine was chosen as an additive for this reaction for being a weak organic base and being readily available in the lab. A weak base was chosen primarily as the effect of including any additive was unknown. A systematic series of experiments using a variety of bases; both strong and weak; would be valuable to this research

Table 6: crude Hydrosilylation conversions using additives to the microwave method.

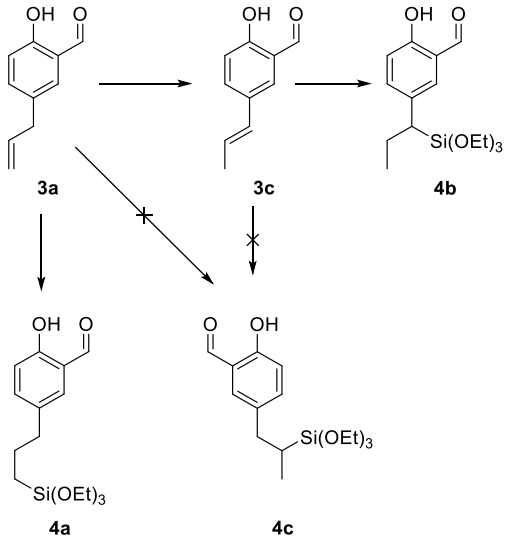

Exp	Additive	3A %	4A %	3C%	4B%
8a	-	-	69	17	14
10-E	0.1 ml Et_3N	-	-	-	>99%
10-H	0.1 ml Et_3N	-	-	-	>99%
10-F	0.1 ml Acetic acid	-	74	11	15
10-I	0.1 ml Acetic acid	-	81.9	<1	18

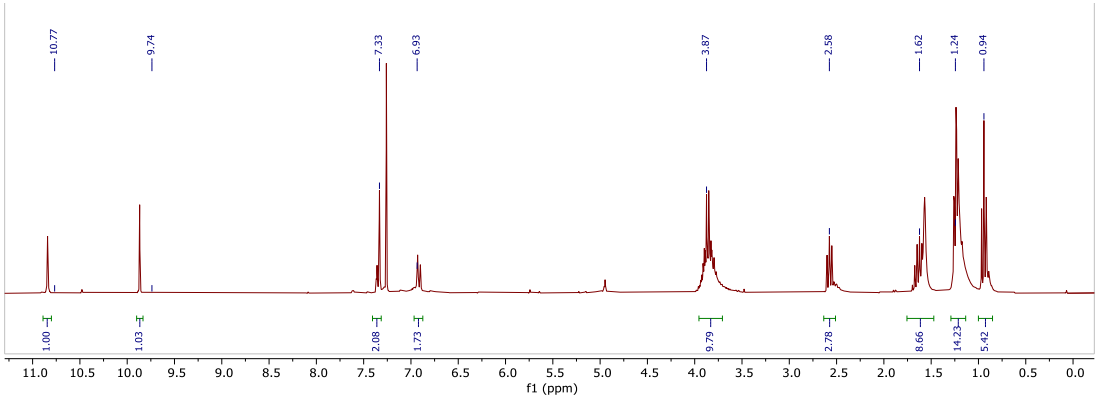

Figure 28: ^{1}H-NMR spectrum of sample C-10-E, microwave excited hydrosilylation rection conducted with 0.1ml of Et_3N

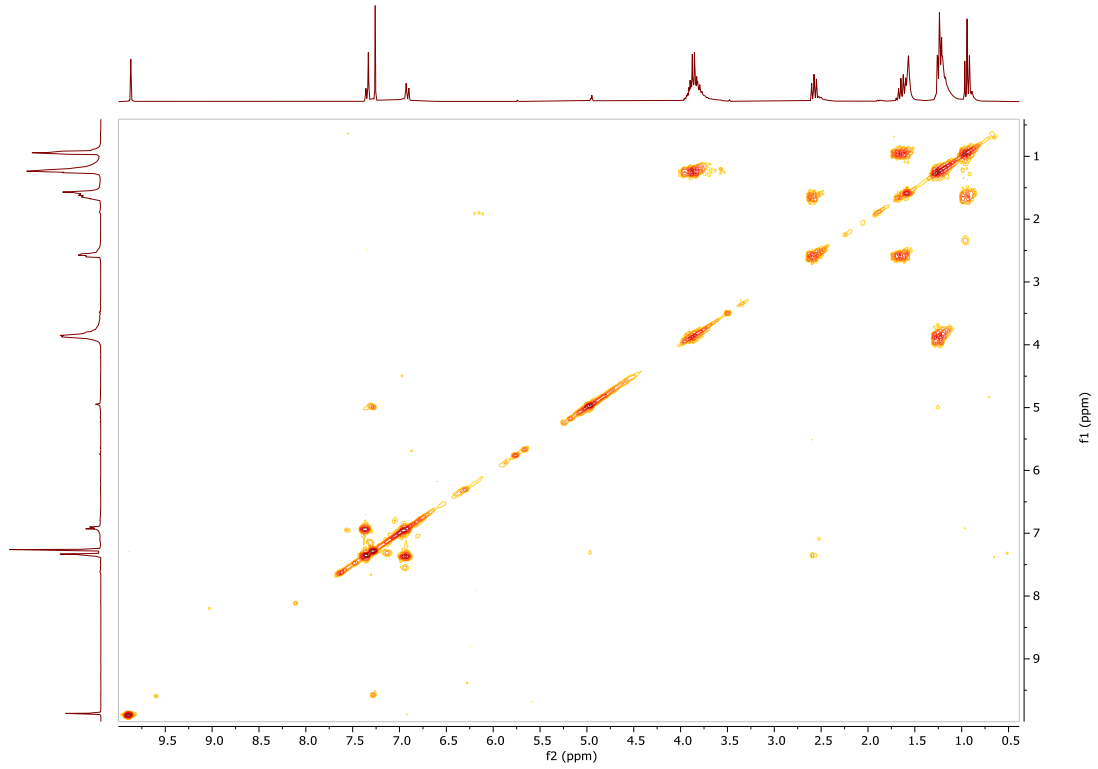

Figure 29: ^{1}H-COSY-NMR spectrum of sample C-10-E, microwave excited hydrosilylation rection conducted with 0.1ml of Et_3N

The spectra of the product produced in this was not identical to the spectra of **4b** obtained in the baseline (neutral) conditions. There are slight changes in the chemical shifts of the propyl chain, which are marginally shifted upfield by inclusion of the base, and the peaks formed by the phenolic and aldehyde hydrogens are reduced in intensity, when compared to the unaltered reaction.

Following this result, acidic conditions were speculated to show the opposite selectivity, in favour product **4a.** A similar experiment was conducted under acidic condition, 0.1 ml of glacial acetic acid (125 Mol %) was added to the reaction mixture. A weak acid was selected for this as any hydrogen halides may have added across the alkene. The crude ^{1}H-NMR of the reaction mixture shown in Figure 30, showed a slight improvement of selectivity compared to neutral conditions; with a conversion of 74% to **4a**, 15% to **4b** and 10% to **3b**.

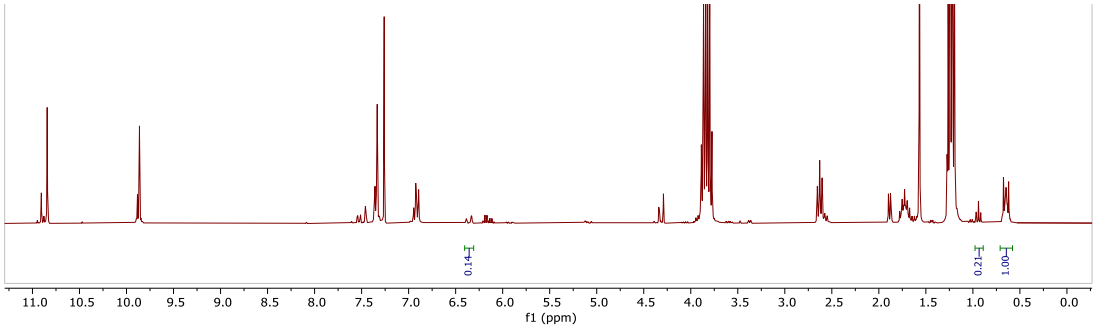

*Figure 30: ^{1}H-NMR spectrum of C-10-F, microwave excited hydrosilylation of **3a** containing 0.1ml of glacial acetic acid*

These conditions represent the single highest selectivity for **4a**, higher selectivity may be possible by further investigation.

3.4.5- Green Chemistry Analysis

As a hydrosilylation, the ideal form of this reaction produces no by-products as all atoms within the reagents appear in the desired product, thus it has a theoretical atom efficiency of 100%, this is true even when both isomers **4a** and **4b** are considered as both can be used to produced immobilised salophens. As all reagents become the final product, given any individual reaction. The result is that under any specific reaction the yield can proxy as effective atom economy. With the initial conditions: a 35% yield was obtained, thus a 35% atom economy. By utilising the microwave and including an additive, basic or acidic, the atom economy becomes 94% or 86% respectively.

$$\%\ Atom\ economy = \frac{Mass\ of\ atoms\ in\ desired\ product}{Mass\ of\ atoms\ in\ all\ products}\ x\ 100$$

$$\%\ Atom\ economy = \frac{278.47\ gmol^{-1}}{278.47\ gmol^{-1}}\ x\ 100 = 100\%$$

This reaction performs well in E-factor analysis, as there is no solvent, no by products and the heterogeneous PtO_2 catalyst can likely be recovered and reused, thus not qualifying as waste. The only waste from this reaction is the small excess of $HSi(OEt)_3$ when used. If the PtO_2 catalyst is classed as waste an E-Factor of 0.0417 is obtained. This is an excellent score and trends towards zero as the equivalents of $HSi(OEt)_3$ is reduced and if the PtO_2 is not considered as waste.

$$E\ Factor = \frac{Total\ Mass\ of\ Waste}{Total\ Mass\ of Product}$$

$$= \frac{+\ 3.40\ mg\ (PtO_2) + 16.4\ mg\ (average\ excess\ of\ HSi(OEt)_3\ )}{475\ mg}$$

$$E\ Factor = 0.0417$$

This reaction excels in other areas of the PoGCs too; a heterogeneous catalyst is utilised and can likely be utilised multiple times, no solvent is used, and very little waste is produced. One of the key developments, using microwave excitation, drastically reduced both the energy and time cost of this transformation and removes the need for purification, Developments such as this may be demonstrative of advances that can be applied on a larger scale. This shows the effectiveness of microwave excitation for heating purposed

compared to more traditional forms of heat generation. It is likely that flow chemistry procedures could employ this in a highly efficient manner, even on the industrial scale.

3.5- Imine Formation

The synthesis of **5a** by the formation of the secondary aldimine bond was achieved by the condensation reaction of **4a** and a 1,2 diamine (Scheme 11). This straightforward reaction is the standard method of producing both salens and salophens. By combining **4a** and 1,2-phenylenediamine in a 2:1 molar ratio in ethanol and heating to 60°C for 3 hours, **5a** was obtained in >99% purity.

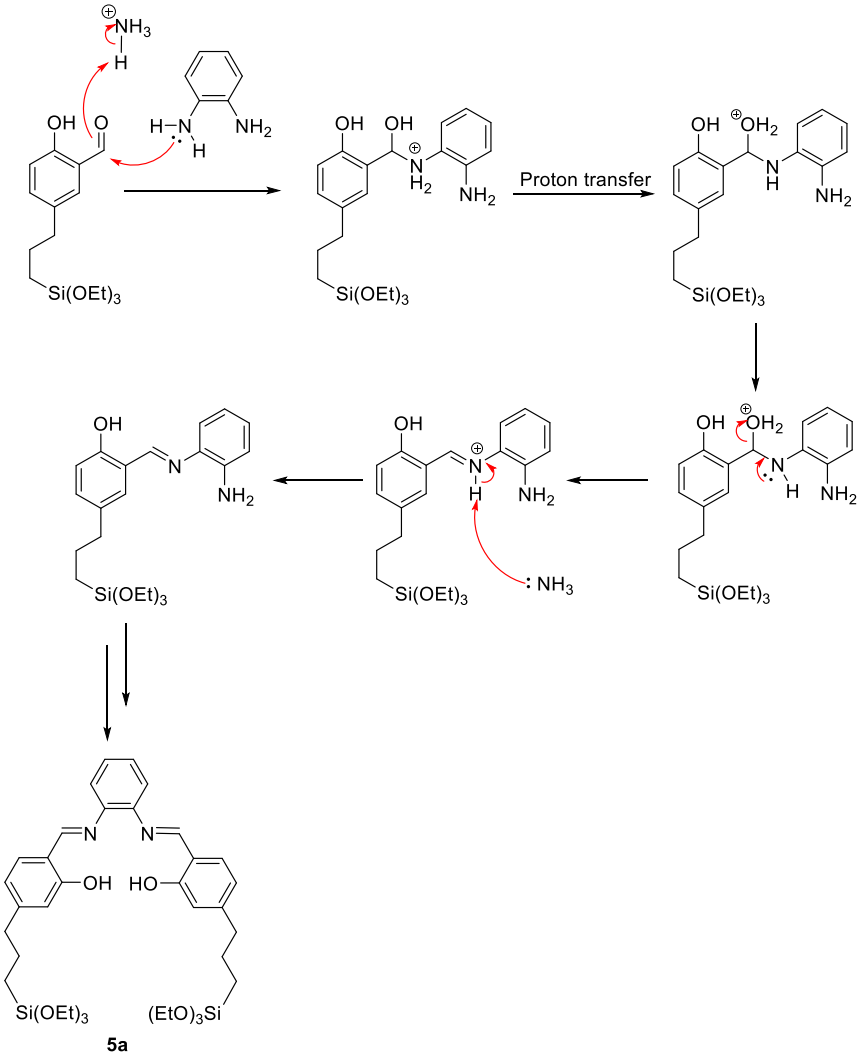

*Scheme 11 Mechanism of Imine formation of **4a** and a 1,2 diamine*

Characterization of **5a** was again accomplished via ^{1}H-NMR, ^{13}C-NMR, IR spectroscopy and Mass Spectroscopy. This material suffers from the same difficulty in isolating as **4a**,

so was not purified and isolated. This did not allow for high quality NMR, however samples were placed under a high vacuum for 16 hours before crude NMRs were taken.

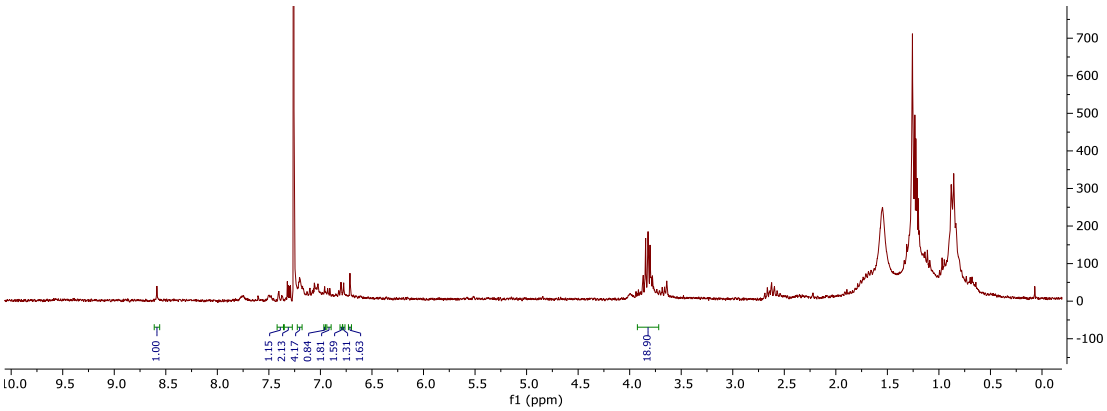

*Figure 31: Crude ^{1}H-NMR of species **5a***

^{1}H-NMR, shown in Figure 31, shows a lack of peaks for both the aldehyde hydrogen and the phenolic hydrogen, present in the spectra for species **4a.** The imine hydrogens can be seen as sharp singlets at 8.59ppm. The aromatic region has become more complex, due to the inclusion of the central aromatic ring. Little else can be gained from the crude spectra, as large peaks between 0.5 and 1.8 ppm wash out any resolution.

Once the product of this reaction was confirmed, and crude yield obtained, little further effort was needed for this reaction. As no purification was possible, the product would be immediately proceeded onto the immobilisation onto silica.

It was crucial to use exact stoichiometric ratios in this reaction. In the case of there being too much 1,2-phenylenediamine, the result is production of the half-salophen, that is one unit of **4a** bonded to 1,2-phenylenediamine. The final result of this would be a mixture of **5a** and the half salophen. In the opposite case, of there being insufficient 1,2-phenylenediamine, unreacted **4a** would remain in the reaction mixture. As purification via column chromatography was not possible for **5a**, separation of these different products was not achieved. This may have altered the incorporation ratios during the

immobilisation of the ligands. However, given that there was little evidence of either the phenolic hydrogen or the aldehyde hydrogen in either the ^{1}H-NMR, or the IR spectra, the total effect of imperfect measuring of the reagents is unknown.

In future work, a different approach to this reaction may be possible by using a 1:1 ratio of **4a** to 1,2-phenylenediamine, producing only the half salophen. This mixture could then be added to an equimolar amount of **4a** to produce the salophen. This method does not eliminate the issues discussed above it does, however present options for developing asymmetric salophens by utilising other derivatives of salicylaldehyde. Using a species that did not contain the silyl-group would then allow for any excess salicylaldehyde to be removed from the products by washing with solvent. This would produce an asymmetric salophen that was only immobilised on one side, which may affect both the catalytic properties and the ability for the species to be recovered and reused.

3.6- Silica Incorporation

The immobilisation of **5a** onto silica was achieved using a sol-gel method, the condensation reaction of tetraethyl orthosilicate (TEOS) and **5a**.[104] This was accomplished by combining the reagents in a dilute solution of ammonium hydroxide within a glass vial, and heating at 40° C for 36 hours, then increasing the temperature to 110°C for a further 48 hours. The product was then washed with ethanol, EtOAc and water before being dried in a vacuum oven overnight, yielding dry **6a.** The product of this reaction was characterised with a combination of solid state ^{13}C-NMR, IR Spectroscopy and CHN analysis. Having been rendered insoluble it was not possible to perform solution state NMR analysis on the product of this reaction.

The full range of solid-state ^{13}C-NMRs can be found in appendix sections- S.3-6, but an example can be seen in Figure 32. The three carbon environments in the propyl chain can be seen at 11.3, 24.0, 36.2 ppm likely to be assigned according to proximity to the aromatic ring. A small peak at 60 ppm is possibly caused from the presence of ethoxy group remaining within the structure, though it may also be caused from the spinning sidebands of the major aromatic peaks. Within the higher chemical shift region seven peaks are distinguishable at 114.2, 119.1, 123.6, 132.6, 141.3, 153.5, 158.7 ppm. These are too few compared to the number of carbon environments within this molecule, however the peaks are broad and clearly overlapping, with a strong likelihood of there being more peaks underneath.

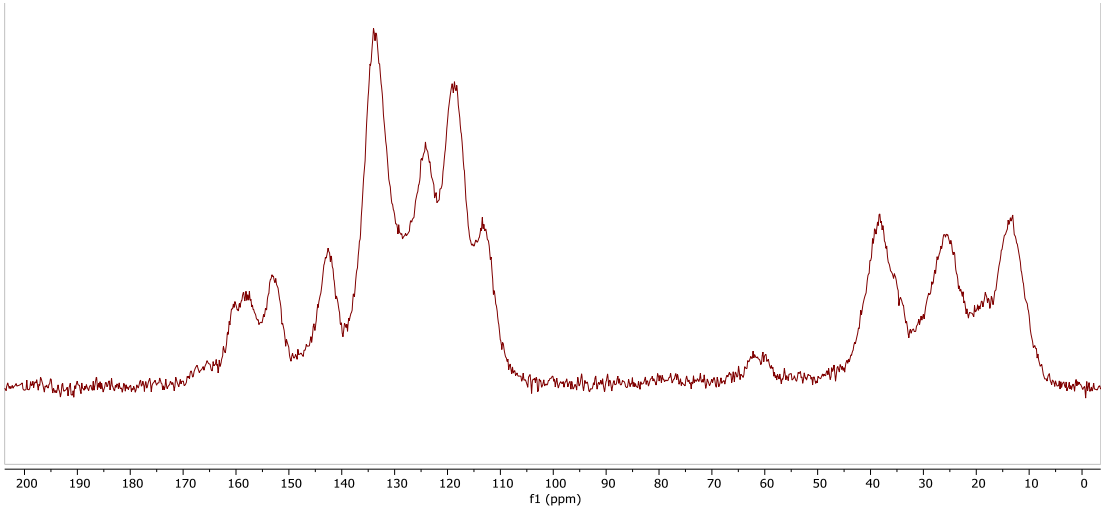

Figure 32: Solid state ^{13}C-NMR of 7:1 Immobilised salophen

Under IR analysis (Figure 33), **6a** proved difficult to analyse, with the spectrum being dominated by a large Si-O-Si stretching peak at 1100 cm^{-1}. This is not unpredictable due to the large mass of silica present and demonstrates the limitation of this technique for this material.

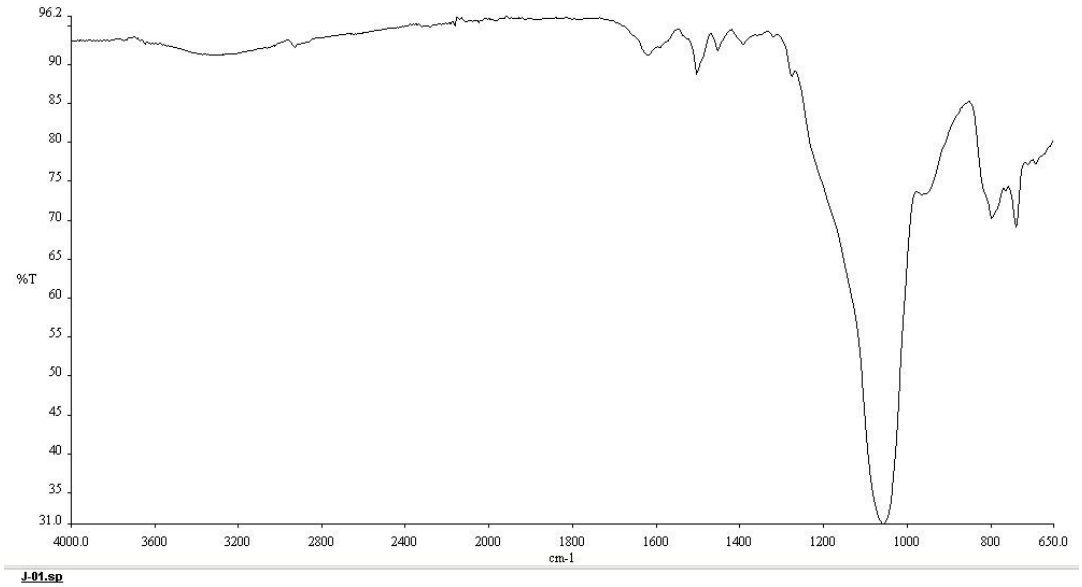

Figure 33: IR Spectrum of 7:1 Immobilised salophen

CHN elemental analysis was used for determining the mass percentage of the of carbon, nitrogen, and hydrogen of the immobilised salophens. The elemental formulae of the

samples were then calculated by obtaining the closest fit to the experimentally obtained values.

There are several shortcomings when fitting the calculated ratios to the CHN results. Firstly, the solid-state NMR taken of these species suggests that ethanol and ethoxy groups are trapped within the silica structure or bound to it. It is also possible that water remained within the samples and was not entirely removed during the drying process. The quantity of water and ethanol trapped within the silica appeared to be independent of the silica: ligand ratio, and no modification of the stirring, heating or drying methods produced any trend. Secondly, as stated in the previous section, any imperfection of the ratio of **4a** and 1,2-phenylenediame would result in a mixture of **5a**, half salophen and **4a**. Both the half salophen and **4a** were inseparable from **5a**, and both are potentially active for this reaction. Therefore, it is possible that the product of this reaction contains a mixture of **5a**, half salophen and **4a** immobilised onto silica. As CHN analysis only provides information about the elemental composition, this technique cannot provide information about the distribution of these products.

In most cases, close matches were found between the computational formulae and experimental results, though these did not always line up with the targeted silica: salophen ratios. When these catalysts were employed in reactions the fitted formula was used to calculate the required mass.

3.6.1- Silica: Ligand: Silica Ratio Control

General control over the incorporation ratio of silica to ligand was demonstrated via control over the stoichiometric ratio of **5a** and TEOS, however exact control has yet to be achieved. Table 7 shows the complete selection of immobilised salophens produced, their target immobilisation ratios and their calculated immobilisation ratios. In general, the

immobilisation ratio was higher (in favour of silica) than the target ratio. The cause of this is unknown. As the mass of TEOS used was calculated specifically for the sample of **5a** in use, the most likely cause of this "overshooting" of the target ratio was **5a** containing solvent, adding to the observed mass. Therefore, more TEOS would have been used than needed. If this hypothesis is correct, it would easily be solved my more rigorous drying of the **5a** used.

Table 7: Incorporation ratios for silica supported salophens.

Target ratio	*Experimental formula*	*Calculated immobilisation ratio*	*Mass of catalyst /g*	***Yield***
5:1	$C_{26}H_{26}N_2Si_8O_{20} \cdot H_2O$	6:1	0.1959	60%
15:1	$C_{26}H_{26}N_2Si_{17}O_{38}$	15:1	0.4375	86%
20:1	$C_{26}H_{26}N_2Si_{27}O_{58} \cdot 9H_2O$	25:1	0.5128	65%
5:1	$C_{26}H_{26}N_2Si_9O_{22} \cdot H_2O$	7:1	0.9496	91%
5:1	$C_{26}H_{26}N_2Si_9O_{22} \cdot 2.5H_2O$	7:1	0.4484	74%
**10:1*	$C_{26}H_{26}N_2Si_{18}O_{40}$ $1H_2O$	16:1	0.6028	66%

- *Material produced using **4b***

In each case of this reaction, it is likely that there is a dispersion of immobilised salophens being formed with a range of silica: ligand ratios, that average out to the calculated formula. This non-uniformity of the product should not affect the overall properties of the immobilised catalyst. It is possible that MALDI-MS may be useful in determining more information regarding the dispersity of the silica: salophen ratio and could provide more insight. It is not currently certain that the desired immobilised salophen has been produced. However, any unsupported salophen would have been removed from the silica by the rigorous washing procedure. The catalytic activity of the material produced indicates that there are salophens present within the material, and therefore likely chemically bound to the silica.

3.6.2- Green Chemistry Analysis

The ideal atom economy of the formation of the salophen via the imine condensation reaction is 94.5% this high value is derived from the fact that the reaction is a coupling of three molecules and only produces two molecules of water as a by-product. The high mass of the product reduces the effect of producing two equivalents of waste.

$$\%\ Atom\ economy = \frac{Mass\ of\ atoms\ in\ desired\ product}{Mass\ of\ atoms\ in\ all\ products}\ x\ 100$$

$$\%\ Atom\ economy = \frac{623.42\ gmol^{-1}}{(2x\ 18.01)\ gmol^{-1} + \ 623.42\ gmol^{-1}}\ x\ 100 = 94.5\%$$

As this reaction is not isolated or purified, a precise mass of product is not known therefore E Factor analysis is not able to be performed accurately, however an estimation is possible.

$$E\ Factor = \frac{Total\ Mass\ of\ Waste}{Total\ Mass\ of Product}$$

$$= \frac{0.789\ g\ (Solvent) + \ 0.0253\ (H_2O)}{0.242\ g}$$

$$E\ Factor = \ 3.36$$

This value is positive and unlikely to be improved upon as neither the solvent or the liberated H_2O can be reduced. This value may be decreased with decreasing yield and is highly dependant of precise measuring of both reagents involved, as to much of either could lead to the production of by-products.

The measurement of atom economy for the immobilisation onto silica is more difficult as it is dependent on the immobilisation ratio; for a 10:1 immobilised salophen 10 equivalents of tetraethyl orthosilicate is used, each liberating 4 molecules of ethanol. This provides an atom economy of 30.1 %. This value is not ideal, however the ethanol produced could be recovered and recycled.

$$\%\ Atom\ economy = \frac{Mass\ of\ atoms\ in\ desired\ product}{Mass\ of\ atoms\ in\ all\ products}\ x\ 100$$

$$\%\ Atom\ economy = \frac{793.0\ gmol^{-1}}{(40x\ 46.07)\ gmol^{-1} + \ 793.0 gmol^{-1}}\ x\ 100 = 30.1\%$$

E Factor analysis is, again, difficult to accomplish on this reaction however an approximation can be attained.

$$E\ Factor = \frac{Total\ Mass\ of\ Waste}{Total\ Mass\ of Product}$$

$$= \frac{20\ g\ (Water) + \ 35\ g\ (wash\ Solvents) + 2\ g\ (reacton\ solvents) + 71\ mg\ (EtOH)}{0.4375\ g}$$

$$E\ Factor\ = \ 130.4$$

The overall environmental impact of these reactions is difficult to determine, with values shown above being approximations. These results are by no means conclusive or concrete, and a significant body of work remains in accessing the environmental impact of producing **6a**. LCA, as mentioned previously would provide a deep insight into the effective CO_2 per gram of **6a**, considering all starting materials, and the processing of all waste. This analysis is essential for assessing the viability of this material as a potential method of combating the rising atmospheric CO_2 levels.

Chapter 4 Catalytic Activity of Silica Immobilized Salophens

4.1.1- - Catalytic Synthesis of Cyclic Carbonates

Salophens have been demonstrated to behave as homogeneous organo-catalysts for the synthesis cyclic carbonates from epoxides and CO_2, Scheme 12.[21–24,41,42] The immobilised salophens produced in this work, were therefore tested for their ability to catalyse the same reaction as heterogeneous catalysts.

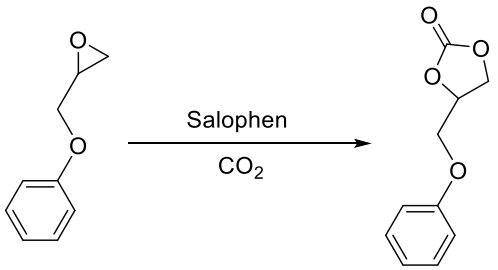

Scheme 12: Synthesis of 4-(phenoxy)methyl-1,3-dioxolane-2-one

4.1.2- Synthesis of 4-(phenoxy)methyl-1,3-dioxolane-2-one

Initially 3-phenoxypropylene oxide was investigated, as it was known to be a highly reactive substrate for this reaction with the homogeneous analogue. Previously this reaction had been undertaken at 120°C pressurised to 1-10 bar pressure of CO_2 with 1% molar ratio of catalyst and would reach >99% conversion after 210 minutes. Initially the extremes of these conditions were replicated with a sample from the same batch of 7:1 immobilised salophen, shown in Table 8.

Table 8:Initial catalytic activity of a 5:1 immobilised salophen at 1 and 10 bar

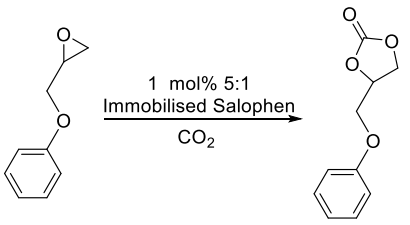

Catalyst	*Time (mins)*	*Temp (°C)*	*Pressure (Bar)*	*Crude Conversion*
Silica	210	120	10	1.8%
7:1	210	120	10	66% *
7:1	210	120	1	50%
	*66% Cyclic carbonate product, remaining 34% formed unknown product likely the corresponding 1,2- diol.			

The testing carried out at 1 bar was accomplished by combining the epoxide and the immobilised salophen inside a 5 ml vial equipped with a stirrer bar and a Suba seal. The system was flushed three times using a CO_2 balloon. This method was simple to conduct, however the balloons would deflate over the duration of the reaction and required replacing. Additionally, the actual pressure of CO_2 within the vials is not precisely known, although this can be assumed to be at roughly atmospheric pressure. Initial results show that at 1 bar, the activity of the immobilised salophens is similar to that of the unsupported salophens (46%).[23]

An additional blank run using pure silica, produced via the same sol-gel procedure, was carried out to ascertain whether the structure of the silica contributed to the total activity of the catalyst. As seen in Table 8, the blank produced a total conversion of 1.8% to the cyclic carbonate product, showing that there is some contribution of the silica to the overall transformation of epoxide to carbonate, however, these results were not replicated in repeat experiments. The initial positive result of the silica blank was obtained using the same equipment as a previous experiment using active catalyst, so it is possible that the

small amount of cyclic carbonate found may have been residue left over from imperfect cleaning of the equipment, as during repeat testing no activity was found it is likely that the initial result is erroneous.

Table 8 also shows the effect of increasing the pressure of the reaction from 1 to 10 bar pressure of CO_2. At 1 bar, 50% of the 3-phenoxypropylene oxide had reacted to form 3-phenoxypropylene carbonate, whilst at 10 bar, the reaction proceeded to completion, with no indication of any epoxide remaining. The crude NMR spectrum of this reaction indicated that 66% of the product had become the cyclic carbonate, with the remaining material likely becoming the corresponding 1,2 diol, possibly caused by the presence of water within the reaction mixture. This was not investigated further, rather effort was directed to purging the system of water prior to the start of the reaction and supressing this reaction. The conversion of the cyclic carbonate to the diol was not confirmed and remains an avenue for future investigation. The conversion at 10 bar is incredibly high, and comparable to that of the equivalent homogeneous catalysts (100%), however it should be noted that reported conversion includes the use of a co-catalyst and was conducted at a lower temperture.[21,23]

The increase in conversion is attributed to a higher rate of reaction when the reaction is conducted at higher pressures, likely due to effectively a higher concentration of CO_2, more favourable kinetics, and a reliably sealed and constant reaction vessel.

Salophens with an immobilisation ratio of 5:1, 16:1, 15:1 and 25:1 were also tested in this manner at both 1 bar and 10 bar, results shown in Table 9 and Table 10 respectively. In all cases increasing the pressure drastically increased the rate of reaction, and therefore the conversion.

Table 9:synthesis of 3phenoxypropylene carbonate at 1 bar CO_2

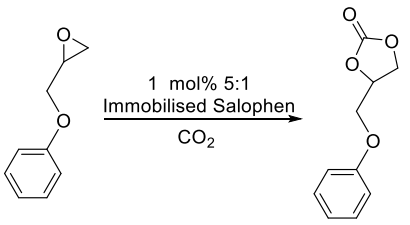

Catalyst	*Time (minutes)*	*Temp / °C*	*Pressure / Bar*	*Conversion percentage*
7:1	210	120	1	50%
**16:1*	210	120	1	56%
15:1	210	120	1	23%
25:1	210	120	1	42%

**- material produced only using 4b*

The difference in catalytic activity of these species does not appear to follow a trend. This is to be expected as each contained the same mass of salophen, only the incorporation ratio and the mass of silica changes. This is the equivalent of diluting the catalyst within solid silica. Increasing the incorporation ratio does not appear to have any noticeable effective on the potency of the ligand, given that the calculated mass of ligand remains the same. The differences in conversion in Table 9 are more likely attributed to imperfect pressurisation with CO_2, temperature variations in an imperfect experimental setup and off-centred stirring. The more valuable interpretation of Table 9 shows that there does not appear to be any effective difference between using supported catalysts produced from either **4a** and **4b** or a mixture thereof, this is supported by the results presented in Table 10.

Table 10: Synthesis of 3-phenoxyproylene carbonate conducted at 10 Bar

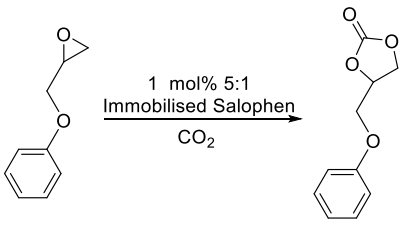

Catalyst	*Time (minutes)*	*Temp / °C*	*Pressure / Bar*	*Conversion percentage*
7:1	210	120	10	99 %
**16:1*	210	120	10	96 %
15:1	210	120	10	88 %
25:1	210	120	10	92 %

**- material produced only using 4b*

At 10 bar, each sample produced 80-100% conversion within 3.5 hours, though not with 100% reliability. Though crucially all material was shown to be highly active, regardless of the mass of silica attached to it. The catalyst was easily recovered, by simply dissolving the sample in approximately 2ml of EtOAc or $CHCl_3$ and spinning on a benchtop centrifuge for 5 minutes.

Purification of this product was achieved by column chromatography using a 3g silica column, eluting with petroleum ether-40:60 (6:4) EtOAc yielding a white powder. The purified ^{1}H-NMR can be seen in Figure 34, the ^{13}C-NMR in Figure 35, the IR in, Figure 36, and the ESI Mass spectra is shown in Figure 37.

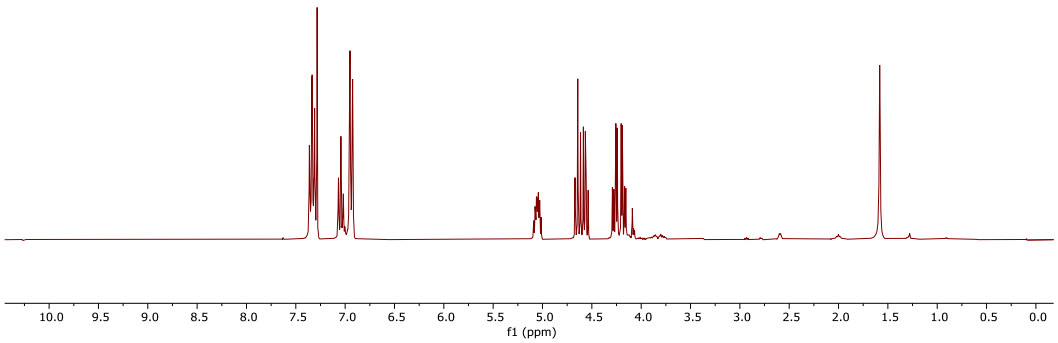

Figure 34: [1]H-NMR of 4-(phenoxy)methyl-1,3-dioxolane-2-one

The [1]H-NMR shows six hydrogen environments: A doublet of doublets at 7.33 (*J=7.3, 1.4 Hz*) relating to the hydrogens *meta* to the alkoxy substituent, a triplet at 7.04 ppm (*J=8.5 Hz*) for the *para* hydrogen, and a doublet of doublet at 6.94 ppm (*J=8.5 Hz)* relating to the *ortho* hydrogens. Further upfield, a doublet of doublet of triplets is formed at 5.05 ppm (*J= 8.1, 6.1, 4.0 Hz*) for the hydrogen on position two of the propyl chain, the diasteriotopic hydrogens on position 1 of the propyl chain appear as a multiplet at 4.58 ppm. The diasteriotopic hydrogens on position 3 of the propyl chain form two doublets of doublets at 4.24 ppm (*J=10.6, 4.0 Hz*) and 4.14 ppm (*J=10.6, 6.1 Hz*).

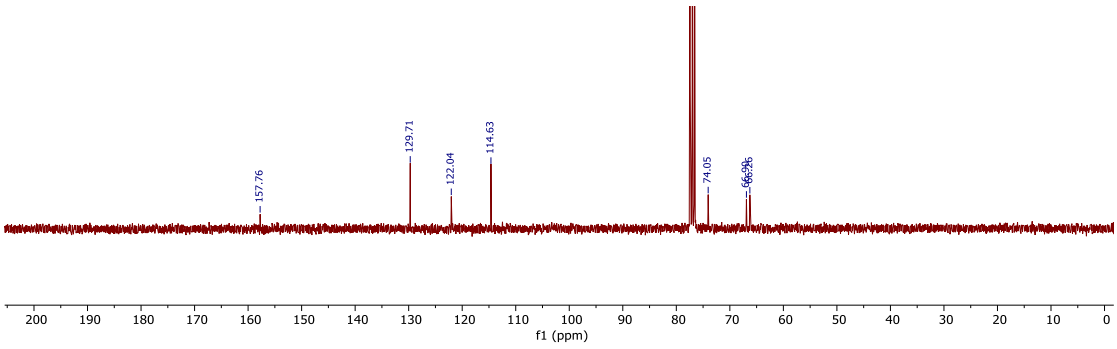

Figure 35: [13]C-NMR spectrum of 4-(phenoxy)methyl-1,3-dioxolane-2-one

The [13]C NMR shown in Figure 35 show the spectrum produced by 4-(phenoxy)methyl-1,3-dioxolane-2-one, containing a carbonyl at 157, three aromatic peaks at 129.0, 122.0 and 114.0 ppm and the three carbons in the propyl chain can be seen at 66.2 and 66.9

ppm for the CH_2 groups and at 74.0 ppm for the OCH carbon on position 2. This NMR is supported by the IR spectrum shown in Figure 36, with the strong carbonyl peak at 1790 cm^{-1}.

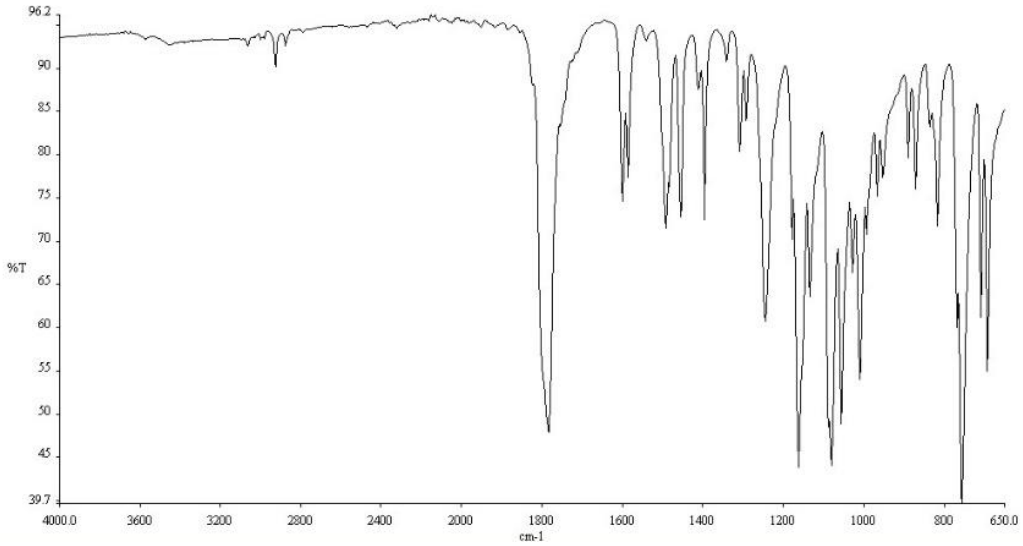

Figure 36: IR spectrum of 4-(phenoxy)methyl-1,3-dioxolane-2-one

The ESI-Mass spectrum shown in Figure 37 shows a molecular ion peak at 217.0465 m/z which aligns with the calculated value of 217.0476 for the $[M+Na]^+$ ion.

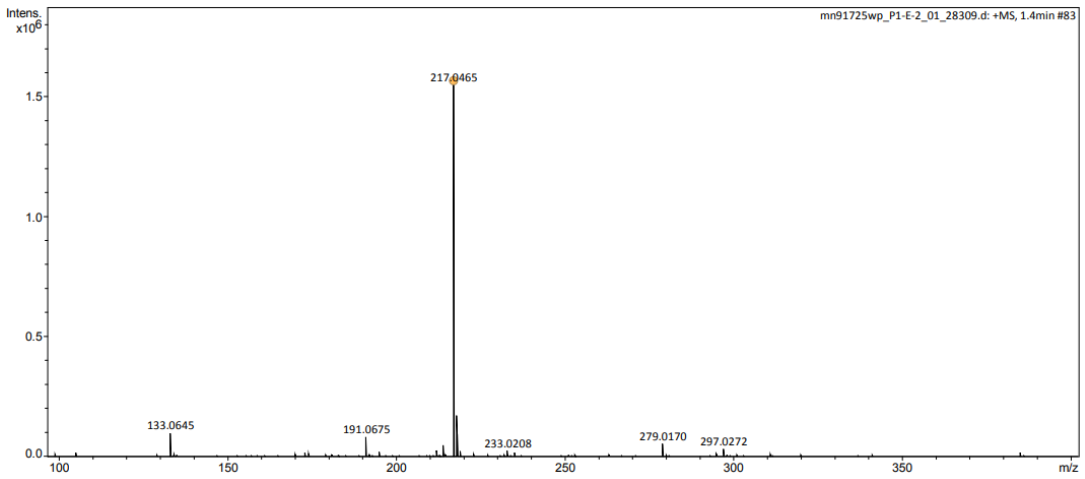

Figure 37: ESI mass spectrum of 4-(phenoxy)methyl-1,3-dioxolane-2-one

4.1.3- Synthesis of 4-Phenyl-1,3-dioxolan-2-one

Having demonstrated high activity of the silica immobilized catalysts for the synthesis of 3-phenoxypropylene carbonate, investigations were conducted into use of styrene oxide. Work on this material was hampered by poor rates of recovery from the sealed reaction vessel. Typically, anywhere from 30-95% off the mass of the reagents would be lost during a reaction procedure. Attempts at finding where this mass was being lost too were not successful, it is possible that the material was evaporating and being lost when the reaction vessels were open, however given that the pressure of the vessel is reduced to a vacuum before being opened, this is unlikely.

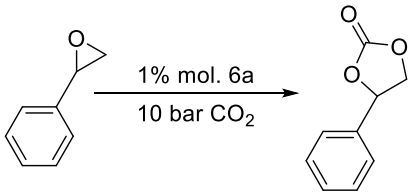

Scheme 13 Synthesis of 4-phenyl-1,3-dioxolan-2-one

It is possible that the styrene oxide was reacting with the rubber on the Suba-seals used to contain the reagents. This idea is cemented by the images shown in Figure 38, which clearly show severe deformation of the rubber seals, when weighed these seals had increased in mass by a similar amount to the mass loss of the reaction mixture, though this measurement was not exact

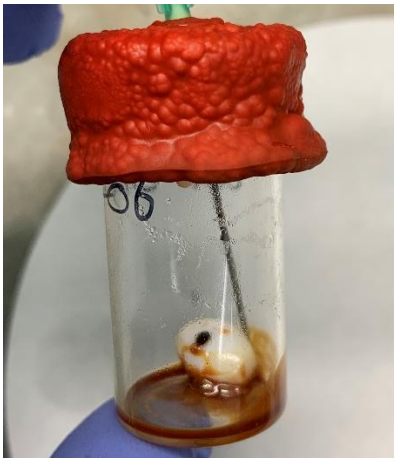

Figure 38: Suba seal exposed to styrene oxide at 120°C and 10 Bar CO_2.

No further investigation was carried out on the seals. To replace them hard plastic lids, with the paper lining and glue removed and a hole drilled through the centre, were used. After switching to this new method, the mass of material lost dropped to less than 5% per reaction.

With the replacement lids, it was found that full conversion of styrene oxide to 4-phenyl-1,3-dioxolan-2-one was achieved after 24 hours of stirring at 120°C under 10 bar pressure of CO_2. The product, a dark yellow oil was purified via column chromatography eluting with petroleum ether-40:60 (6:4) EtOAc to yield a white powder. Characterisation was achieved by ^{1}H-NMR (Figure 39), ^{13}C-NMR (Figure 40), IR spectrometry (Figure 41) and ESI Mass spectrometry (Figure 42).

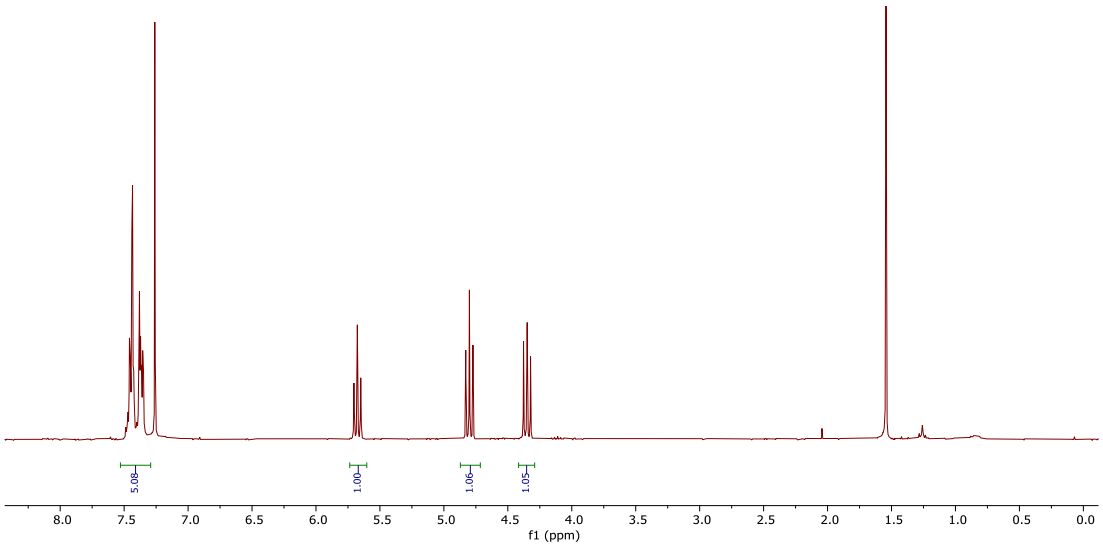

Figure 39: [1]H-NMR spectrum of 4-Phenyl-1,3-dioxolan-2-one

The [1]H-NMR of 4-phenyl-1,3-dioxolan-2-one (Figure 39) contains a non-aromatic doublet of doublets peak at 5.70 ppm (*J= 8.4, 8.2 Hz*) caused by the CH hydrogen on position 4 and two doublets at 4.82 ppm (*J= 8.4 Hz*) and 4.37 (*J= 8.2 Hz*) ppm from the two CH_2 hydrogens on position 5. The [13]C-NMR (Figure 40) of this species contains seven peaks, one for each unique carbon environment. Carbon 2, the carbonyl group is visible at 154.4 ppm, the aromatics at 137.0, 129.8, 129.3 and 123.7 ppm and the aliphatic carbons at 79.1 and 70.1 ppm.

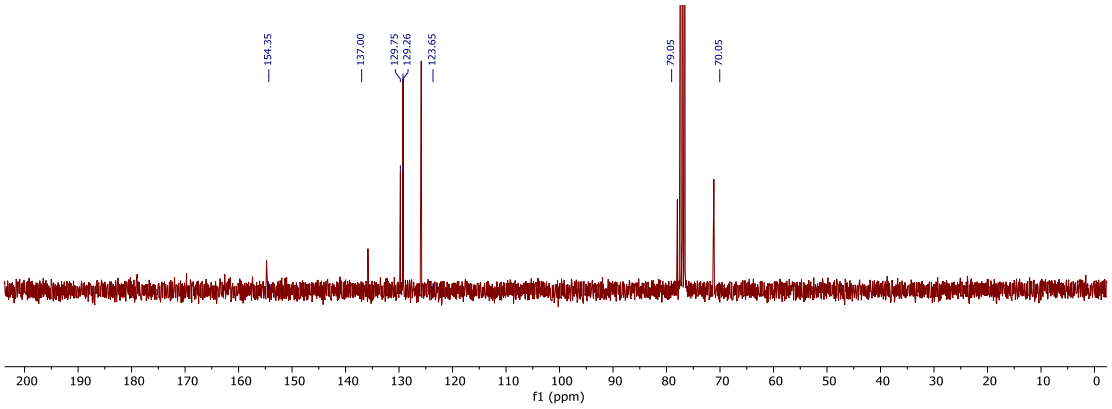

Figure 40: 13 C NMR Spectrum of 4-Phenyl-1,3-dioxolan-2-one

They key peak within the IR spectrum (Figure 41) is the strong peak at 1790 cm^{-1}, caused by the carbonyl bond. The aromatic and alkyl carbon-hydrogen stretches can also be seen between 2850 cm^{-1} and 3000 cm^{-1}.

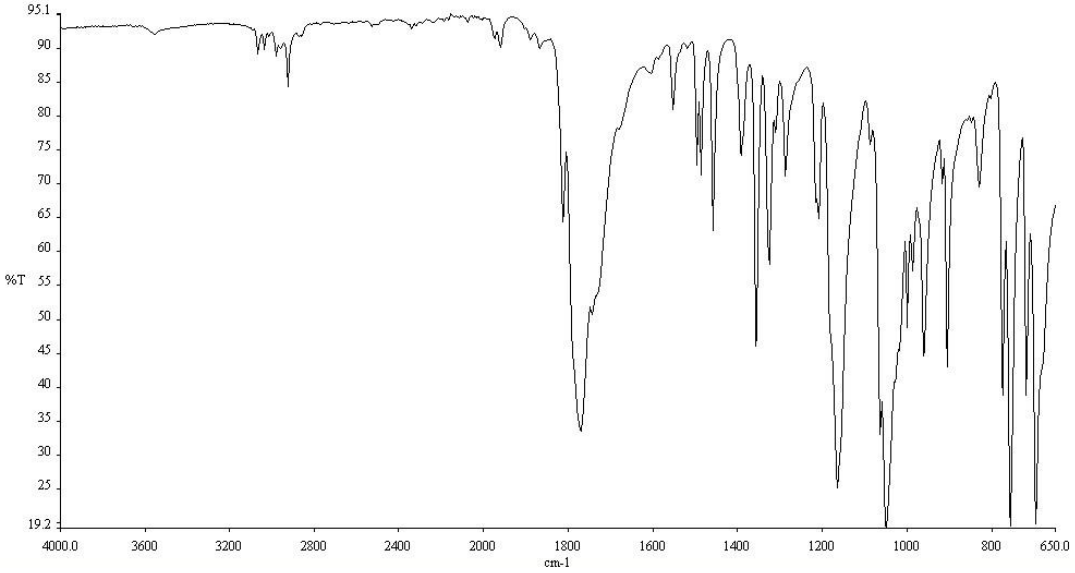

Figure 41: Infrared spectrum of 4-phenyl-1,3-dioxolan-2-one

Finally, the mass spectrum (Figure 42) shows a molecular ion peak of 187 m/z, this corelates to the mass of 4-phenyl-1,3-dioxolan-2-one with the addition of one sodium atom.

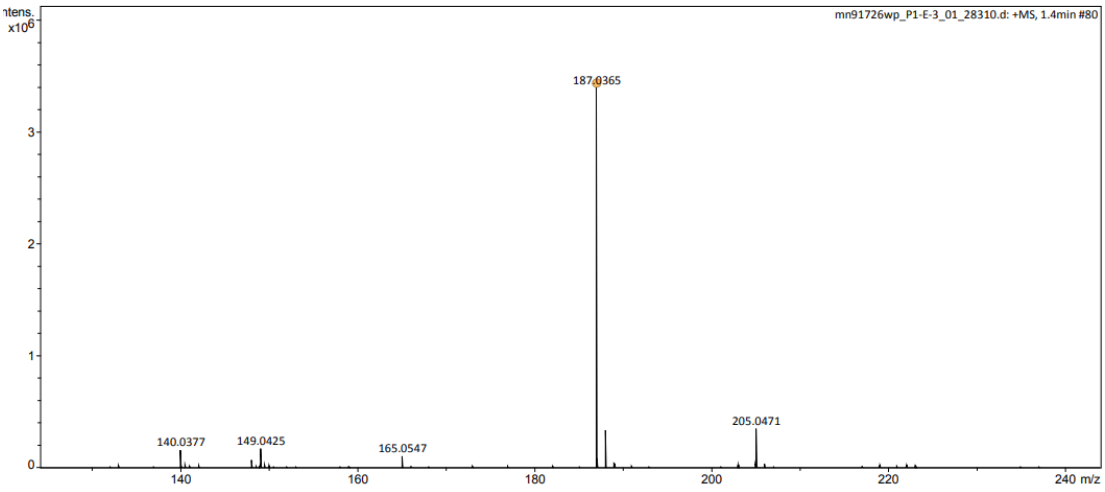

Figure 42: ESI Mass spectrum of 4-phenyl-1,3-dioxolan-2-one

4.1.4- Synthesis 4-(4-chlorophenyl)-[1,3]-dioxolan-2-one

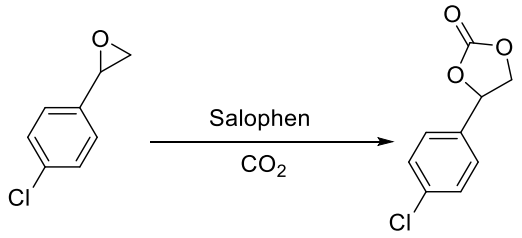

Scheme 14: Synthesis 4-(4-chlorophenyl)-[1,3]-dioxolan-2-one

Chlorostyrene oxide was investigated to study the effect of the electron withdrawing group attached para to the epoxide substituent. As previously, this reaction was conducted using 1 mol% catalyst and 10 bar of CO_2. It was discovered that this substrate is highly reactive under these conditions, with the reaction going to completion within 3 hours. The product was isolated via column chromatography eluting with petroleum ether-40:60 (6:4) EtOAc yielding a viscous yellow oil, which was subsequently characterised by ^{1}H-NMR, IR spectroscopy and ESI Mass spectrometry. ^{13}C-NMR was attempted on this species, however the sample appeared to have degraded as far more peaks were present than can be explained. The mass recovery was far higher than that of the unsubstituted styrene oxide (>99%). The reason for this is not known.

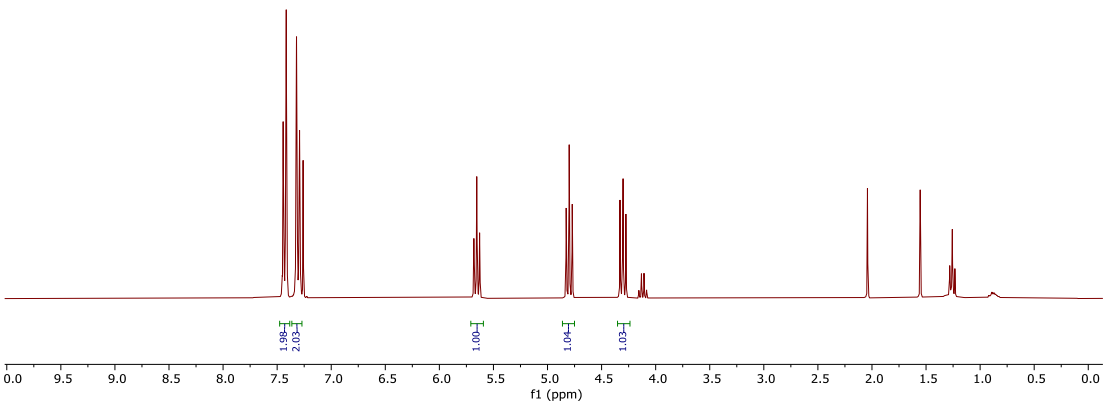

Figure 43: ^{1}H-NMR spectrum 4-(4-chlorophenyl)-[1,3]-dioxolan-2-one

Figure 43 shows the purified ^{1}H-NMR spectrum of 4-(4-chlorophenyl)-[1,3]-dioxolan-2-one, It contains to aromatic peaks, relating to each of the two aromatic hydrogen environments, each integrating to approximately two. There are three doublets of doublets at 5.65 (*J=8.3, 7.9 Hz*), 4.79 (*J= 8.7, 8.3 Hz*) and 4.30 (*J= 8.7, 7.9 Hz*) ppm relating to the hydrogens on position 4 and 5 respectively. The hydrogen NMR is supported by the IR spectrum shown in Figure 44. There are weak aromatic C-H stretches around 3000 cm^{-1} however the spectrum is dominated by strong carbonyl return at 1790 cm^{-1}.

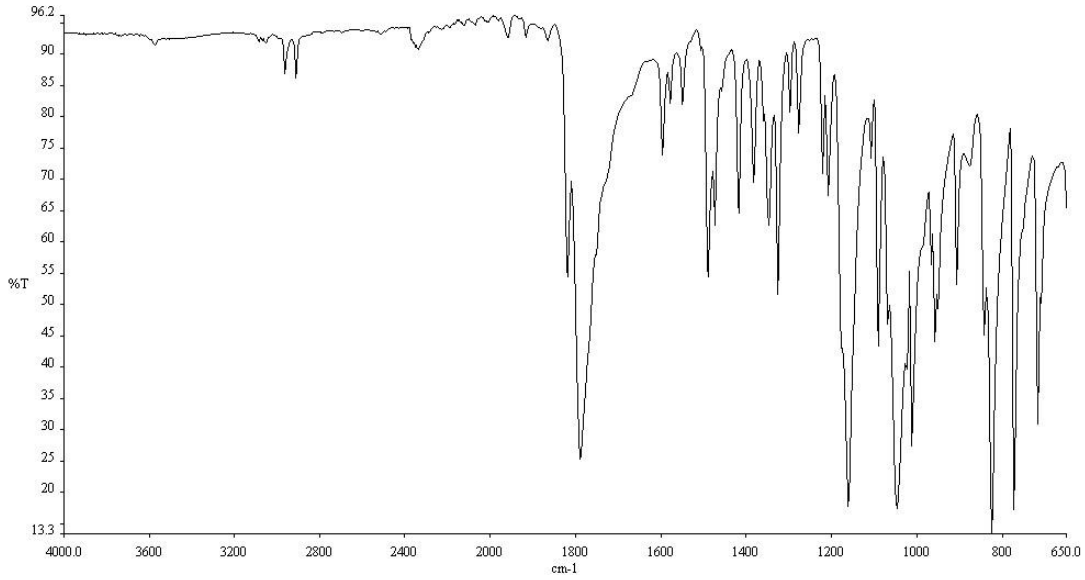

Figure 44: Infrared spectrum 4-(4-chlorophenyl)-[1,3]-dioxolan-2-one

The mass spectrum (Figure 45) contains additional support for the presence of 4-(4-chlorophenyl)-[1,3]-dioxolan-2-one, with a molecular ion peak of 199.0156 m/z corresponding to the protonated ion of the molecule.

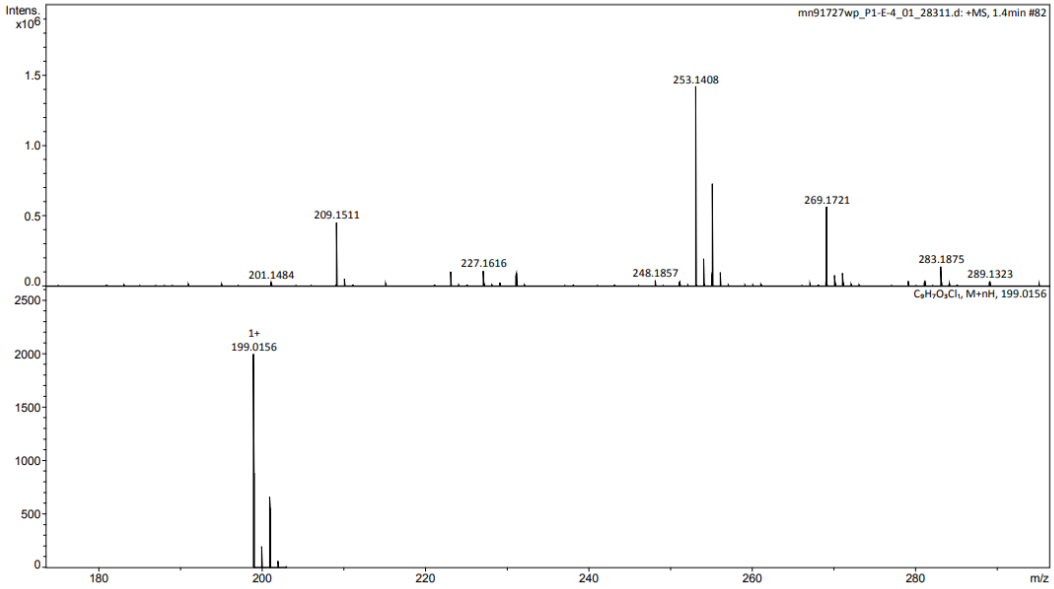

Figure 45: ESI Mass spectrum 4-(4-chlorophenyl)-[1,3]-dioxolan-2-one

4.1.5- Synthesis 4-octyl-1,3-dioxolan-2-one

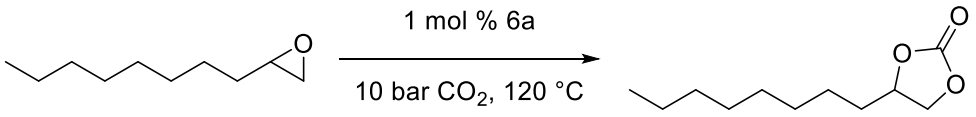

Scheme 15:Synthesis 4-octyl-1,3-dioxolan-2-one

Decene oxide was chosen as a potential substrate for this reaction as it is markedly different in structure to the previous epoxides, but it had been shown to be active in this synthesis using an analogous homogeneous catalyst (Scheme 14).[23] Decene oxide is an interesting reactant in this reaction due to its lack of aromaticity and heteroatoms present.

Under the conditions used previously, decene oxide proved to be less reactive than the substrates previously tested. A crude ^{1}H-NMR of a test conducted at 10 bar and 120 °C for 3 hours is shown in Figure 46. The crude spectrum does contain 4-octyl-1,3-dioxolan-2-one, as can be seen by the three peaks at 4.69 ppm (*J= 7.5, 7.5, 5.5 Hz*), 4.52 ppm (*J= 8.2,7.5 Hz*) and 4.06 ppm (*J= 8.2, 7.5 Hz*), but in under 20% conversion.

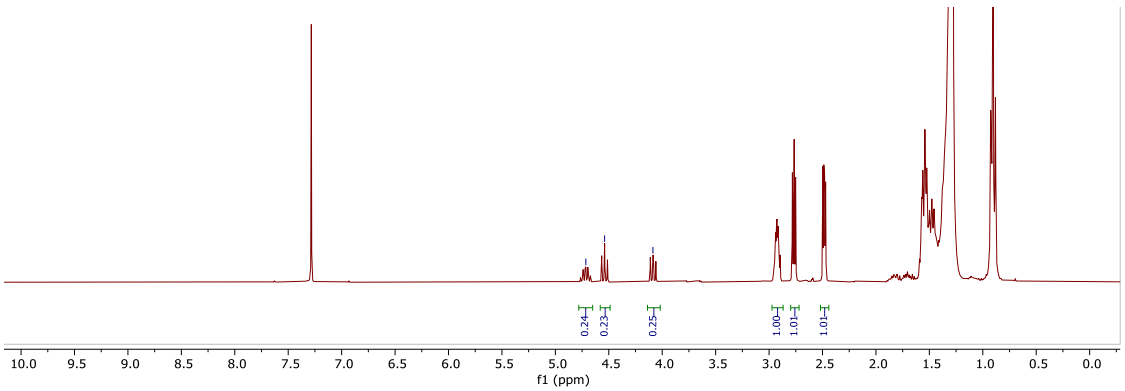

Figure 46:Crude ^{1}H-NMR of 4-octyl-1,3-dioxolan-2-one

Rather than alter the pressure or temperature of the reaction, it was decided to increase the duration of the experiment. This was chosen because of the positive result of doing this with styrene oxide, and the presence of 4-octyl-1,3-dioxolan-2-one after 3 hours indicating that the reaction does proceed under the conditions used but at a rate too slow

to reach completion within that time. Tests were then conducted for 24 hours and 48 hours with the results shown in Table 11. Full conversion was achieved after 48 hours, producing 4-octyl-1,3-dioxolan-2-one in 78% isolate yield. The "lost" material is again unaccounted for, though loss during the reaction and purification are likely to explain this. The product was purified by column chromatography eluting with petroleum ether 40-60 (6:4) EtOAc yielding pure 4-octyl-1,3-dioxolan-2-one as a pale-yellow powder. Following these results no further investigation of this reaction as undertaken.

Table 11: Crude conversions of 4-octyl-1,3-dioxolan-2-one after different duration reactions.

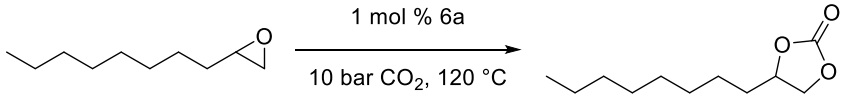

Epoxide	Crude reaction conversion		
	3.5h	**24h**	**48h**
1,2-epoxydecane	19%	40%	**>99%**

Characterisation of 4-octyl-1,3-dioxolan-2-one was accomplished using the combined data from ^{1}H-NMR (Figure 47) ^{13}C-NMR (Figure 48), IR and Mass Spectrometry. As much of the decene oxide is unchanged during this reaction, the majority of the carbons, the terminal CH_3 and six CH_2 appear as a triplet at 0.88 ppm and a broad multiplet at 1.27 pm respectively. The six CH_2 units should produce a unique signal each , however due to the overlapping chemical shift they resolve as one large peak. The diasteriotopic hydrogens adjacent to the cyclic carbonate appear as a multiplet at 1.74 ppm. Two doublets of doublets are visible at 4.06 ppm (*J= 8.2, 7.5 Hz*) and 4.52 ppm (*J= 8.2,7.5 Hz*) caused by the two CH_2 hydrogens on position 5 and the CH hydrogen on position 4 can be seen at 4.69 ppm (*J= 7.5, 7.5, 5.5 Hz*) as a doublet of doublet of triplets.

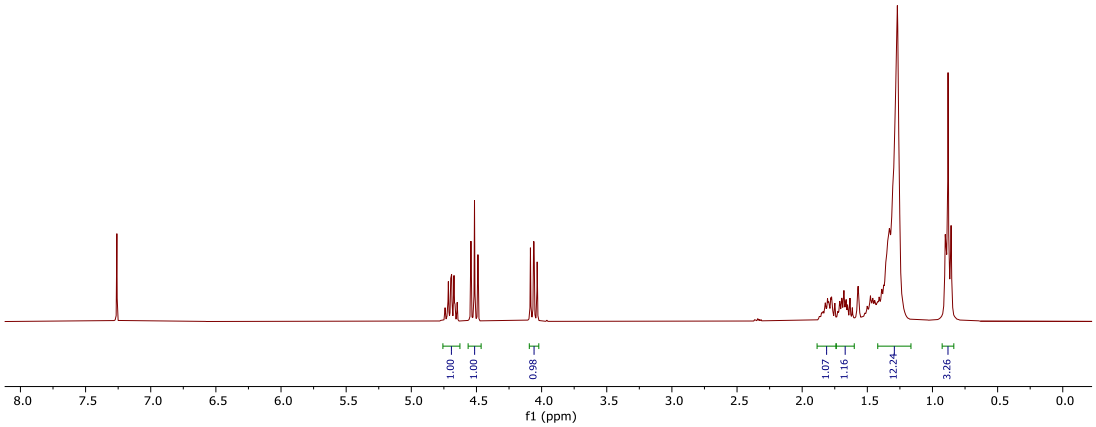

Figure 47 [1]H-NMR of 4-octyl-1,3-dioxolan-2-one

The [13]C-NMR specrtrum (Figure 48) contains a peak at 155.0 ppm, assigned to carbon 2 of the cyclic carbonate ring. There are eight peaks ranging from 14.1 ppm to 33.9 ppm referring to the 8 alkyl carbons.

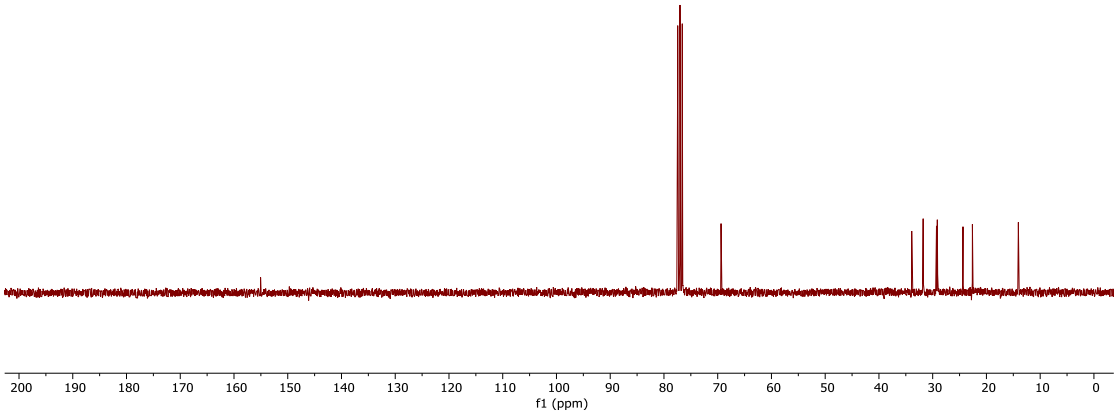

Figure 48: [13]C-NMR spectrum of 4-octyl-1,3-dioxolan-2-one

The molecular ion peak of 4-octyl-1,3-dioxolan-2-one can be seen at 201 m/z, additionally a strong return at 223 m/z correlates to the sodium ion peak of the molecule (Figure 49). Within the IR spectrum (Figure 50) a strong carbonyl peak can be seen at 1790 cm^{-1} as well as a medium strength return in the C-H region at 3000 cm^{-1}.

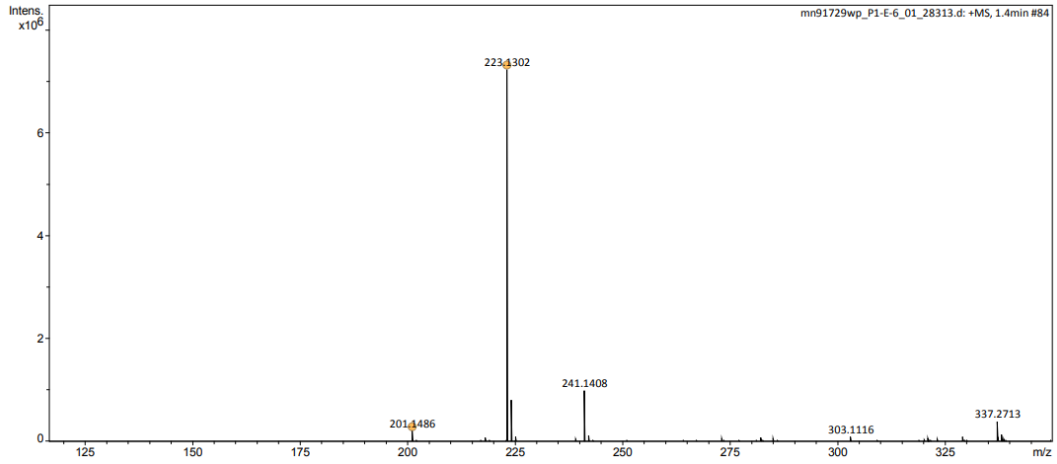

Figure 49: ESI Mass Spectrum of 4-octyl-1,3-dioxolan-2-one

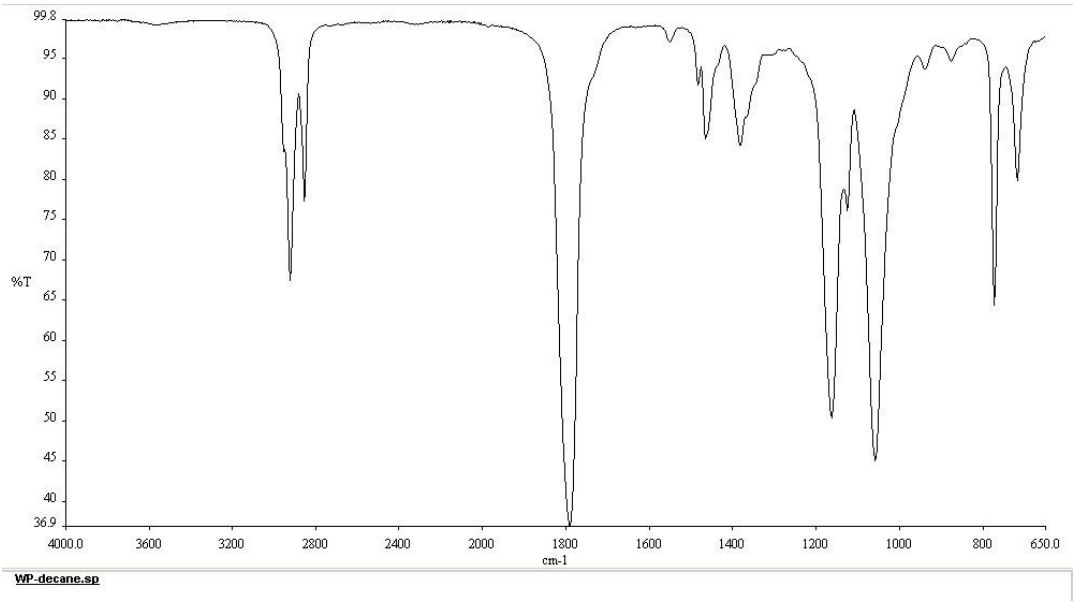

Figure 50: IR spectrum of 4-octyl-1,3-dioxolan-2-one

4.1.6- Synthesis 4-decyl-1,3-dioxolan-2-one

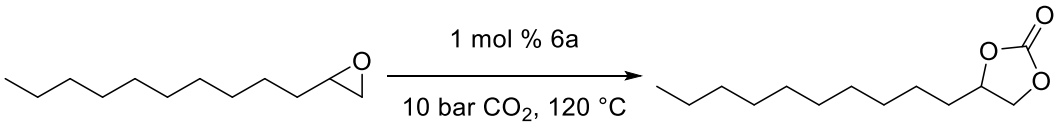

Scheme 16: Synthesis 4-decyl-1,3-dioxolan-2-one

Dodecane oxide was tested concurrently with Decane oxide due to the similarity in structure of the two species and as it was known to be a suitable substrate for this reaction.[23] This similarity resulted in near identical reactivities, as shown in Table 12. Full conversion was achieved after 48 hours, The product was purified by column chromatography eluting with petroleum ether 40-60 (6:4) EtOAc . yielding 4-decyl-1,3-dioxolan-2-one in 88%. The slightly higher yield of this reaction, compared to 1,2-epoxydeacne, may support the hypothesis that the material lost is being lost during the sublimation of the solid CO_2 after the reaction vessel is opened. Though this was not investigated further.

Table 12: Crude conversions of 4-decyl-1,3-dioxolan-2-one and 4-octyl-1,3-dioxolan-2-one after different duration reactions.

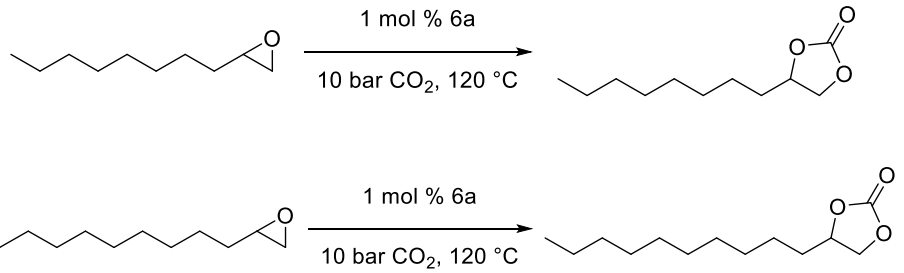

Epoxide	Crude reaction conversion		
	3.5h	**24h**	**48h**
1,2-epoxydecane	19%	40%	**>99%**
1,2-epoxydodecane	12%	40%	**>99%**

Characterisation of 4-decyl-1,3-dioxolan-2-one was accomplished using the combined data from ^{1}H-NMR (Figure 51) ^{13}C-NMR (Figure 52), IR (Figure 54) and Mass Spectrometry (Figure 53). The ^{1}H NMR spectrum of 4-decyl-1,3-dioxolan-2-one is similar to that of 4-octyl-1,3-dioxolan-2-one, the only real change being a difference in integration of the broad multiplet CH_2 peak at 1.29 pm, reflecting the presence of 4 additional hydrogens. The terminal CH_3 appear as a triplet at 0.90 ppm The diasteriotopic hydrogens adjacent to the cyclic carbonate appear as a multiplet stretchinmg between 1.92 ppm and 1.61 ppm. Two doublets of doublets are visible at 4.08 ppm (*J = 8.2, 7.2 Hz*) and 4.54 ppm (*J = 8.2, 7.5 Hz*) caused by the two CH_2 hydrogens on position 5 and the CH hydrogen on position 4 can be seen at 4.72 ppm (*J = 7.5, 7.2, 5.4 Hz*) as a doublet of doublet of triplets.

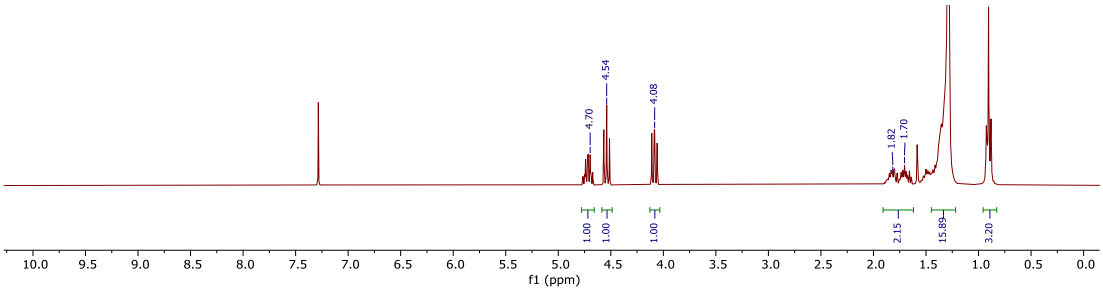

Figure 51: ^{14}H-NMR spectrum of 4-Decyl-1,3-dioxolan-2-one

Again, similar to 4-octyl-1,3-dioxolan-2-one the key peak in the ^{13}C-NMR, is at 155ppm caused by carbon 2 of the cyclic carbonate ring. There are ten peaks ranging from 14.1 ppm to 33.9 ppm referring to the ten alkyl carbons. And an additional peak at 69.4 ppm, which is likely caused by carbon 5 of the carbonate ring.

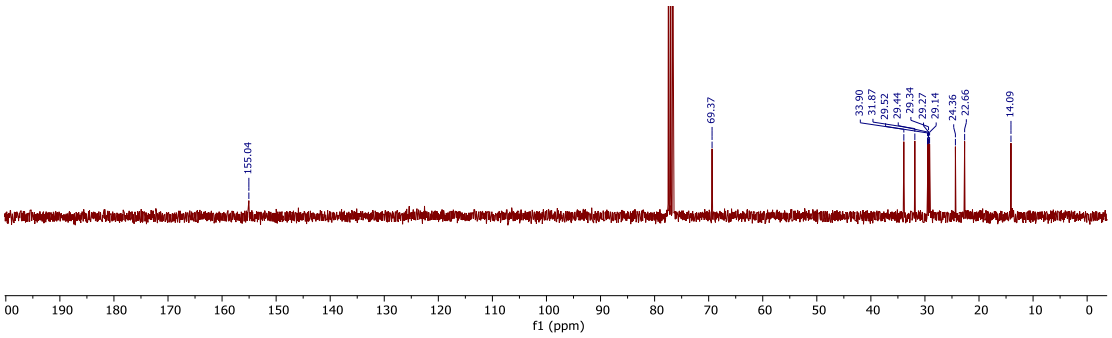

Figure 52: ^{13}C NMR of 4-Decyl-1,3-dioxolan-2-one

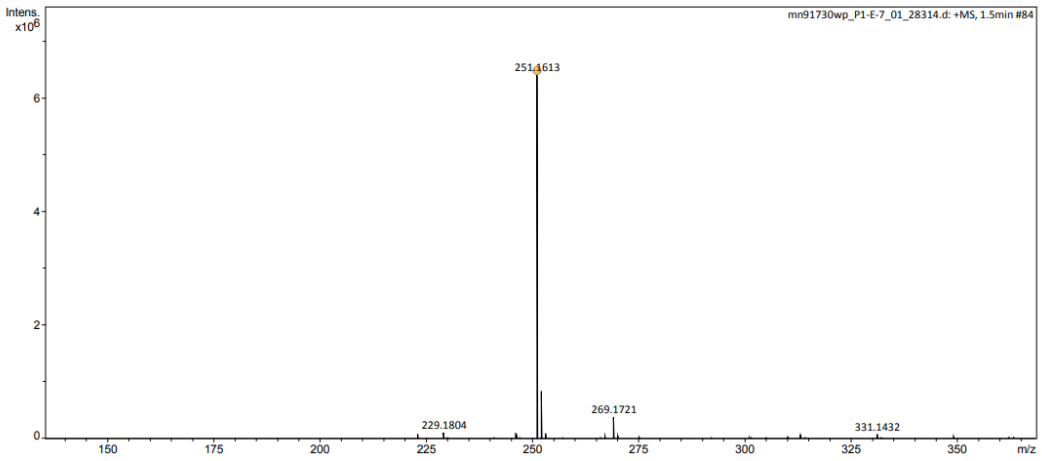

Figure 53: ESI Mass spectrum of 4-decyl-1,3-dioxolan-2-one

The molecular ion peak of 4-decyl-1,3-dioxolan-2-one can be seen at 229 m/z, additionally a strong return at 251 m/z correlates to the sodium ion peak of the molecule (Figure 53). Within the IR spectrum (Figure 54) a strong carbonyl peak can be seen at 1790 cm^{-1} as well as a medium strength return in the C-H region at 3000 cm^{-1}.

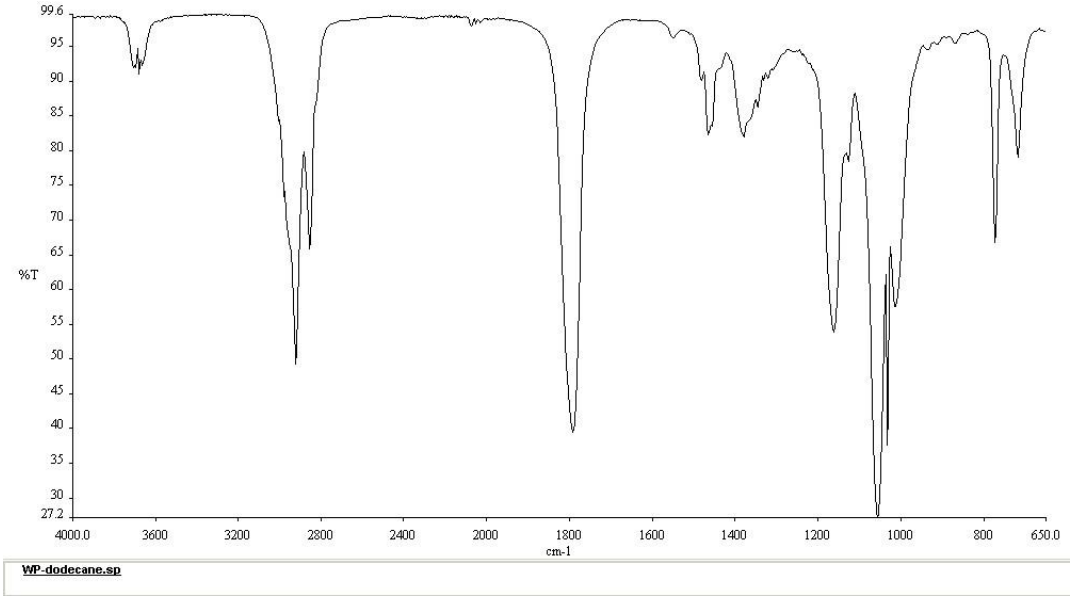

Figure 54: IR spectrum of 4-Decyl-1,3-dioxolan-2-one

4.1.7- Attempted synthesis of 4-(fluoromethyl)-1,3-dioxolan-2-one and 4-chloromethyl-[1,3]dioxolan-2-one

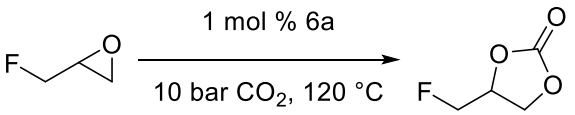

Scheme 17: synthesis of 4-(fluoromethyl)-1,3-dioxolan-2-one

Epifluorohydrin proved to be an incredibly difficult material to utilise for this reaction. Very low (<5%) mass recovery was achieved using this material, meaning up to 95% of the mass of the starting material was unaccounted for after the culmination of the reaction. Where this material is lost to remains unknown, it is possible that the epifluorohydrin had evaporated whilst the reactor was being heated to 120°C and being lost from the reactor by the necessity of the system being unsealed. To overcome this, the reactor was heated prior to the insertion of the reagents, then quickly sealed and pressurised with CO_2. This did not solve the mass loss issue however, with recovery still being negligible. It is also possible that the species fragments under this condition, and that the epifluorohydrin simply could not survive the high temperatures and pressures. The same reaction was conducted at a lower temperature 50°C, with no more success than at 120°C. A system using a suba-seal, such as that discussed previously, was not used in this experiment, it is possible that using a seal would aid in mass recovery, however this was not investigated.

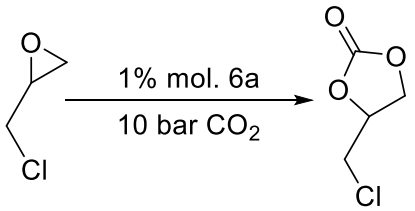

Scheme 18: Scheme synthesis of 4-chloromethyl-[1,3]dioxolan-2-one

Synthesis of 4-chloromethyl-[1,3]dioxolan-2-one (was attempted via the use of epichlorohydrin (Scheme 18) with positive initial results, however full isolation and characterisation was not achieved.

4.1.8- Synthesis 4-bromomethyl-[1,3]dioxolan-2-one

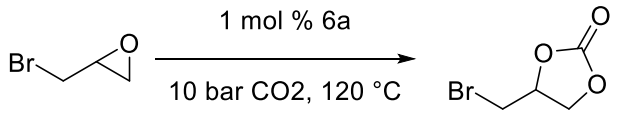

Scheme 19: Synthesis 4-bromomethyl-[1,3]dioxolan-2-one

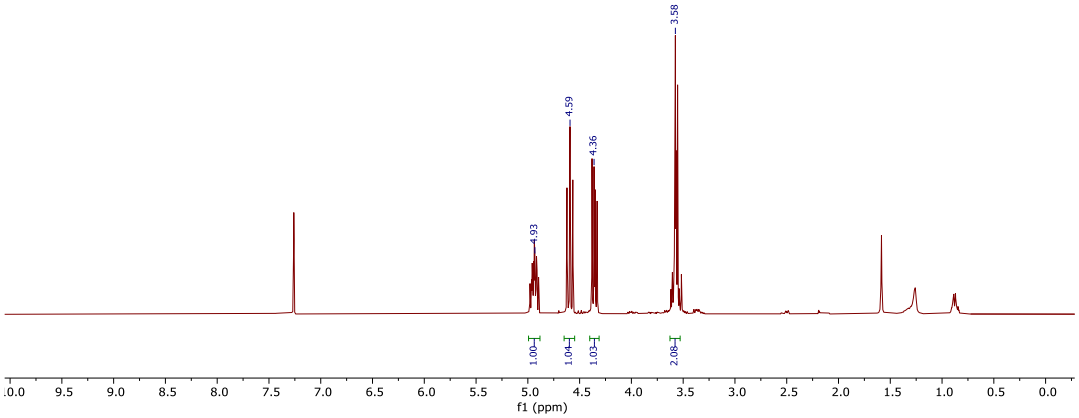

Figure 55: ^{1}H-NMR spectrum of 4-bromomethyl-[1,3]dioxolan-2-one

Synthesis of 4-bromomethyl-[1,3]dioxolan-2-one was attempted via the use of epibromohydrin (3-bromoproylene oxide) and the standard conditions of 120°C, 10 bar CO_2 and 1 mol% of immobilized salophen. More success was achieved in this reaction than with epiflourohudrin, with there being sufficient mass recovery to allow for purification and characterisation. The crude NMR showed a high percentage conversion (>99%) however the purified yield was only 58%. This indicates that, whilst this species is active for this reaction, the conditions used were not optimal, as starting material was being lost. The activity of bromohydrin is an indicator that more work needs to be conducted on epichlorohydrin and epifluorohydrin in order to find conditions for those substrates to be utilised in this reaction.

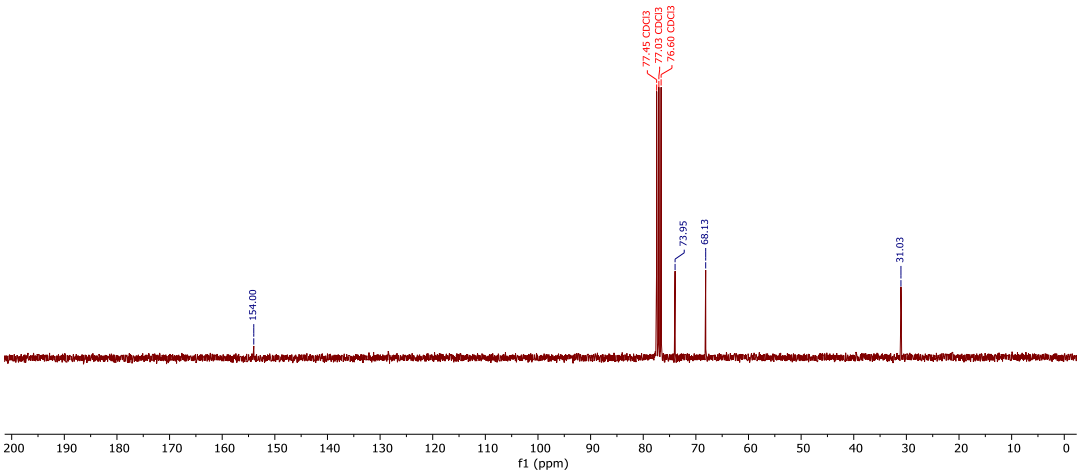

Figure 56: ^{13}C-NMR spectrum of 4-bromomethyl-[1,3]dioxolan-2-one

As previously, 4-bromomethyl-[1,3]dioxolan-2-one was puriofied by column chromatography eluting with petroleum ether-40:60 (6:4) EtOAc to yield pure 4-bromomethyl-[1,3]dioxolan-2-one (58%). The purified hydrogen ^{1}H-NMR contains four peaks, one for each Hydrogen within the cyclic carbonate ring and the terminal CH_2Br.

The ^{13}C-NMR contains four peaks (Figure 56), 154.0 ppm, assigned to carbon 2 of the cyclic carbonate ring. There are three further peaks ranging from 31.0 ppm to 74.0 ppm referring to the three alkyl carbons. As is consistent for the IR spectrum of cyclic carbonates, Figure 57, contains a strong carbonyl peak at 1800 cm^{-1} and a weaker return at 3000 cm^{-1} caused by the alkyl CH Stretch. The ESI spectrum (Figure 58) shows a molecular ion peak at 182.9472 m/z and a second large peak at 184 m/z, this pattern is characteristic of the two isotopes of bromine.

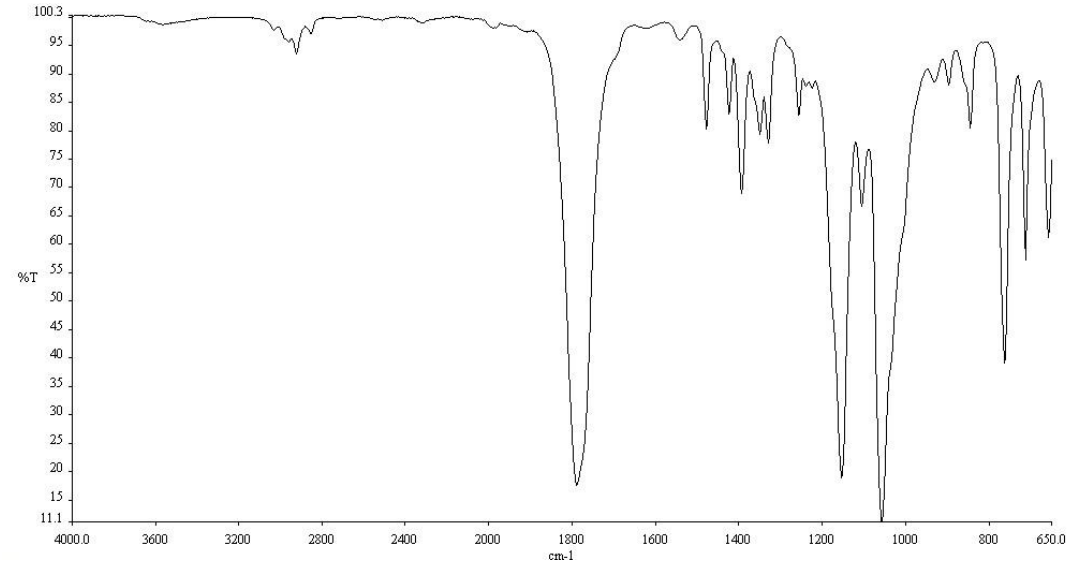

Figure 57: IR spectrum of 4-bromomethyl-[1,3]dioxolan-2-one

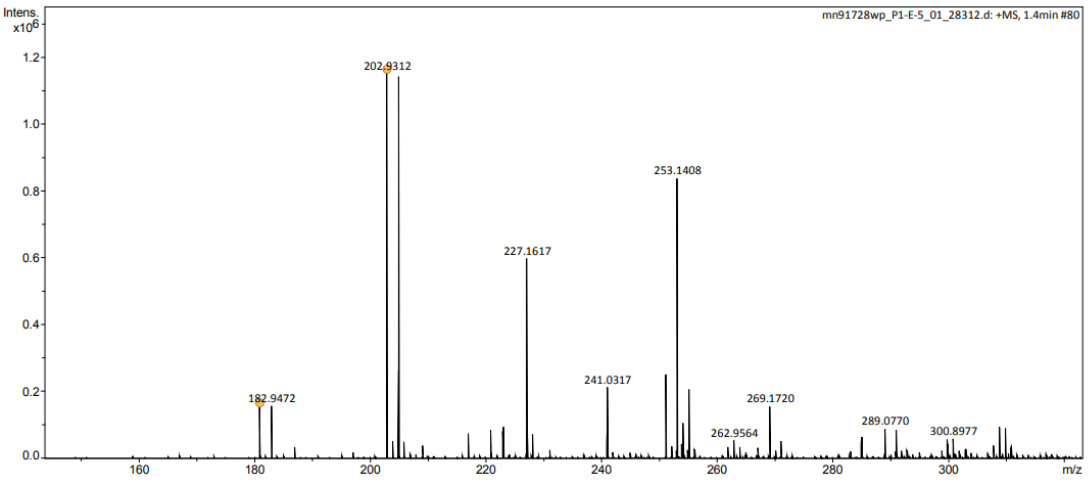

Figure 58: ESI Mass spectrum of 4-bromomethyl-[1,3]dioxolan-2-one

Conclusions

A novel method for producing symmetric silica immobilised salophens has been developed using a five-step synthesis route, starting from a renewable, natural product. The initial demethylation has been improved via the elimination of the production of a by-product and high conversions with reduced equivalents of BBr_3 has been demonstrated. The orthoformylation of 4-allylphenol proceeds in high conversions and yields but has room for further improvement due to the necessity of large equivalents of paraformaldehyde and $MgCl_2$. Large advances in the PtO_2 catalysed hydrosilylation of 2-hydroxy-5-allylbenzaldehyde have been achieved by the development of a novel microwave excited procedure, reducing the reaction time from 24 hours to 60 minutes while simultaneously increasing the enantioselectivity of the reaction via the inclusion of an acidic additive. Immobilisation onto amorphous silica was accomplished via a sol-gel method using tetraethoxy orthosilicate, with control over the stoichiometric ratios defining the ratio of silica to salophen. A range of immobilised salophens have been produced with immobilisation ratios ranging from 5:1 (silica:salophen) to 25:1. These species have subsequently been used to catalyse the synthesis of cyclic carbonates from a range of epoxides and CO_2.

High activity has been demonstrated for a number of epoxides, notably 3-phenoxypropene oxide, styrene oxide, chlorostyrene oxide, 1,2-epoxydecane and 1,2-epoxydodecane. These species have been utilised in the afore mentioned reaction to produce their corresponding cyclic carbonates in high yield. The crude conversions and isolated yields for the formation of cyclic carbonates are comparable, and in some cases higher than, those obtained using the equivalent homogeneous catalysts.[21,23] **6a**, demonstrated higher activity for the synthesis of 4-phenyl-1,3-dioxolan-2-one (99%

conversion, 95% isolated yield) than the homogeneous manganese(III) salen complexes produced by Baiker *et al.* (35% isolated yield), whilst operating under milder conditions.[21] A resin supported bimetallic aluminium salen complex produced by the North group produced 4-phenyl-1,3-dioxolan-2-one in 79% yield, lower than the yield obtained by the silica immobilised salophen. Similar yields were obtained to that of electrochemically driven attempts at synthesising cyclic carbonates as demonstrated by Yuan *et al.* (66-98% isolated yield of 4-phenyl-1,3-dioxolan-2-one).[21]

Future Work

There is scope for a large amount of work to conducted based on the research presented in this thesis. Firstly, this synthesis route has been designed for versatility and can be easily modified to produce asymmetric immobilised salophens, immobilised salens (with many different imine bridge structures) and asymmetric immobilised salens.

Secondly, only the insertion of CO_2 into epoxides has been examined in this thesis, but as discussed in section 1.5- salens and salophens are able to host a wide variety of metal ions and catalyse a vast number of commercially and academically relevant reactions. The materials produced in the route described should be investigated for these two factors.

Thirdly, the activity of these silica immobilised salophens for the insertion of CO_2 into epoxides has been demonstrated and presents an opportunity for the development of CO_2 utilisation technology and methodologies within the production of cyclic carbonates, especially with regard to carbon capture and utilisation within flow conditions.

Chapter 5 Experimental

5.1- Synthesis of 4-Allylphenol-**2a**

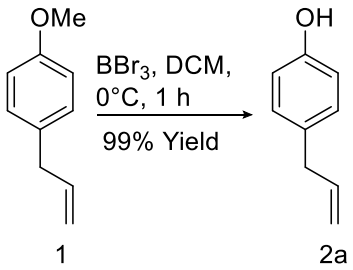

5.1.1- Synthesis using aqueous quench

To a solution of 4-allylanisole, **1,** (1.501 mmol, 2.224 g) in CH_2Cl_2 (14.50ml), 1.1 molar equivalents of BBr_3 (16.50 mL, 1 M in CH_2Cl_2) were added dropwise at 273K. The reaction mixture was stirred at 273K for 60 minutes, then quenched dropwise with ice-cold deionised H_2O (30mL). The product was extracted with CH_2Cl_2 (2x30mL), washed with H_2O (2x20ml), brine (20mL) and dried with $MgSO_4$. The solvent was removed in vacuo and the residue was purified by column chromatography using silica gel (50g) eluting with EtOAc/Hexane (1/9) to yield pure 4-allylphenol, **2a,** (1.038 g, 51%) as a yellow oil. ^{1}H-NMR ($CDCl_3$, 300MHz) δ 7.08 (d, 2H, *J = 8.3 Hz*), 6.80 (dt, 2H, *J = 8.3, 2.1 Hz*), 5.98 (ddt 1H, *J = 16.0, 10.7, 6.7 Hz*), 5.09 (dt, 1H, *J = 16.0, 1.6 Hz*), 5.08 (dt, 1H, *J = 10.7, 1.6 Hz*), 3.33 (d, 2H, *J= 6.7 Hz*); ^{13}C-NMR ($CDCl_3$, 300MHz)= 153.8 , 137.8 , 132.3 , 129.7 , 115.5 , 115.2 , 39.2; IR (neat) ν̃= 3314, 1220, 1180 cm^{-1}; HRMS (ESI^+): calcd for C_9H_9O $[M-H]^+$ 133.0653 found at 133.0645

5.1.2- Basic work-up procedure

To a solution of 4-allylanisole **1** (1.501 mmol, 2.224 g) in CH_2Cl_2 (14.50 mL), 1.1 molar equivalents of BBr_3 (16.50 mL, 1M in CH_2Cl_2) were added dropwise at 273K. The

reaction mixture was stirred at 273K for 60 minutes. The reaction mixture was added dropwise to a 2M solution of NaOH in H_2O. The resulting mixture was then neutralised with 1M HCl solution The product was extracted with CH_2Cl_2 (2x30mL), washed with H_2O (2x20 mL), brine (20 mL) and dried with $MgSO_4$. The solvent was removed in vacuo and the residue was purified by column chromatography using silica gel (50g) eluting with EtOAc/Hexane (1/9) to give 4-allylphenol, **2a,** (1.801g, 88%) as a yellow oil. ^{1}H-NMR ($CDCl_3$, 300MHz) δ 7.08 (d, 2H, *J = 8.3 Hz*), 6.80 (d, 2H, *J = 8.3Hz*), 5.98 (ddt 1H, *J = 16.0, 10.7, 6.7 Hz*), 5.09 (dt, 1H, *J* = 16.0, 1.6 Hz), 5.08 (dt, 1H, *J = 10.7, 1.6 Hz*), 3.33 (d, 2H, *J= 6.7 Hz*); ^{13}C-NMR ($CDCl_3$, 300MHz)= 153.8 (Phenol-C), 137.8 (ArC), 132.3 (ArCH), 129.7 (ArCH), 115.5 (C=CH), 115.2 ($C=CH_2$), 39.2 (CH_2);IR (neat) ῡ= 3314, 1220, 1180 cm^{-1}; HRMS (ESI^+): calcd for C_9H_9O $[M-H]^+$ 133.0653 found at 133.0645

5.2- Synthesis of 2-hydroxy-5-allylbenzaldehyde **3a**

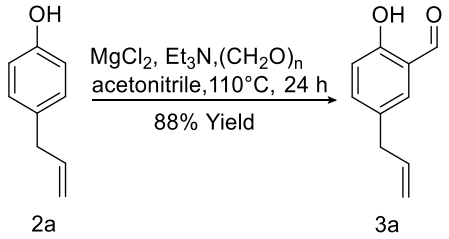

4-Allylphenol, **2a,** (6.400 mmol, 1.038 g) was dissolved in MeCN (30ml), to which was added 2.5 equivalents of $MgCl_2$ (19.49 mmol,1.856g) , 4 equivalents of Et_3N (31.20 mmol, 3.157g) and 10 equivalents of paraformaldehyde (77.92 mmol, 2.340g) . The reaction mixture was heated to 383K and stirred at 490 rpm for 24 hours. The reaction was quenched with aqueous HCl (40 mL, 1 M), the product was extracted with EtOAc (3x30 mL) and the combined organic phase was washed with H_2O (2x30 mL) and brine (30 mL), then dried with $MgSO_4$. The solvent was removed in vacuo, and the residue purified

via column chromatography using silica gel (35g) eluting with petroleum ether 15:1 EtOAc to yield 2-hydroxy-5-allylbenzaldehyde, **3a,** as a yellow oil (1.102 g, 88 %). ^{1}H-NMR ($CDCl_3$, 300MHz) δ 10.9 (s, 1H), 9.98 (s, 1H), 7.38 (m, 2H), 6.95 (m, 1H), 5.94 (m, 1H), 5.12 (m, 2H), 3.40 (d, 2H, *J=6 Hz*) ^{13}C-NMR ($CDCl_3$, 300MHz)= 196.5, 160.1, 137.6, 136.9, 133.2, 131.5, 120.5, 117.6, 116.4, 38.8; IR (neat) ῡ= 2980, 1650, 1590 cm^{-1}; HRMS (ESI^+) calcd for $C_{10}H_9O_2$ $[M-H]^+$ 161.0603 found at 161.0616.

5.3- Synthesis of 2-hydroxy-5-(3-triethoxysilylpropyl) benzaldehyde -**4a**

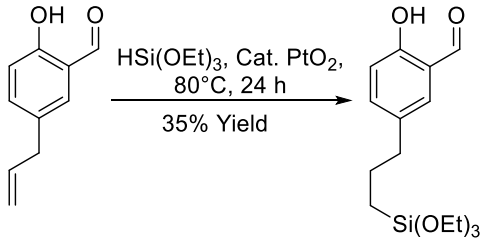

3a **4a**

5.3.1- Synthesis **4a** by reflux

2-Hydroxy-5-allylbenzaldehyde, **3a,** (1.498 mmol, 0.2430g) was combined with 1.1 equivalents of $HSi(OEt)_3$ (1.7 mmol, 0.2790 g) and 0.01 equivalents of solid PtO_2 ($1.5x10^{-2}$ mmol, 3.4 mg) and heated to 358K with stirring at 300rpm for 24 hours in a sealed glass vial.

5.3.2- Synthesis of **4a** by microwave

2-Hydroxy-5-allylbenzaldehyde, **3a,** (1.498 mmol, 0.2430g) was combined with 1.1 equivalents of $HSi(OEt)_3$ (1.698 mmol, 0.2790g) and 0.01 equivalents of solid PtO_2 ($1.5x10^{-2}$mmol, 3.4mg) in a 7 mL glass microwave vial. The mixture was microwaved in a CEM Discover microwave set to 385 K for 15 minutes with a power setting of 80 watts.

5.3.3- Extraction of **4a**

The reaction mixture was spun in a benchtop centrifuge for 5 minutes. The PtO_2 catalyst was recovered and the remaining liquid placed under a vacuum to yield crude 2-hydroxy-5-(3-triethoxysilylpropyl) benzaldehyde -**4a**. (0.4753 g, 94%) ^{1}H-NMR ($CDCl_3$, 300MHz) δ 10.78 (s, 1H), 9.79 (s, 1H) 7.37 (m, 2H), 6.91(dd, 1H, *J= 9.2, 2.1 Hz*), 3.80 (q, 6H, *J=6.9 Hz*), 2.56 (t, 2H, *J= 7.6 Hz*), 1.72 (m, 2H), 1.14 (t, 9H, *J= 6.9 Hz*) 0.57 (t, 2H, *J=8.1 Hz*); ^{13}C-NMR ($CDCl_3$, 300MHz)= 196.6, 159.8, 137.5, 133.9, 133.0, 120.4, 117.4, 59.2, 58.4, 37.8, 24.8, 18.3, 10.0; HRMS (ESI^+) calcd for $C_{16}H_{26}O_5SiNa$ $[M+Na]^+$ 349.1447 found at 349.1448

5.4- Imine formation and Immobilisation onto silica

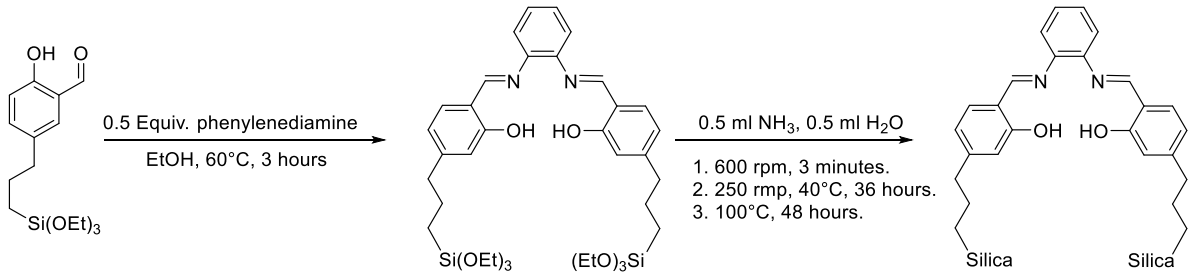

5a **6a**

2-Hydroxy-5-(3-triethoxysilylpropyl)benzaldehyde, **4a**, (0.7692 mmol, 0.2285g) was dissolved in EtOH 99.9% (1 mL) to which was added 0.5 equivalents of phenylenediamine (0.3588 mmol, 0.0388g). The mixture was heated to 333K for 3 hours before being cooled to 298 K, producing salophen **5a.**

To 1mL a solution of NH_3 in H_2O (1:1 by volume) was added dropwise tetraethyl orthosilicate (5-20 equivalents) and stirred at 600 rpm for 3 minutes. To this mixture was then added the solution containing salophen **5a.** The resulting reaction was heated to 313 K and left stirring at 250 rpm for 36 hours. The temperature was then increased to 483 K

and the reaction vessel was heated for a further 2 days with no stirring. The resulting product was then washed with H_2O (2x10 mL), EtOH (2x10 mL) and EtOAc (2x10 mL) and dried at 353K for 24 hours in a vacuum oven, yielding silica immobilised salophen **6a** as a yellow powder (0.4380 g, 86%).^{13}C-NMR (Solid state, 300MHz) δ=158.7, 153.5, 141.3, 132.6, 123.6, 119.1, 114.2, 36.2, 24.0 11.3; IR (neat) ῡ= 1100 cm^{-1}; Found: C, 21.1; H, 2.3; N, 2.2%; calculated for $C_{26}H_{26}N_2O_{38}Si_{17}$: C, 21.2; H, 1.9; N, 1.9%.

5.5- Cyclic carbonate synthesis

5.5.1- Synthesis of 4-(phenoxy)methyl-1,3-dioxolane-2-one at 1bar.

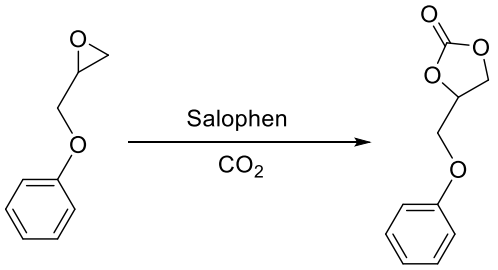

3-Phenoxypropylene oxide (2mmol) was weighed into a 7 mL glass vial equipped with a stirrer bar. 1 mol % of immobilised salophen **6a** ($1.0x10^{-2}$ mmol, 14 mg) was added to the vial, before the vial was sealed with a Suba seal. The vial was purged of air using a CO_2 balloon 3 times before being fitted with two CO_2 balloons. The reaction vessel was then heated to 393 K with a stirring rate of 300 rpm for 3.5 hours, after which the vessel was cooled to room temperature and the balloons removed. $CHCl_3$ (2 mL) was added to the vial and the mixture was transferred to a 2 mL centrifuge vial. The reaction mixture was spun in a benchtop centrifuge for 5 minutes, the solvent was collected and evaporated in vacuo yielding crude 3-phenoxypropylene carbonate. The catalyst remaining in the centrifuge vial was collected for re-use. The crude mixture was purified by column chromatography using silica gel (10 g) eluting with petroleum ether-40:60 (6:4) EtOAc to yield pure 4-(phenoxy)methyl-1,3-dioxolane-2-one. (Lit.[23,24]);^{1}H-NMR ($CDCl_3$, 300MHz) δ= 7.33 (dt, 2H, *J=7.3, 1.4 Hz*), 7.04 (t, 1H, *J=8.5 Hz*), 6.94(d, 2H, *J=8.5 Hz*), 5.04 (ddt, 1H, *J= 8.1, 6.1, 4.0 Hz*), 4.58 (m, 2H) , 4.24(dd, 1H, *J=10.6, 4.0 Hz*), 4.16(dd, 1H, *J=10.6, 6.1 Hz*); ^{13}C-NMR ($CDCl_3$, 300MHz)=157.0, 129.0, 122.0, 114.0, 72.0, 67.0, 66.2; IR (neat) ῡ= 3000, 1790 cm^{-1}; HRMS (ESI^+) calcd for $C_{10}H_{10}O_4Na$ $[M+Na]^+$ 217.0476 found at 217.0465

5.5.2- Synthesis of 4-(phenoxy)methyl-1,3-dioxolane-2-one at 10 bar

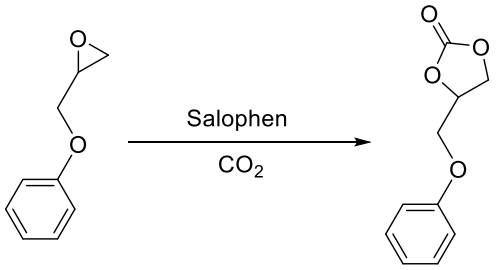

3-Phenoxypropylene oxide (0.3579g, 2.383 mmol) was weighed into a 7 mL glass vail equipped with a stirrer bar. 1 mol % of immobilised salophen **6a** ($1.0x10^{-2}$ mmol, 14mg) was added to the vial. The vial was placed inside a 500 mL steel autoclave preheated to 120°C. The autoclave was sealed and flushed with CO_2 three times before being pressurised to 10 bar with CO_2. The vessel was held at reaction temperature with stirring of 350 rmp for 3.5 hours. The autoclave was rapidly cooled with liquid N_2. The autoclave was opened and left to equilibrate to room temperature. EtOAc (2 mL) was added to the reaction vial, and the mixture was transferred to a 2ml centrifuge vial. The reaction mixture was spun in a benchtop centrifuge for 5 minutes, the solvent was removed in vacuo yielding crude 4-(phenoxy)methyl-1,3-dioxolane-2-one. The solid catalyst was recovered from the centrifuge vial and dried on a high-vacuum line for 24 hours. Crude 4-(phenoxy)methyl-1,3-dioxolane-2-one was purified by column chromatography using silica gel (10g) eluting with petroleum ether-40:60 (6:4) EtOAc yielding pure 4-(phenoxy)methyl-1,3-dioxolane-2-one (0.3982g, 78%) (Lit.[23,24]). ^{1}H-NMR ($CDCl_3$, 300MHz) δ= 7.33 (dt, 2H, *J=7.3, 1.4 Hz*), 7.04 (t, 1H, *J=8.5 Hz*), 6.94(d, 2H, *J=8.5 Hz*), 5.04 (ddt, 1H, *J= 8.1, 6.1, 4.0 Hz*), 4.58 (m, 2H), 4.24(dd, 1H, *J=10.6, 4.0 Hz*), 4.16(dd, 1H, *J=10.6, 6.1 Hz*); ($CDCl_3$, 300MHz)=157.0, 129.0, 122.0, 114.0, 72.0, 67.0, 66.2; IR (neat) ν̃= 3000, 1790 cm^{-1} HRMS (ESI^+) calcd for $C_{10}H_{10}O_4Na$ $[M+Na]^+$ 217.0476 found at 217.0465

5.5.3- Synthesis of 4-Phenyl-1,3-dioxolan-2-one at 10 bar

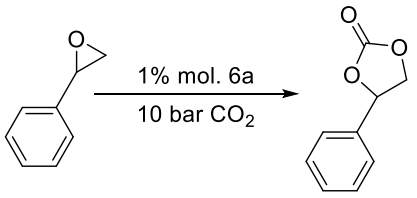

Styrene oxide (0.2400 g, 2.0 mmol) was weighed into a 7 mL glass vail equipped with a stirrer bar. 1 mol % of immobilised salophen **6a** (1.0×10^{-2} mmol, 14mg) was added to the vial. The vial was placed inside a 500ml steel autoclave preheated to 120°C. The autoclave was sealed and flushed with CO_2 three times before being pressurised to 10 bar with CO_2. The vessel was held at reaction temperature with stirring of 350 rmp for 3.5 hours. The autoclave was rapidly cooled with liquid N_2. The autoclave was opened and left to equilibrate to room temperature. EtOAc (2 mL) was added to the reaction vial, and the mixture was transferred to a 2ml centrifuge vial. The reaction mixture was spun in a benchtop centrifuge for 5 minutes, the solvent was removed in vacuo yielding crude 4-Phenyl-1,3-dioxolan-2-one. The solid catalyst was recovered from the centrifuge vial and dried on a high-vacuum line for 24 hours. Crude 44-Phenyl-1,3-dioxolan-2-one was purified by column chromatography using silica gel (10 g) eluting with petroleum ether-40:60 (6:4) EtOAc yielding pure 4-Phenyl-1,3-dioxolan-2-one(0.3096g, 95%,) (Lit.[23,24]); ^{1}H-NMR ($CDCl_3$, 300MHz) δ= 7.42(m, 5H), 5.70(dd, 1H, *J= 8.4, 8.2 Hz*), 4.82d, 1H, *J= 8.4 Hz*), 4.37(d, 1H, *J= 8.2 Hz*); ^{13}C-NMR ($CDCl_3$, 300MHz)=154.4, 137.0, 127.8, 129.2, 123.7, 79.0, 70.0; IR (neat) $\tilde{\nu}$= 3000, 2850, 1790 cm^{-1}; HRMS (ESI^+) calcd for $C_9H_8O_3Na$ $[M+Na]^+$ 187.0371 found at 187.0436

5.5.4- Synthesis of 4-(4-chlorophenyl)-[1,3]-dioxolan-2-one at 10 bar

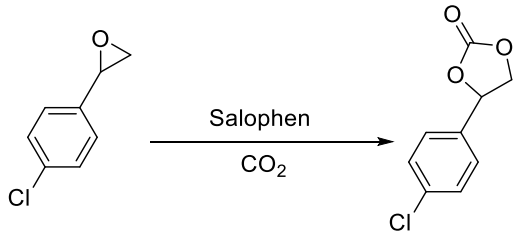

4-chlorostyrene oxide (0.2901g, 1.876 mmol) was weighed into a 7 mL glass vail equipped with a stirrer bar. 1 mol % of immobilised salophen **6a** (1.0×10^{-2} mmol, 14mg) was added to the vial. The vial was placed inside a 500ml steel autoclave preheated to 120°C. The autoclave was sealed and flushed with CO_2 three times before being pressurised to 10 bar with CO_2. The vessel was held at reaction temperature with stirring of 350 rmp for 3.5 hours. The autoclave was rapidly cooled with liquid N_2. The autoclave was opened and left to equilibrate to room temperature. EtOAc (2 mL) was added to the reaction vial, and the mixture was transferred to a 2 mL centrifuge vial. The reaction mixture was spun in a benchtop centrifuge for 5 minutes, the solvent was removed in vacuo yielding crude 4-(4-chlorophenyl)-[1,3]-dioxolan-2-one one. The solid catalyst was recovered from the centrifuge vial and dried on a high-vacuum line for 24 hours. Crude 4-(4-chlorophenyl)-[1,3]-dioxolan-2-one was purified by column chromatography using silica gel (10 g) eluting with petroleum ether-40:60 (6:4) EtOAc yielding 4-(4-chlorophenyl)-[1,3]-dioxolan-2-one (0.3307g, 89%) (Lit.[23,24]); ^{1}H-NMR ($CDCl_3$, 300MHz) δ= 7.42(m, 2H), 7.30 (m, 2H), 5.65 (dd,1H, *J=8.3, 7.9 Hz*), 4.79 (dd,1H, *J= 8.7, 8.3 Hz*), 4.30 (dd,1H, *J= 8.7, 7.9 Hz*); IR (neat) ῡ= 3000,1790 cm^{-1}.HRMS (ESI^+) calcd for $C_9H_8ClO_3$ $[M+H]^+$ 199.0161 found at 199.0156.

5.5.5- Synthesis of 4-octyl-1,3-dioxolan-2-one at 10 bar

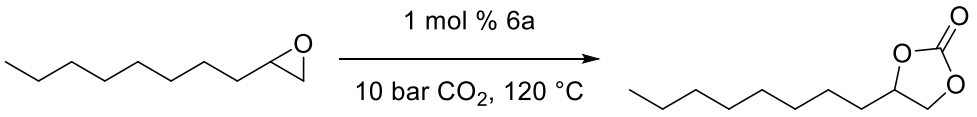

1,2 epoxy decane (0.3068g, 1.963 mmol) was weighed into a 7 mL glass vail equipped with a stirrer bar. 1 mol % of immobilised salophen **6a** (1.0 $x10^{-2}$ mmol, 14 mg) was added to the vial. The vial was placed inside a 500 mL steel autoclave preheated to 120 °C. The autoclave was sealed and flushed with CO_2 three times before being pressurised to 10 bar with CO_2. The vessel was held at reaction temperature with stirring of 350 rmp for 3.5, 24 or 48 hours. The autoclave was rapidly cooled with liquid N_2. The autoclave was opened and left to equilibrate to room temperature. EtOAc (2 mL) was added to the reaction vial, and the mixture was transferred to a 2ml centrifuge vial. The reaction mixture was spun in a benchtop centrifuge for 5 minutes, the solvent was removed in vacuo yielding crude -octyl-1,3-dioxolan-2-one. The solid catalyst was recovered from the centrifuge vial and dried on a high-vacuum line for 24 hours. Crude -octyl-1,3-dioxolan-2-one was purified by column chromatography using silica gel (10g) eluting with petroleum ether-40:60 (6:4) EtOAc yielding pure -octyl-1,3-dioxolan-2-one (0.3066g, 78%) (Lit.[23,24]); ^{1}H-NMR ($CDCl_3$, 300MHz) δ= 4.69 (ddt, 1H, *J= 7.5, 7.5, 5.5 Hz*), 4.52 (t, H, *J= 8.2,7.5 Hz*), 4.06(dd, 1H, *J= 8.2, 7.5 Hz*), 1.74 (m, 2H), 1.27 (m, 12H), 0.88 (m, 3H); ^{13}C-NMR ($CDCl_3$, 300MHz)= 155.0, 77.0, 69.4, 33.9, 31.8, 29.2, 29.1, 29.1, 24.4, 22.6, 14.1; IR (neat) ῡ= 3000, 1790 cm^{-1}; HRMS (ESI^+) calcd for $C_{11}H_{21}O_3$ $[M+H]^+$ 201.1490 found at 201.1486.

5.5.6- Synthesis of 4-decyl-1,3-dioxolan-2-one at 10 bar

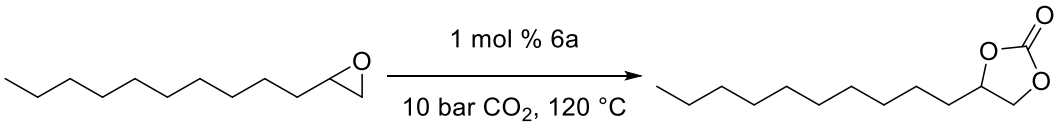

1,2 epoxy dodecane (0.3688g, 2.001 mmol) was weighed into a 7 mL glass vail equipped with a stirrer bar. 1 mol % of immobilised salophen **6a** (1.0 x10^{-2} mmol, 14mg) was added to the vial. The vial was placed inside a 500 mL steel autoclave preheated to 120 °C. The autoclave was sealed and flushed with CO_2 three times before being pressurised to 10 bar with CO_2. The vessel was held at reaction temperature with stirring of 350 rmp for 3.5, 24 or 48 hours. The autoclave was rapidly cooled with liquid N_2. The autoclave was opened and left to equilibrate to room temperature. EtOAc (2 mL) was added to the reaction vial, and the mixture was transferred to a 2ml centrifuge vial. The reaction mixture was spun in a benchtop centrifuge for 5 minutes, the solvent was removed in vacuo yielding crude 4-decyl-1,3-dioxolan-2-one. The solid catalyst was recovered from the centrifuge vial and dried on a high-vacuum line for 24 hours. Crude 4-decyl-1,3-dioxolan-2-one was purified by column chromatography using silica gel (10g) eluting with petroleum ether-40:60 (6:4) EtOAc yielding pure 4-decyl-1,3-dioxolan-2-one (0.3882g, 88%) (Lit.[23,24]); ^{1}H-NMR ($CDCl_3$, 300MHz) δ= 4.72 (ddt, 1H, *J = 7.5, 7.2, 5.4 Hz*), 4.54 (dd, 1H, *J = 8.2, 7.5 Hz*), 4.08 (dd, 1H, *J = 8.2, 7.2 Hz*), 1.92–1.61 (m, 2H), 1.55–1.20 (m, 17H), 0.96 – 0.82 (m, 3H); ^{13}C-NMR ($CDCl_3$, 300MHz) δ=155.0, 69.4, 52.1, 33.9, 31.9, 29.5, 29.4, 29.3, 29.3, 29.1, 24.4, 22.7, 14.1; IR (neat) ῡ= 3000, 1790 cm^{-1}; HRMS (ESI^+) calcd for $C_{13}H_{25}O_3$ $[M+H]^+$ 229.1803 found at 229.1803.

5.5.7- Attempted synthesis of 4-(fluoromethyl)-1,3-dioxolan-2-one at 10 bar

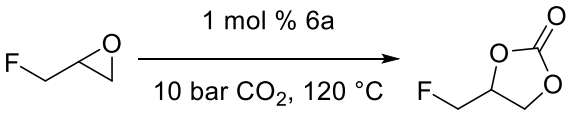

Epiflourohydrin (2mmol) was weighed into a 7 mL glass vail equipped with a stirrer bar. 1 mol % of immobilised salophen **6a** ($1x10^{-2}$ mmol, 14mg) was added to the vial. The vial was placed inside a 500ml steel autoclave preheated to 120°C. The autoclave was sealed and flushed with CO_2 three times before being pressurised to 10 bar with CO_2. The vessel was held at reaction temperature with stirring of 350rmp for 3.5 hours. The autoclave was rapidly cooled with liquid N_2. The autoclave was opened and left to equilibrate to room temperature. EtOAc (2ml) was added to the reaction vial, and the mixture was transferred to a 2ml centrifuge vial. The reaction mixture was spun in a benchtop centrifuge for 5 minutes, the solvent was removed in vacuo yielding crude 4-(fluoromethyl)-1,3-dioxolan-2-one

5.5.8- Synthesis of 4-bromomethyl-[1,3]dioxolan-2-one at 10 bar

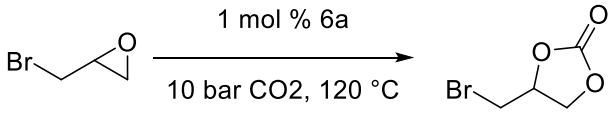

Epibromohydrin (0.2915g, 2.172 mmol) was weighed into a 7 mL glass vail equipped with a stirrer bar. 1 mol % of immobilised salophen **6a** ($1.0\ x10^{-2}$ mmol, 14 mg) was added to the vial. The vial was placed inside a 500ml steel autoclave preheated to 120°C. The autoclave was sealed and flushed with CO_2 three times before being pressurised to 10 bar with CO_2. The vessel was held at reaction temperature with stirring of 350 rmp for 3.5, 24 or 48 hours. The autoclave was rapidly cooled with liquid N_2. The autoclave was

opened and left to equilibrate to room temperature. EtOAc (2 mL) was added to the reaction vial, and the mixture was transferred to a 2 mL centrifuge vial. The reaction mixture was spun in a benchtop centrifuge for 5 minutes, the solvent was removed in vacuo yielding crude 4-bromomethyl-[1,3]dioxolan-2-one. The solid catalyst was recovered from the centrifuge vial and dried on a high-vacuum line for 24 hours. 4-bromomethyl-[1,3]dioxolan-2-one was purified by column chromatography using silica gel (10g) eluting with petroleum ether-40:60 (6:4) EtOAc yielding pure 4-bromomethyl-[1,3]dioxolan-2-one (0.2462, 58%) (Lit.[23,24]) ;^{1}H-NMR ($CDCl_3$, 300MHz) δ= 4.96 (ddd, 1H, *J = 8.1, 6.5, 5.9 Hz*), 4.62 (dd, 1H, *J = 8.9, 8.1 Hz*), 4.38 (dd, 1H, *J = 8.9, 5.9 Hz*), 3.59 (d, 3H, *J = 6.5 Hz*);^{13}C-NMR ($CDCl_3$, 300MHz) δ = 154.0, 73.9, 68.1, 31.0; IR (neat) ῡ= 3000, 1800 cm^{-1}; HRMS (ESI^+) calcd for $C_4H_5BrO_3Na$ 202.9319 found at 202.9312.

References

1 Intergovernmental Panel on Climate Change and O. Edenhofer, Eds., *Climate change 2014: mitigation of climate change: Working Group III contribution to the Fifth Assessment Report of the Intergovernmental Panel on Climate Change*, Cambridge University Press, New York, NY, 2014.

2 [Core Writing Team, R.K. Pachauri and L.A. Meyer (eds.)]., *Climate Change 2014: Synthesis Report. Contribution of Working Groups I, II and III to the Fifth Assessment Report of the Intergovernmental Panel on Climate Change*, IPCC, Geneva, Switzerland, 2014.

3 Global Temperture Vital Signs, https://climate.nasa.gov/vital-signs/global-temperature/, (accessed 7 March 2021).

4 K. Jahnke, C. F. Fendt, M. Fouesneau, T. Herbst and *et. al*, *Nat. Astron.*, 2020, **4**, 4.

5 M. Collins, R. Knutti, J. Arblaster, J.-L. Dufresne, T. Fichefet, P. Friedlingstein, X. Gao, W.J. Gutowski, T. Johns, G. and Krinner, M. Shongwe, C. Tebaldi, A.J. Weaver and M. Wehner, *Long-term Climate Change: Projections, Commitments and Irreversibility. In: Climate Change 2013: The Physical Science Basis. Contribution of Working Group I to the Fifth Assessment Report of the Intergovernmental Panel on Climate Change*, Cambridge University Press, Cambridge, United Kingdom and New York, NY, USA.

6 T. Barnett, R. Malone, W. Pennell, D. Stammer, B. Semtner and W. Washington, *Clim. Change*, 2004, **62**, 1–11.

7 T. P. Barnett, D. W. Pierce, H. G. Hidalgo, C. Bonfils, B. D. Santer, T. Das, G. Bala, A. W. Wood, T. Nozawa, A. A. Mirin, D. R. Cayan and M. D. Dettinger, *Science*, 2008, **319**, 1080–1083.

8 *Kyoto Protocol to The United Nations Framework Convention on Climate Change*, United Nations Framework Convention on Climate Change (UNFCCC), 1997.

9 L. Bengtsson, *Environ. Res. Lett.*, 2010, **5**, 025202.

10 D. A. Lashof and D. R. Ahuja, *Nature*, 1990, **344**, 529–531.

11 Global Warming Potentials (IPCC Second Assessment Report), https://unfccc.int/process/transparency-and-reporting/greenhouse-gas-data/greenhouse-gas-data-unfccc/global-warming-potentials.

12 S. Solomon, Intergovernmental Panel on Climate Change and Intergovernmental Panel on Climate Change, Eds., *Climate change 2007: the physical science basis: contribution of Working Group I to the Fourth Assessment Report of the Intergovernmental Panel on Climate Change*, Cambridge University Press, Cambridge ; New York, 2007.

13 M. Maiss and C. A. M. Brenninkmeijer, *Environ. Sci. Technol.*, 1998, **32**, 3077–3086.

14 W. R. L. Anderegg, J. W. Prall, J. Harold and S. H. Schneider, *Proc. Natl. Acad. Sci.*, 2010, **107**, 12107–12109.

15 A. E. Creamer and B. Gao, *Environ. Sci. Technol.*, 2016, **50**, 7276–7289.

16 J. N. Knudsen, J. N. Jensen, P.-J. Vilhelmsen and O. Biede, *Energy Procedia*, 2009, **1**, 783–790.

17 E. S. Sanz-Pérez, C. R. Murdock, S. A. Didas and C. W. Jones, *Chem. Rev.*, 2016, **116**, 11840–11876.

18 J. Koornneef, A. Ramírez, W. Turkenburg and A. Faaij, *Prog. Energy Combust. Sci.*, 2012, **38**, 62–86.

19 Z. Yuan, M. R. Eden and R. Gani, *Ind. Eng. Chem. Res.*, 2016, **55**, 3383–3419.
20 D. G. Madden, H. S. Scott, A. Kumar, K.-J. Chen, R. Sanii, A. Bajpai, M. Lusi, T. Curtin, J. J. Perry and M. J. Zaworotko, *Philos. Trans. R. Soc. Math. Phys. Eng. Sci.*, 2017, **375**, 20160025.
21 M. North, R. Pasquale and C. Young, *Green Chem.*, 2010, **12**, 1514.
22 D. O. Meléndez, A. Lara-Sánchez, J. Martínez, X. Wu, A. Otero, J. A. Castro-Osma, M. North and R. S. Rojas, *ChemCatChem*, 2018, **10**, 2271–2277.
23 J. A. Castro-Osma, M. North and X. Wu, *Chem. - Eur. J.*, 2016, **22**, 2100–2107.
24 Y. A. Rulev, Z. T. Gugkaeva, A. V. Lokutova, V. I. Maleev, A. S. Peregudov, X. Wu, M. North and Y. N. Belokon, *ChemSusChem*, 2017, **10**, 1152–1159.
25 J. van de Loosdrecht, F. G. Botes, I. M. Ciobica, A. Ferreira, P. Gibson, D. J. Moodley, A. M. Saib, J. L. Visagie, C. J. Weststrate and J. W. Niemantsverdriet, in *Comprehensive Inorganic Chemistry II*, Elsevier, 2013, pp. 525–557.
26 Y. H. Choi, Y. J. Jang, H. Park, W. Y. Kim, Y. H. Lee, S. H. Choi and J. S. Lee, *Appl. Catal. B Environ.*, 2017, **202**, 605–610.
27 T. Riedel, M. Claeys, H. Schulz, G. Schaub, S.-S. Nam, K.-W. Jun, M.-J. Choi, G. Kishan and K.-W. Lee, *Appl. Catal. Gen.*, 1999, **186**, 201–213.
28 G. Leonzio, *Chem. Eng. J.*, 2016, **290**, 490–498.
29 E. Moioli, N. Gallandat and A. Züttel, *Chem. Eng. J.*, 2019, **375**, 121954.
30 E. E. Adams and K. Caldeira, *Elements*, 2008, **4**, 319–324.
31 Y. Teng and D. Zhang, *Sci. Adv.*, 2018, **4**, eaao6588.
32 V. Gutknecht, S. Ó. Snæbjörnsdóttir, B. Sigfússon, E. S. Aradóttir and L. Charles, *Energy Procedia*, 2018, **146**, 129–134.
33 S. Kwon, M. Fan, H. F. M. DaCosta and A. G. Russell, *J. Environ. Sci.*, 2011, **23**, 1233–1239.
34 W.-L. Dai, S.-L. Luo, S.-F. Yin and C.-T. Au, *Appl. Catal. Gen.*, 2009, **366**, 2–12.
35 S. Fukuoka, M. Kawamura, K. Komiya, M. Tojo, H. Hachiya, K. Hasegawa, M. Aminaka, H. Okamoto, I. Fukawa and S. Konno, *Green Chem*, 2003, **5**, 497–507.
36 B. Schäffner, F. Schäffner, S. P. Verevkin and A. Börner, *Chem. Rev.*, 2010, **110**, 4554–4581.
37 M. Yoshida and M. Ihara, *Chem. - Eur. J.*, 2004, **10**, 2886–2893.
38 G. Rokicki and W. Kuran, *Bull. Chem. Soc. Jpn*, 1984, **57**, 1662–1666.
39 H. Komura, T. Yoshino and Y. Ishido, *Bull. Chem. Soc. Jpn.*, 1973, **46**, 550–553.
40 D. C. Webster, *Prog. Org. Coat.*, 2003, **47**, 77–86.
41 F. Castro-Gómez, G. Salassa, A. W. Kleij and C. Bo, *Chem. - Eur. J.*, 2013, **19**, 6289–6298.
42 L. Guo, K. J. Lamb and M. North, *Green Chem.*, 2021, **23**, 77–118.
43 V. Butera and H. Detz, *ACS Omega*, 2020, **5**, 18064–18072.
44 T. Marino, F. Ponte, G. Mazzone, E. Sicilia, M. Toscano and N. Russo, *Dalton Trans.*, 2017, **46**, 9030–9035.
45 A. Sukumaran Nair, S. Cherian, N. Balachandran, U. G. Panicker and S. K. Kalamblayil Sankaranarayanan, *ACS Omega*, 2019, **4**, 13042–13051.
46 Y. Ecochard and S. Caillol, *Eur. Polym. J.*, 2020, **137**, 109915.
47 T. Bürgel and M. Fedtke, *Polym. Bull.*, 1993, **30**, 61–68.
48 G. Rokicki and C. Wojciechowski, *J. Appl. Polym. Sci.*, 1990, **41**, 647–659.
49 D. J. Darensbourg, *Chem. Rev.*, 2007, **107**, 2388–2410.
50 N. Chawla, N. Bharti and S. Singh, *Batteries*, 2019, **5**, 19.
51 E. S. Takeuchi, P. J. Quattrini and W. Greatbatch, *Pacing Clin. Electrophysiol.*, 1988, **11**, 2035–2039.

52 J. Chai, Z. Liu, J. Zhang, J. Sun, Z. Tian, Y. Ji, K. Tang, X. Zhou and G. Cui, *ACS Appl. Mater. Interfaces*, 2017, **9**, 17897–17905.
53 X. Zuo, K. Chang, J. Zhao, Z. Xie, H. Tang, B. Li and Z. Chang, *J. Mater. Chem. A*, 2016, **4**, 51–58.
54 S. D. Tillmann, P. Isken and A. Lex-Balducci, *J. Power Sources*, 2014, **271**, 239–244.
55 C.-C. Su, M. He, R. Amine, Z. Chen, R. Sahore, N. Dietz Rago and K. Amine, *Energy Storage Mater.*, 2019, **17**, 284–292.
56 *Basic Principles in Applied Catalysis*, Springer Berlin Heidelberg, Germany, 2013.
57 B. Cornils and W. A. Herrmann, *J. Catal.*, 2003, **216**, 23–31.
58 C. W. Gellings and K. E. Parmenter, *Encycl. Life Support Syst.*, 2004, 1–15.
59 F. Haber, Nobel lectures in chemistry 1901-2921, Elsevier, Amsterdam, 1966.
60 G. C. Koltsakis, I. P. Kandylas and A. M. Stamatelos, *Chem. Eng. Commun.*, 1998, **164**, 153–189.
61 *Industrial Catalyst Market: Global Industry Trends, Share, Size, Growth, Opportunity and Forecast 2021-2026*, IMARC Group, 2021.
62 G. f. Swieglers, *Mechanical catalysis: Methods of Enzymatic, homogeneous, and heteroeneous catalysis*, John Wiley & Sons Inc., Hoboken, New Jersey, 2008.
63 M. V. Twigg, *Catalyst Handbook*, CRC Press Taylor and Francis Group, 2nd edn.
64 P. Van Leeuwen, *Homogeneous catalysis: understanding the art*, Kluwer Acad. Publ, Dordrecht, 2004.
65 J. Védrine, *Catalysts*, 2017, **7**, 341–366.
66 R. C. Ray and D. Montet, *Fermented foods. Part II, Part II*, 2017.
67 E. Buchner, *Cell-free fermentation*, Nobel Lecture, 1907.
68 M. Vitolo, *World J. Pharm. Res.*, **9**, 60–76.
69 S. J. Benkovic, *Science*, 2003, **301**, 1196–1202.
70 J. Kadokawa and S. Kobayashi, *Curr. Opin. Chem. Biol.*, 2010, **14**, 145–153.
71 M. C. Roman-Martinez and C. Salinas-Martinez de lecea, in *New and Future Developments in Catalysis*, Elsevier B.V., 2013.
72 A. Tanimu, S. Jaenicke and K. Alhooshani, *Chem. Eng. J.*, 2017, **327**, 792–821.
73 P. G. Cozzi, *Chem Soc Rev*, 2004, **33**, 410–421.
74 E. N. Jacobsen, W. Zhang, A. R. Muci, J. R. Ecker and L. Deng, *J. Am. Chem. Soc.*, 1991, **113**, 7063–7064.
75 A. Dalla Cort, P. De Bernardin, G. Forte and F. Yafteh Mihan, *Chem. Soc. Rev.*, 2010, **39**, 3863–3876.
76 Md. A. Asraf, C. I. Ezugwu, C. M. Zakaria and F. Verpoort, *Photochem. Photobiol. Sci.*, 2019, **18**, 2782–2791.
77 V. Mirkhani, M. Moghadam, S. Tangestaninejad and B. Bahramian, *Appl. Catal. Gen.*, 2006, **311**, 43–50.
78 M. Bazarganipour and M. Salavati-Niasari, *Appl. Catal. Gen.*, 2015, **502**, 57–64.
79 A. Dalla Cort, L. Mandolini and L. Schiaffino, *Chem. Commun.*, 2005, 3867–3870.
80 J. D. McGilvra and V. H. Rawal, *Synlett*, 2004, 2440–2442.
81 A. Coletti, P. Galloni, A. Sartorel, V. Conte and B. Floris, *Catal. Today*, 2012, **192**, 44–55.
82 R. M. Haak, S. J. Wezenberg and A. W. Kleij, *Chem. Commun.*, 2010, **46**, 2713–2724.
83 K. Tabatabaeian, M. Mamaghani and A. Pourahamad, *Russ. J. Org. Chem*, 2001, **37**, 1287–1288.

84 J. H. Sinfelt, *Sci. Am.*, 1985, **253**, 90–101.
85 A. Scheurer, H. Maid, F. Hampel, R. W. Saalfrank, L. Toupet, P. Mosset, R. Puchta and N. J. R. van Eikema Hommes, *Eur. J. Org. Chem.*, 2005, **2005**, 2566–2574.
86 H. Jing, S. K. Edulji, J. M. Gibbs, C. L. Stern, H. Zhou and S. T. Nguyen, *Inorg. Chem.*, 2004, **43**, 4315–4327.
87 C. Baleizão and H. Garcia, *Chem. Rev.*, 2006, **106**, 3987–4043.
88 M. Abd El Sater, N. Jaber and E. Schulz, *ChemCatChem*, 2019, **11**, 3662–3687.
89 A. Zulauf, M. Mellah, X. Hong and E. Schulz, *Dalton Trans.*, 2010, **39**, 6911–6936.
90 M. A. Esteves, B. Gigante, C. Santos, A. M. Guerreiro and C. Baleizão, *Catal. Today*, 2013, **218–219**, 65–69.
91 S.-H. Cho, B. Ma, S. T. Nguyen, J. T. Hupp and T. E. Albrecht-Schmitt, *Chem Commun*, 2006, 2563–2565.
92 Q. Xia, Y. Liu, Z. Li, W. Gong and Y. Cui, *Chem. Commun.*, 2016, **52**, 13167–13170.
93 A. H. Chughtai, N. Ahmad, H. A. Younus, A. Laypkov and F. Verpoort, *Chem. Soc. Rev.*, 2015, **44**, 6804–6849.
94 P. T. Anastas, L. B. Bartlett, M. M. Kirchhoff and T. C. Williamson, *Catal. Today*, 2000, **55**, 11–22.
95 H. Bilel, N. Hamdi, C. Fischmeister and C. Bruneau, *ChemCatChem*, 2020, **12**, 5000–5021.
96 M. Hassam, A. Taher, G. E. Arnott, I. R. Green and W. A. L. van Otterlo, *Chem. Rev.*, 2015, **115**, 5462–5569.
97 D. G. Vassão, D. R. Gang, T. Koeduka, B. Jackson, E. Pichersky, L. B. Davin and N. G. Lewis, *Org Biomol Chem*, 2006, **4**, 2733–2744.
98 J. L. Hayes, B. L. Strom, L. M. Roton and L. L. Ingram, *J. Chem. Ecol.*, 1994, **20**, 1595–1615.
99 M. D. Vincenzi, M. Silano, F. Maialetti and B. Scazzocchio, *Fitoterapia*, 2000, **71**, 725–729.
100 P. Anastas and N. Eghbali, *Chem Soc Rev*, 2010, **39**, 301–312.
101 H. Jo, M. Choi, M. Viji, Y. Lee, Y.-S. Kwak, K. Lee, N. Choi, Y.-J. Lee, H. Lee, J. Hong, M. Lee and J.-K. Jung, *Molecules*, 2015, **20**, 15966–15975.
102 N. Hofslokken and L. Skattebol, *Acta Chem. Scandiavia*, 1999, **53**, 258–262.
103 A. S. Amarasekara, A. R. Oki, I. McNeal and U. Uzoezie, *Catal. Commun.*, 2007, **8**, 1132–1136.
104 L. L. Hench and J. K. West, *Chem. Rev.*, 1990, **90**, 33–72.

List of Abbreviations

In the order of appearance

IPCC	-International panel on climate change
IR	-Infrared
GHG	-greenhouse gas
HFCs	-Hydrofluorocarbon
PFCs	-Perfluorocarbons
GWP	-Global warming potential
CC	-Carbon capture
MOF	-Metal organic framework
VOC	-Volatile organic compounds
PoGCs	-The principles of green chemistry
NMR	-Nuclear magnetic resonance
ppm	-Parts per million
ESI	-Electrospray ionisation
MS	-Mass Spectrometry
1M	-1 Molar (Mol L^{-1})
EtOAc	-Ethyl acetate
Et_3N	-Triethyl amine
^{1}H-COSY	-Hydrogen COrrelated SpectroscopY
TEOS	- tetraethyl orthosilicate
CHN	-Carbon Hydrogen Nitrogen
MALDI	-Matrix assisted laser desorption/ionisation
EtOH	-Ethanol

Appendix

5.5.9- Spectra

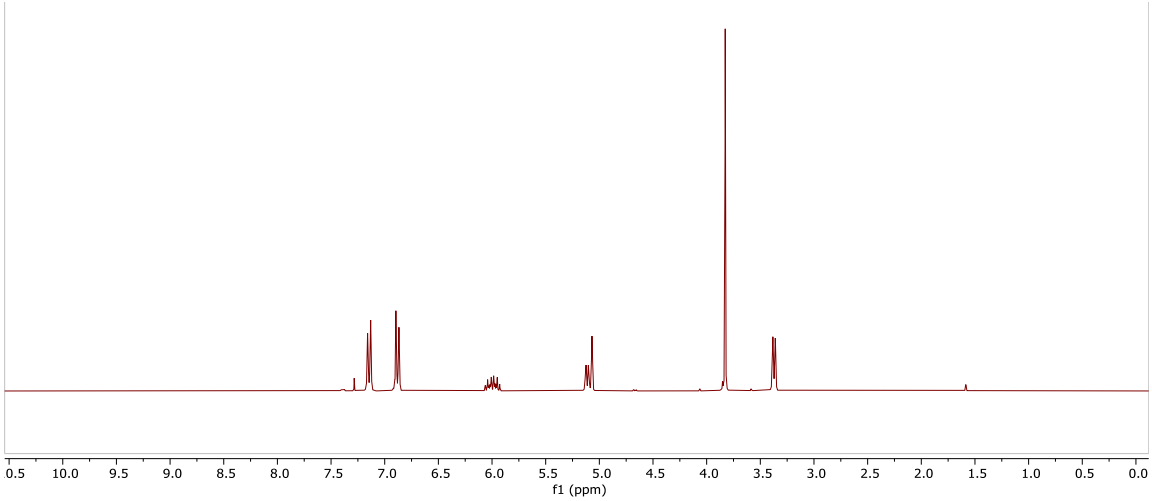

S. 1- 1H NMR spectra of 4-allylanisole, 1a

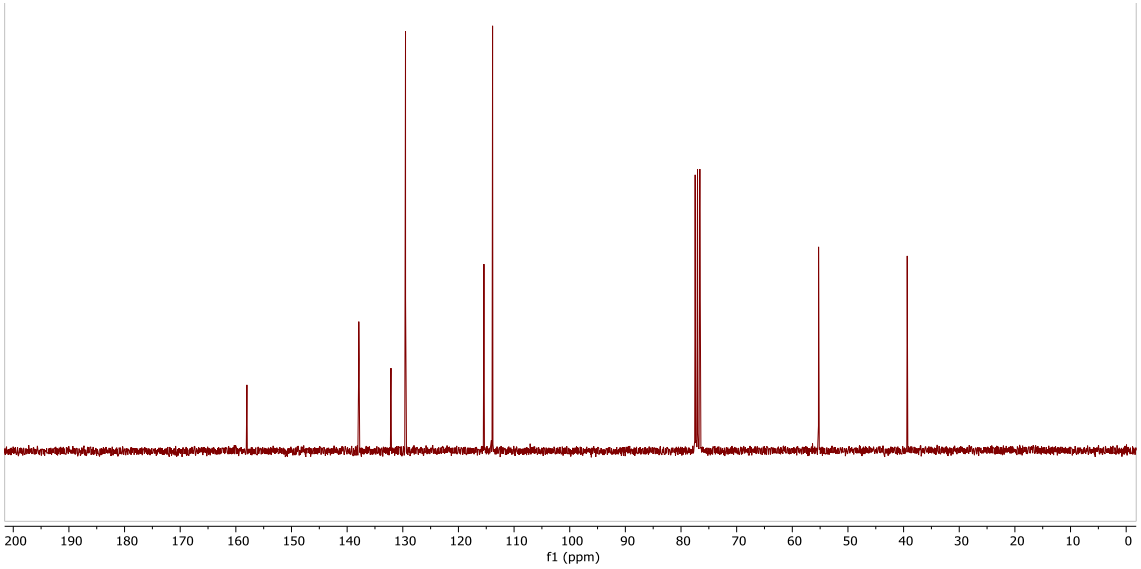

S. 2 13C-NMR Spectra of 4-allylanisole, ***1a***

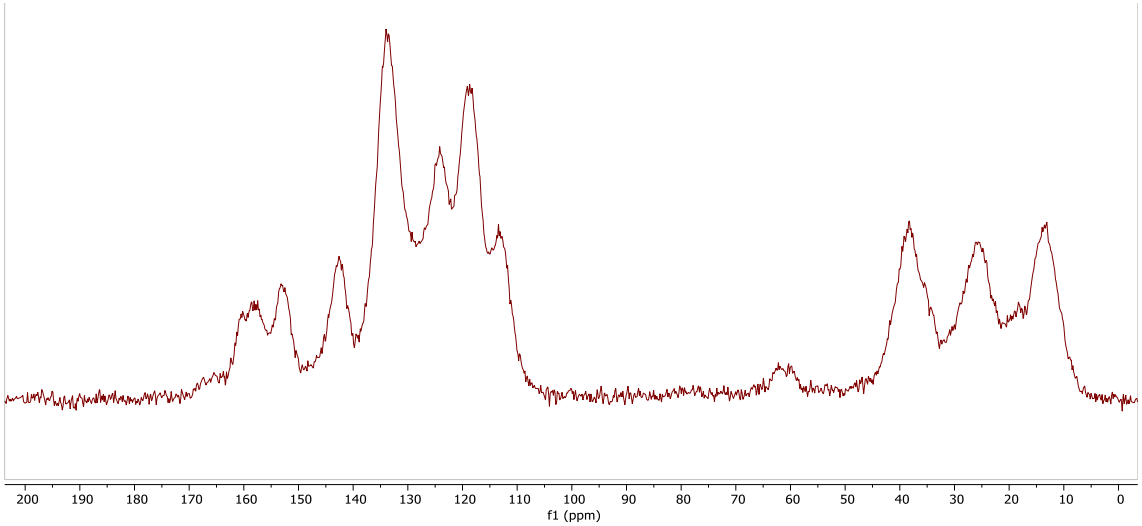

S. 3: Solid state ^{13}C-NMR of 7:1 Immobilised salophen

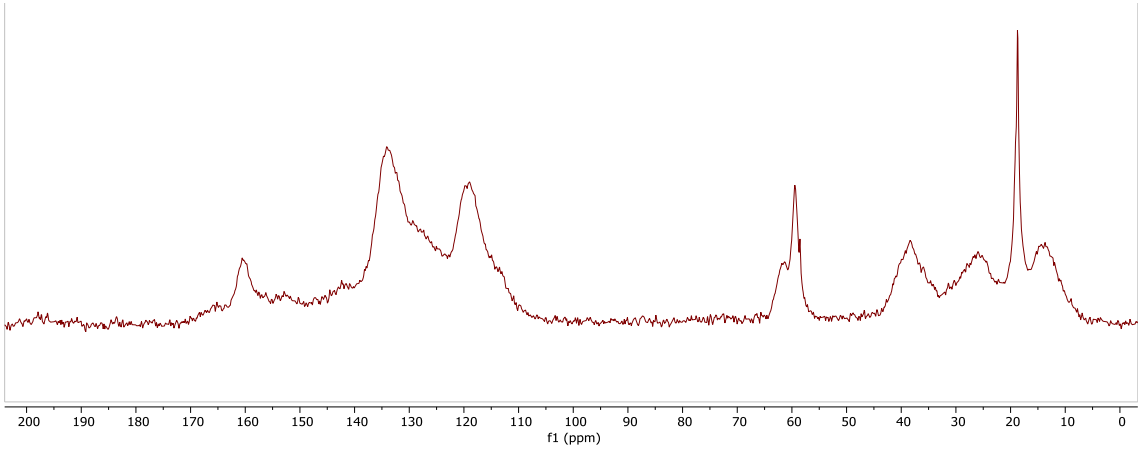

S. 4: Solid state ^{13}C-NMR of 15:1 Immobilised salophen

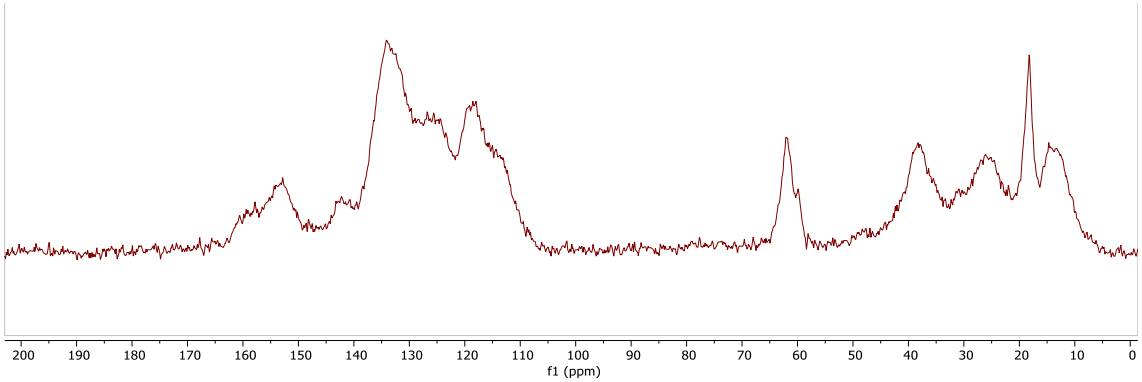

S. 5: Solid state ^{13}C-NMR of 25:1 Immobilised salophen

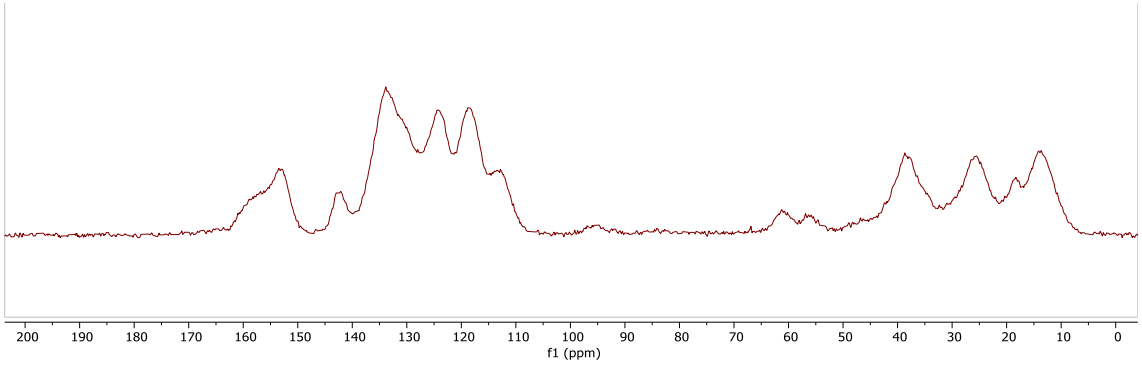

*S. 6: Solid state ^{13}C-NMR of 16:1 Immobilised salophen formed with **4b***